

## ABSTRACT

Title of Thesis: MOLECULAR PHYLOGENETICS IN THE FAMILY  
SPHINGIDAE (LEPIDOPTERA: BOMBYCOIDEA)

Andre Arthur Mignault, Master of Science, 2004

Thesis directed by: Professor Charles W. Mitter

Department of Entomology

Moths in superfamily Bombycoidea (Lepidoptera) exhibit a range of strongly divergent life history traits, especially concerning larval herbivory and adult feeding. Building on Regier *et al.* (2001), this study aimed to provide a context for investigation of life history evolution by reconstructing molecular phylogenetic hypotheses of relationships within one bombycoid family, Sphingidae. Coding nucleotide sequence data were collected from two genes, Elongation Factor 1-alpha (1,274bp) and Dopa Decarboxylase (1,373bp), across 65 & 67 sphingids and 40 & 51 lepidopteran outgroups, respectively. Variation in both genes was concentrated in third codon positions, and phylogenetic signal between them proved discordant. Analyses under criteria of Maximum Parsimony and Maximum Likelihood generated six unique hypotheses of sphingid relatedness, each of which was evaluated for concordance with Kitching & Cadiou's (2000) classification. Given weak bootstrap support within and conflicting basal relationships among these topologies, they are best viewed as novel hypotheses subject to further testing via collection of new molecular data.

MOLECULAR PHYLOGENETICS IN THE FAMILY SPHINGIDAE  
(LEPIDOPTERA: BOMBYCOIDEA)

By

Andre Arthur Mignault

Thesis submitted to the Faculty of the Graduate School of the  
University of Maryland, College Park, in partial fulfillment  
of the requirements for the degree of  
Master of Science  
2004

Advisory Committee:

Professor Charles W. Mitter, Chair  
Professor Jerome C. Regier  
Professor Charles F. Delwiche

*To Kimberly*



## ACKNOWLEDGMENTS

Charlie Mitter nurtured and guided the progress of this work and my general intellectual development with boundless wisdom and patience. Jerry Regier fostered a stimulating laboratory environment, making possible effective collection of these molecular data. My understanding of molecular systematic principles and methods is traced with gratitude to Chuck Delwiche. Members of the Regier Lab, especially Diane Shi, Chris Desjardins and Chris Cook, provided invaluable support during wet-bench work. I feel fortunate to have tapped Ian Kitching's exceptional reserve of knowledge on matters of sphingid taxonomy and natural history. Paul Somers and Jerry Regier contributed valuable comments on the manuscript. This research was made possible by the indispensable support of a network of sphingid collectors and enthusiasts, including: James Adams, Martin Andree, Manuel Balcazar Lara, Ed Ballard, George Balogh, Charles Bordelon, Jr., David Boucher, Don Bowman, Tom Burbidge, Ken Davenport, John DeBenedictis, Bob Denno, Willy DePrins, Duke Elsner, Chuck Ely, Les Ferge, Pete Haggard, Chuck Harp, Dan Janzen, Bill Kelly, Ian Kitching, Ed Knudson, Jim Kruse, Pete Landolt, Ron Leuschner, Mark Mello, Julio & Charyn Micheli, Bill & Byrne Mooney, Marcela More, James Mouw, John Nelson, Mike Nelson, Mogens Nielsen, John Noble, Jim Oberfoell, Paul Opler, Ric Peigler, Owen Perkins, Rob Raguso, John Richards, Kelly Richers, Craig Rudolph, Glen Smart, Dick Smith, Mike Smith, Fred Stehr, Paul Thompson, Jim Tuttle, Bruce Walsh, Reggie Webster and Kirby Wolfe. Finally, this study was inspired and motivated by the comprehensive research programme of Dan Janzen, whose enthusiasm and passion for bombycid life history evolution provided relevance for a phylogenetic perspective.

# TABLE OF CONTENTS

LIST OF TABLES.....	v
LIST OF FIGURES.....	vi
INTRODUCTION.....	1
<b>MATERIALS &amp; METHODS</b> .....	<b>13</b>
Taxon Sampling.....	13
Specimen Acquisition.....	14
Specimen Curation.....	16
Sequence Collection de novo.....	17
A. Whole Nucleic Acid Extraction.....	18
B.1 Reverse-Transcription Amplification.....	20
B.2 Gel Purification of RT-PCR Products.....	26
B.3 Nested PCR Amplification.....	28
B.4 Gel Purification of Nested PCR Products.....	29
C. Automated Sequencing.....	29
D. Sequence Editing.....	30
E. Sequence Alignment.....	32
Sequence Data Collection in silico.....	33
Data Matrix Construction.....	36
Character Information Content.....	37
Parsimony-Based Preliminary Analyses.....	38
A. PTP Test of Information Content.....	38
B. Parsimony-Based Searches.....	39
C. Nonparametric Bootstrap Analysis.....	41
D. Incongruence Length Difference (ILD) Test.....	42
Evaluating Alternative Parsimony Topologies.....	44
Selection of a Model of Nucleotide Substitution.....	46
Likelihood-Based Analyses.....	48
<b>RESULTS</b> .....	<b>50</b>
Taxon Sampling.....	50
Data Matrix Construction.....	54
Information Content.....	55
Parsimony-Based Preliminary Analyses.....	60
A. Testing for Information Content.....	60
B. Parsimony Searches.....	61
C. Nonparametric Bootstrap Analysis.....	65
D. ILD Test.....	65
Evaluating Alternative Parsimony Topologies.....	66
Qualification of Parsimony-Based Topologies.....	68
Likelihood-Based Parameter Estimation.....	72
Evaluating Topologies from Likelihood Analyses.....	76
Evaluating the Likelihood of All Candidate Topologies.....	79
<b>DISCUSSION</b> .....	<b>80</b>
<b>DIRECTIONS FOR FURTHER ANALYSIS</b> .....	<b>89</b>
<b>REFERENCES</b> .....	<b>92</b>

## LIST OF TABLES

- Table 1. Selected life history contrasts between Sphingidae and Saturniidae (Lepidoptera: Bombycoidea).
- Table 2. Taxonomic classification and phylogenetic sequence of genera in Sphingidae (Lepidoptera: Bombycoidea) presented by Kitching & Cadiou (2000).
- Table 3. Elongation Factor 1-alpha (EF) Primers.
- Table 4. Dopa Decarboxylase (DDC) Primers.
- Table 5. Amplification strategies for DDC employed (a) in this study and (b) in the Regier Lab.
- Table 6. RT-PCR and Nested PCR reaction conditions.
- Table 7. Survey of GenBank accessions for EF and DDC across Lepidoptera.
- Table 8. Ingroup samples (Bombycoidea: Sphingidae) for which EF and/or DDC sequences were obtained.
- Table 9. Outgroup samples (Lepidoptera) for which EF and/or DDC sequences were obtained.
- Table 10. New Sphingidae specimens.
- Table 11. Distribution of EF and DDC sequence accessions in GenBank across Lepidoptera.
- Table 12. Summary of character information content and nucleotide composition in data matrices by gene, taxon set and partition.
- Table 13. Amino acid alignment for EF.
- Table 14. Amino acid alignment for DDC.
- Table 15. Empirical base compositions for EF and DDC among ingroup taxa (Bombycoidea: Sphingidae).
- Table 16. Empirical base compositions for EF and DDC among outgroup taxa (Lepidoptera).
- Table 17. Empirical pairwise distance matrix for EF data.
- Table 18. Empirical pairwise distance matrix for DDC data.
- Table 19. Preliminary maximum parsimony (MP) heuristic searches.
- Table 20. Performance of data on alternative topologies, evaluated under the criterion of maximum parsimony (MP).
- Table 21. Iterative maximum likelihood (ML) model parameter estimation and heuristic searches.
- Table 22. Performance of data on alternative topologies, evaluated under the criterion of maximum likelihood (ML).

## LIST OF FIGURES

- Figure 1. Phylogenetic relatedness among fourteen genera of Sphingidae (Lepidoptera: Bombycoidea) presented in the pilot study of Regier, *et al.* (2001).
- Figure 2. Instructions distributed to sphingid collectors.
- Figure 3. Data entry page of the University of Maryland Lepidoptera Collections Database.
- Figure 4. Reference sequence for Elongation Factor 1-alpha (EF)
- Figure 5. Reference sequence for Dopa Decarboxylase (DDC)
- Figure 6. Exemplar most parsimonious phylogram reconstructed from phylogenetic inference on EF ntall data for the Sphingidae&2OG taxon set
- Figure 7. Exemplar most parsimonious phylogram reconstructed from phylogenetic inference on DDC ntall data for the Sphingidae&2OG taxon set.
- Figure 8. Exemplar most parsimonious phylogram reconstructed from phylogenetic inference on combined EF&DDC ntall data for the Sphingidae&2OG taxon set.
- Figure 9. Maximum likelihood phylogram from phylogenetic inference on EF ntall data for the Sphingidae&2OG taxon set.
- Figure 10. Maximum likelihood phylogram from phylogenetic inference on DDC ntall data for the Sphingidae&2OG taxon set.
- Figure 11. Exemplar maximum likelihood phylogram from phylogenetic inference on combined EF&DDC ntall data for the Sphingidae&2OG taxon set.

## INTRODUCTION

Extraordinary numerical, morphological and behavioral diversity within insects (Arthropoda: Hexapoda) has made them potent model systems for examining the connection between ecological phenomena and evolutionary history (Dobler & Farrell 1999; Farrell 1993, 1998, 2001; Farrell *et al.* 2001; Hufbauer & Via 1999; Kelley & Farrell 1998; Kelley *et al.* 2000; Mitter *et al.* 1988; Pierce 1987, 1995; Powell *et al.* 1999; Sequeira *et al.* 2000; Shaw 1996a,b). Studies on insect ecology and evolution are complementary and synergistic, and can be viewed broadly from two perspectives: (i) short-term interactions between an organism and its environment (ecology) can influence long-term patterns and processes of stasis or change in organismal traits (evolution) (e.g., Costa *et al.* 1996; Hawthorne & Via 2001); and (ii) evolutionary history constrains the genesis of novel ecological habits (e.g., Farrell *et al.* 1992; Farrell & Mitter 1994; Mitter *et al.* 1991; Mitter & Farrell 1991; Wiegmann *et al.* 1993). Application of an evolutionary perspective to long-standing ecological questions may provide insight into the origin and maintenance of traits considered key elements of an organism's natural history. By comparing the observed distribution of ecologically relevant characters with independently derived estimates of organismal evolutionary history, the link between pattern and process can be inferred (Harvey & Pagel 1991). Refinement of molecular phylogenetic methodology has made available robust and novel tools for inferring evolutionary history. In conjunction with traditional and contemporary ecological studies, these methods have made feasible the examination of natural history within an evolutionary context.



Moths in the superfamily Bombycoidea (Lepidoptera: Macrolepidoptera) represent a potent study system for exploration of the connection between ecology and life history evolution. Bombycoidea is one of 43 superfamilies in the hyper-diverse Ditrysia, a lepidopteran clade characterized by explosive diversity in life history strategies which accounts for approximately 98.5% of the over 200,000 species of Lepidoptera (Wagner 2001). As currently delimited, Bombycoidea consists of 3,554 described species distributed across nine families, and is presumed monophyletic on the basis of at least four robust morphological synapomorphies (Lemaire & Minet 1999; Minet 1991 & 1994; Wagner 2001): (a) ultimate instar prothoracic coxae anteriorly fused, each having lost its independent mobility; (b) larval abdominal segment VIII with D1 setae arising from middorsal protuberance, usually a scolus; (c) flexors in valvae of male genitalia originate on the tegumen, not the vinculum; and (d) forewing with Rs1+Rs2 closely parallel to or fused to stem Rs3+Rs4. Bombycoid moths and their close relatives have a cosmopolitan distribution, are among the largest and most conspicuous Lepidoptera (e.g., *Hyalophora*, the cecropia silkworm; *Actias*, the luna moth) and have in some cases even acquired cultural significance (e.g., *Acherontia*, the death's head sphinx). They have served as model systems for studies in insect biochemistry and physiology (Bartholomew & Casey 1978; Casey 1976; Fink 1995; Goldsmith & Wilkins 1995; Gopfert & Wasserthal 1999; Heinrich 1971a,b; Heinrich & Bartholo 1971; Liu *et al.* 1998; O'Brien 1999 ; Ojeda-Avila *et al.* 2001, 2003; Raguso *et al.* 1996; Raguso & Light 1998; Raguso & Willis 2002; Scriber 1979; Wasserthal 2001; Willmott & Ellington 1997a,b; Willmott *et al.* 1997), development (Hatzopoulos & Regier 1987; Leclerc & Regier 1993; Mazur *et al.* 1989; Regier *et al.* 1993, 1995; Regier & Kafatos 1991) and

functional morphology (Bullock & Pescador 1983; Buttiker *et al.* 1996; Fanger 1999; Fleming 1968; Fullard & Yack 1993; Ghiradella 1998; Gopfert *et al.* 2002; Gopfert & Wasserthal 1999; Grant & Eaton 1973; Grodnitsky 1999; Krenn 1990; Miller 1997a,b; Robinson & Robinson 1972; Roeder 1972; Roeder *et al.* 1968, 1970; Roeder & Treat 1970; Schmitz & Wasserthal 1999; Scoble 1992; Wannemacher & Wasserthal 2003; Yack & Fullard 1993a,b, 2000), with special attention focused on agricultural pests (e.g., *Manduca*, the tobacco & tomato hornworms; *Erinnyis*, a potent euphorb crop pest in the New World, see Dillon *et al.* 1983 and Winder 1976) and species of economic significance (e.g., *Bombyx*, the silkworm; also see Batra 1983; Coffelt & Schultz 1990, 1991, 1993). Furthermore, bombycoid moths have assumed central roles in studies of insect community ecology (Bernays & Janzen 1988; Janzen 1981,1984,1988; Janzen & Waterman 1984; Young 1972), nutritional ecology (O'Brien *et al.* 2000) and pollination biology (Darwin 1862; Eisikowitch & Galil 1971; Grant & Grant 1983a,b; Haber 1984; Haber & Frankie 1982, 1989; Kitching 2002; Miller 1981; Nilsson 1988,1998; Nilsson *et al.* 1985, 1987; Paige & Whitham 1985; Raguso & Willis 2002; Wasserthal 1996,1997,1998; White *et al.* 1994).

In a paper entitled “Two ways to be a tropical big moth: Santa Rosa saturniids and sphingids”, Janzen (1984) highlighted and reformulated interest in bombycoid natural history in the context of tropical ecology. Janzen identified stark contrasts in life history strategies between and among moths in two prominent lepidopteran components of a Costa Rican tropical forest community: the bombycoid families Sphingidae and Saturniidae. Superficially, Sphingidae and Saturniidae share many similarities. Both families contain large, conspicuous moths whose larvae struggle to meet demanding

metabolic requirements to support their size. As a result, the larvae of both families can be quite large and feed externally on plant tissues, making them prime targets for suites of predators and parasites (Dyer 1995; Janzen 1988; Price 1997; Stamp & Casey 1993). The biogeographic distribution of both families overlaps both within the Santa Rosa forest and at broader spatial scales. Finally, the sexes in both families pursue common strategies: adult males strive to locate reproductively viable females, and mated females strive to locate suitable plants and/or microhabitats for oviposition. Despite these shared attributes, however, members of the Sphingidae and Saturniidae have adopted starkly divergent life history strategies (Table 1).

A critical difference between sphingid and saturniid moths, which broadly impacts many aspects of their life histories, is the ability for the adult moths to feed (Miller 1996). Sphingidae are renowned for their impressive proboscises (Krenn 1990,1997,1998,2000; Krenn & Kristensen 2000), which permit penetration into sometimes deep and morphologically specialized flower corolla tubes to extract nutrient-rich nectar, and indeed have been prominent figures in studies of pollination biology (Nilsson 1998; Nilsson *et al.* 1985, 1987; Raguso & Willis 2002; Wasserthal 1997). In his treatise, *On the Various Contrivances by which British and Foreign Orchids are Fertilised by Insects*, Darwin (1862) predicted that “in Madagascar there must be moths with proboscises capable of extension to a length of between ten and eleven inches”, based on his knowledge of the deep-nectary orchid *Angraecum sesquipedale*. Forty-one years later, Rothschild & Jordan (1903) described the hawkmoth *Xanthopan morgani praedicta* (with a proboscis of length 300 mm or 11.8 inches) as a confirmed pollinator of this orchid (Kritsky 1991). This case illustrates the impressive development of

specialized mouthpart morphology associated with evolution of the feeding habit in Sphingidae. In stark contrast, all adult Saturniidae have reduced or functionally vestigial mouthparts, and the adults are relatively ineffective or incapable feeders.

Potential for adult nutrient intake has been recognized as a critical trait affecting almost every classically important parameter of insect life history, including life span, metabolic rate, activity level, sexual dimorphism and reproduction (Price 1997; see Table 1). For example, sphingid moths which feed continuously throughout their adult stage live much longer than saturniids of comparable size (Janzen 1984). Adult Sphingidae also sustain much higher activity levels and are capable of more controlled and sustained flight maneuvers than saturniids (O'Brien 1999; O'Brien & Suarez 2001). Sphingid male and female adults both share the ability to feed, and they exhibit dampened sexual dimorphism in size and behavior relative to saturniid males and females (Janzen 1984). This drastically affects both the mating habits of the adults and the ways in which female energy is allocated to reproduction. Sphingid males actively court females and are susceptible to female choice and male-male competition (Price 1997), while saturniid females mate indiscriminately with the first male encountered (Janzen 1984). Sphingid females steadily produce eggs throughout their adult lives and oviposit selectively in small clutches, while saturniid females possess their full complement of mature eggs at eclosion and oviposit in large clutches relatively indiscriminately (Janzen 1984).

Notable contrasts in life history strategies are not confined to just the adult stage of Sphingidae and Saturniidae. Janzen (1984) observed a striking series of life history correlates during sphingid and saturniid larval development. For example, sphingid larvae eat a much more restricted set of hostplants and develop much faster than

saturniids of comparable size (Janzen 1984). Characteristics of an insect herbivore's hostplants have long been regarded as central aspects of their biology. Sphingid larvae feed on inconspicuous but nutrient-rich plant materials with highly specific and toxic defensive compounds, including: Asteridae (Asteraceae, Asclepiadaceae, Apocynaceae, Bignoniaceae, Boraginaceae, Convolvulaceae, Lamiaceae, Rubiaceae, Solanaceae, Verbenaceae); Dilleniidae (Dilleniaceae, Euphorbiaceae, Flacourtiaceae); Hamamelidae (Moraceae); Magnoliidae (Lauraceae); and Rosidae (Anacardiaceae, Vitaceae) (Bernays & Janzen 1988; Janzen 1981; Janzen & Waterman 1984; Mabberley 1997; also see Table 4 in Janzen 1984). In contrast, saturniid larvae feed on more readily apparent plant materials (e.g., trees) which are nutrient-poor and rich in simpler and less toxic defensive chemicals (e.g., >50% of saturniids in Santa Rosa feed on Fabaceae [Rosidae]; see Table 3 in Janzen 1984). Finally, the larvae adopt strongly contrasting strategies for defense: sphingids by passive crypsis and mimicry, saturniids with more aggressive chemical and morphological defenses.

Janzen (1984) provided not only insightful recognition of bombycoid life history contrasts, but also a translation of those ecological patterns into a series of questions exploring insect evolution. For example, he framed the question of character evolution polarity by asking whether the sphingid "caricature" arose from a saturniid precursor, or *vice versa* (Janzen 1984, p.130)? Given that both families are members of the same putatively monophyletic superfamily, this question of directionality in life history evolution can be framed as a hypothesis testable via phylogenetic methods (Harvey & Pagel 1991, Farrell & Mitter 1990; Mitter *et al.* 1988, 1991; Wiegmann *et al.* 1993). Phylogenetic inference of relationships within the Bombycoidea may reveal which of the

two syndromes more closely represents the ancestral condition, and which is derived. Assessing such long term evolutionary trends would likewise shed light on a battery of accompanying questions also raised by Janzen. For example, what factors have contributed to much stronger intra- and inter-specific polymorphism in Saturniidae vs. Sphingidae (Janzen 1984, p.113)? Also, what factors (e.g., oviposition constraints, physiological constraints, top-down and bottom-up regulation) have influenced the distinct and nonoverlapping patterns of larval hostplant use between these families, especially when assessed by degree of polyphagy and differential exploitation of various plant growth forms (Janzen 1984, p.122)? Finally, have the selection pressures favoring non-feeding in saturniid adults been imposed by environments unfavorable to those adults, or in habitats conducive to heavy resource accumulation in the larval stage (Janzen 1984, p.130)? Reconstruction of character evolution on a robust phylogenetic hypothesis would assign direction to the contrasting syndromes (i.e., sphingid vs. saturniid) of bombycoid life history evolution, and permit assignment of one habit to the ancestral condition. This would contribute to a more complete understanding of characters impacting the notable diversification of this superfamily.

Importance of a historical perspective in this system is heightened by consideration of one of the three sphingid subfamilies, the Smerinthinae. Though these moths share morphological synapomorphies which position them resolutely in the Sphingidae (see below), smerinthines exhibit striking similarity in many aspects of their life history strategies to saturniids (Janzen 1984; see Table 1). Thus, broad interfamilial contrasts (i.e., Sphingidae vs. Saturniidae) described in Janzen's (1984) study can be considered evolutionarily "replicated" within the Sphingidae (i.e., Smerinthinae vs.

Sphinginae / Macroglossinae). Depending on the relative orientation of the three subfamilies in a tree of Sphingidae, Smerinthinae may provide an independent contrast to test the impact of divergent life history traits on diversification rates. Alternatively, a basal smerinthine position would indicate that the sphingid “caricature” (*sensu* Janzen 1984) arose once in bombycoid evolution. Regardless of the scenario, robust determination of sphingid subfamily relationships will provide a critical clue to investigate the proximate and ultimate factors responsible for the origin and maintenance of such discrepant life histories in the Bombycoidea.

Construction of a robust phylogenetic hypothesis for the Bombycoidea, subsuming all taxa in Janzen’s Santa Rosa study system, would provide a powerful evolutionary backdrop against which to interpret such vast ecological differences between component families. Such a phylogeny may permit reconstruction of the presumed ancestral condition, suggesting possible character transformation pathways by which these relatively closely related families underwent ecological diversification. Ecological polarity implied by this reconstruction may greatly enhance our understanding of the opportunities and constraints governing broad scale evolution of insect life history strategies, with implications for understanding patterns of herbivory, sexual dimorphism, reproduction, population dynamics and the origin of morphological & behavioral novelty.

The bombycoid system offers a rare opportunity for significant progress in *both* construction of a robust molecular phylogeny and application of that phylogenetic hypothesis to interpretation of the connection between ecology and evolution. Initial attempts to assess phylogenetic relationships within the Bombycoidea have focused on the two most prominent members of the superfamily: the Saturniidae and Sphingidae.

The latter has recently benefited from an intersection of comprehensive morphological (Kitching & Cadiou 2000) and molecular (Regier *et al.* 2001) systematic treatments.

Kitching & Cadiou (2000) proposed an exhaustive genus-level systematic revision of Sphingidae based on unpublished cladistic analyses of morphological and behavioral characters conducted by Kitching (Table 2). Their revision exposed and resolved many layers of nomenclatural violations and proposed an approximately phylogenetic arrangement of taxa. However, this coarse treatment left unresolved many of the relationships across every taxonomic level within the family, including many of prime ecological relevance. Of greatest relevance to interpretation of contrasting life history strategies is the monophyly of and relative position among the three subfamilies recognized by Kitching & Cadiou (2000). Monophyly of the family is considered extremely well-supported on the grounds of at least nine morphological synapomorphies: (a) lateral oblique stripes on larval abdominal segments I-VII; (b) exposed hindwings not reaching pupal abdominal segment IV; (c) ventral arm of adult laterocervicale ending abruptly in a thin rod; (d) prescutal clefts of the adult mesonotum very close or fused dorsally; (e) mostly unsclerotized ventral process in tegula; (f) adult forewing vein M2 arising slightly closer to M3 than to M1; (g) adult hindwing margin produced or angulate at the tip of vein 1A+2A; (h) strong sclerotized lobe on metafurcula secondary arms reinforcing the thoraco-abdominal intersegmental membrane close to abdominal sternite II; and (i) cavity broadly open in 'tergal rim' (Minet 1994, p. 85). However, comparable morphological support has not been established for subfamily concepts, prompting Minet (1994) to state the "monophyly of each of these three subfamilies is, obviously, less convincingly established than that of the Sphingidae" (p. 85). It is hoped that a robust



phylogeny based on molecular data will both corroborate the recent classification of Kitching & Cadiou (2000) and offer clarification in the search for strict morphological synapomorphies characterizing clades at all levels within the Sphingidae.

In a pilot study, Regier *et al.* (2001; hereafter called 'Regier 2001') established the efficacy of two unlinked protein-coding nuclear markers in resolving relationships among sphingid genera. Elongation factor 1-alpha (EF) is involved in the initial stages of peptide elongation, and promotes GTP-dependent binding of aminoacyl tRNA to the ribosome A-site during protein biosynthesis (Hovemann *et al.* 1988; Kamiie *et al.* 1993). Dopa decarboxylase (DDC) catalyzes conversion of dopa into dopamine, and ninety percent of DDC activity occurs in epidermal tissues where dopamine derivatives are involved in sclerotization and melanization of insect cuticle (Hiruma *et al.* 1995; Tatarenkov *et al.* 1999). Regier 2001 found comparable information content and no significant conflict in signal between 1,240 bp of EF and 709 bp of DDC across assayed taxa. After partitioning the data into codon positions, they found that 88% of all variable sites occurred at third codon positions (nt3). Despite that 96% of all nucleotide changes were inferred to be synonymous, pairwise divergences at first and second codon positions (nt1 & nt2) increased with increasing taxonomic depth, suggesting character state saturation at those positions had not yet occurred. Phylogenetic inference was conducted under two optimality criteria: (i) maximum parsimony (MP) with differential weightings across partitions; and (ii) maximum likelihood (ML) under general time reversible models with and without parameters accounting for unequal base frequency. Each analysis was performed on a variety of partition schemes, including genes and codon positions both alone and in conjunction. Differential performance of each analytical

method was assessed via a bootstrap taxon bipartition table, which itemized bootstrap support for clades of interest across the entire range of bombycoids sampled (see Table 1 of Regier 2001). A single fully dichotomous topology derived from MP analysis on the nt1&nt2 partition was selected as the best estimate of relationships among taxa sampled (Figure 1). This fully resolved topology revealed no significant conflict with Kitching's morphological hypotheses, however branches of special interest (especially the position of the "saturniid-like" Smerinthinae) were poorly supported by the data.

The current study was designed as the next step toward ultimately building a robust phylogenetic hypothesis of the entire superfamily Bombycoidea, to provide an evolutionary context for interpretation of ecological characters (e.g., those highlighted by Janzen 1984) as determinants of insect life history evolution. Specifically, this study aimed to expand taxon and character sampling as a means to improve resolution of relationships among genera in systematic analyses of the family Sphingidae. While this work touched on the orientation of Sphingidae within the superfamily, obtaining greater support for the position of the family relative to other bombycoids was left for future studies. Establishing a robust hypothesis of genealogical relatedness within the family Sphingidae has two immediate applications: (1) testing existing hypotheses of sphingid classification based on analysis of non-molecular characters (viz. Kitching & Cadiou 2000); and (2) interpreting correlations between a diverse suite of morphological and behavioral traits from an explicitly phylogenetic perspective.

Immediate goals for this work included: (a) testing the broadly accepted concept of Sphingidae monophyly by exploring robustness of the sphingid node under different suites of outgroups; (b) building on the pilot analyses conducted in Regier 2001 by

augmenting their taxon sampling and extending the range of nucleotides collected from DDC; (c) assessing the degree of corroboration between sphingid phylogenetic hypotheses derived from molecular versus morphological data, especially the monophyly of and relationships among subfamilies, tribes & sections delimited by Kitching & Cadiou (2000); (d) confirming the utility of EF and DDC, both separately and in conjunction, for providing robust phylogenetic resolution within Sphingidae; (e) investigating degree of concordance or conflict in phylogenetic signal between EF and DDC; (f) exploring effects of different taxon samples, character partitions and optimality criteria employed in phylogeny reconstruction.

Broader goals to which this study is expected to contribute include: (a) testing Minet's (1991, 1994) morphologically derived taxonomic hypotheses about relationships in Bombycoidea, including monophyly of and interrelationships among his nine recognized families; (b) contributing a robust phylogenetic component toward resolution of a long-standing polytomy at the base of Macrolepidoptera; (c) establishing a connection between ecology and evolution of life history strategies across Bombycoidea, especially through identification of independent contrasts (e.g., adult feeding, reproductive strategies, sexual dimorphism, larval diet breadth) among bombycoid sister lineages across all taxonomic levels.

## MATERIALS & METHODS

### *Taxon Sampling*

A prime focus of the present study was to expand the diversity of taxon sampling beyond that in Regier 2001. That pilot study included representatives of 7 genera across all three tribes in Macroglossinae, 2 genera in only one of the three tribes in Smerinthinae, and 5 genera in only one of the three tribes in Sphinginae (Figure 1 and Table 2). While results of that study were compelling, the current work aimed to improve the breadth of Sphingidae species in the University of Maryland (UMD) Lepidoptera Collections available for collection of nucleotide sequence data. To this end, a global network of collectors was assembled through directed correspondence and the systematic revision by Kitching & Cadiou (2000) was used as the basis for assigning target taxa to different collectors.

Choice of outgroups for systematic analyses of the Sphingidae was relatively straightforward, given the systematic classification of Bombycoidea proposed by Minet, in which nine families, including Sphingidae, were arranged into putatively monophyletic groups (Minet 1991, 1994; Lemaire & Minet 1999). Corroboration of Minet's broader systematic hypotheses by analysis of molecular evidence is forthcoming (Mitter, pers. comm.); thus, for the purposes of this study all non-sphingid bombycoids were considered viable candidates for outgroups to root the tree of Sphingidae. This study was designed primarily to explore relatedness among genera within Sphingidae, and conclusions regarding genealogical relatedness across the broader Bombycoidea were treated only provisionally.

### *Specimen Acquisition*

To build a grassroots network of sphingid collectors, a list of self-identified sphingid enthusiasts was compiled from The Lepidopterists' Society Membership Directory for years 2000 and 2002 (J.P. Donohue, editor; Los Angeles, CA). In addition, names of registered collectors of sphingid taxa were compiled from The Lepidopterists' Society Season Summary for years 1992-2002 (J.P. Tuttle, editor; Tucson, AZ). A letter summarizing the goals of this project within the context of broader arthropod systematic research at the Maryland Center for Systematic Entomology (MCSE) was mailed to each potential collector, soliciting their help in procuring specimens for the upcoming season and/or providing leads for other collectors. Responses to these solicitations were compiled and correlated against the list of target taxa. Special emphasis was placed on enlisting geographically dispersed collectors to maximize sampling diversity across the North American fauna (see genera shaded in Table 2).

After establishing a collaboration with these parties, collecting kits consisting of the following items were assembled and mailed to interested collectors:

- (a) 15mL and/or 50mL screw-cap centrifuge tubes (Corning Life Sciences, catalog nos. 430790 & 430291) filled with 100% (200 proof) ethanol and labeled internally and externally, for preservation of tissues;
- (b) 5.9cm x 9.2cm side-opening glassine envelopes (Bioquip Products, catalog no. 1131B) for collection of wing vouchers and/or whole dried voucher specimens;
- (c) preformatted specimen information data sheets, for recording specimen information;

- (d) a one-page instruction sheet detailing proper field preservation of insect tissue for use in molecular systematic studies (Figure 2);
- (e) permanent (ethanol-resistant) felt-tip markers;
- (f) parafilm sheets, for sealing vial lids after specimen storage;
- (g) pre-paid overnight return postage labels.

Special emphasis was made in preparation of the kits to simplify both the specimen collection/processing and the data recording steps for each collector. The number and size of vials shipped was customized to the anticipated collecting load and taxa commonly encountered by each collector. Individual vials were labeled internally with laser-printed four-digit serial numbers on strips of 65 lb. 96 brightness acid-free archival quality paper (Wausau Bright White, catalog no. 92101), and externally with the same serials hand-written in permanent marker. Specimen data sheets accompanying each kit were pre-labeled with the collectors' name, the series of numbers for corresponding tubes, and ample space for recording collection information was provided.

Field-collected specimens were transferred immediately into 100% ethanol in the provided vials, and kept cool and dark until shipment back to College Park. Ethanol was selected for specimen preservation in this study for several reasons: (a) low toxicity, (b) low melting point to facilitate storage at cryogenic temperatures, (c) rapid evaporation upon removal of specimen tissue for examination, and (d) slow rate of DNA degradation relative to aqueous solutions. Dessauer *et al.* (1996) remarked that prolonged storage of tissue in at low temperatures and in the absence of oxygen retarded the rate of degradation. Post *et al.* (1993) confirmed that samples stored in any medium at room

temperature, or in aqueous solution at any temperature, exhibited very poor yields in DNA extraction.

### *Specimen Curation*

Upon receipt, shipped specimens were processed immediately and curated for end storage in the UMD Lepidoptera Collections. Spent ethanol preservative was decanted and the vials were refilled to capacity with fresh 100% ethanol. Extremely large specimens (e.g., *Cocytius*, *Eumorpha*, *Manduca*, *Pachysphinx*, etc.) were sectioned or slit to ensure proper penetration of the preservative into internal tissues. Extremely small specimens (e.g., *Agrius*, *Erinnyis*, *Hemaris*, *Proserpinus*, etc.) were transferred to appropriately sized vials, making every effort to maximize volume of free ethanol while conserving freezer space. If necessary, wings submersed in ethanol were separated from the specimen at the basal sclerites, blotted dry on Kimwipes and stored in glassine envelopes labeled with the same four-digit serial number. Similarly, serial numbers of wing vouchers processed by the collectors prior to shipment were checked against the specimen from which they were separated.

Both the pickled tissue specimen and the dried wing voucher were reassigned a revised UMD Lepidoptera Collections accession number consisting of the original four-digit random number with a prefix composed of the collector's initials and a two digit code for the year in which the specimen was received [e.g., "WJK-02-1941" denotes a specimen collected by William J. Kelly into vial #1941 and received at College Park in 2002]. Laser-printed labels with these final accession numbers were swapped for the original vial labels, and wing voucher labels summarizing key collection information for

each specimen were inserted into corresponding glassine envelopes. Curated specimens in 100% ethanol were archived into permanent storage at –80 degrees C in the Regier Laboratory at the University of Maryland Biotechnology Institute (UMBI) Center for Biosystems Research (CBR), College Park, MD. Wing vouchers were sorted by accession number and stored in Cornell drawer insect cabinets in the Mitter Laboratory at UMD Entomology, College Park, MD.

After specimen processing, detailed collections information was compiled from collectors' data sheets and entered into a specimen database custom-designed in FileMaker Pro (version 3.1 and 6.0; FileMaker, Inc.) for management and tracking of molecular tissues specimens in the UMD Lepidoptera Collections. Species identification was determined in all cases by the collector and was *not* independently verified prior to curation. Other key pieces of information entered into designated fields in the UMD database included: accession number, collector & determiner name(s), collection date & time, collection locality, number of specimens, life stage, preservation method, higher taxonomic assignment of each genus, wing voucher information and freezer storage location (Figure 3). In addition, specimen physical condition and any oddities in the collection/curation process were recorded in a notes field. Every effort was made to compile exhaustive collection records for each specimen, and in many cases collectors were consulted to *post facto* verify or clarify specific collection or identification data.

#### *Sequence Collection de novo*

Congruence between independent data sets has long been recognized to lend power to any phylogenetic hypothesis (Brown *et al.* 1994; Cunningham 1997; Eernisse &



Kluge 1993; Funk *et al.* 2000; Mickevich & Farris 1981; Miyamoto & Fitch 1995; Penny & Hendy 1986; Yeates & Wiegmann 1999). In this spirit, nucleotide sequence data was gathered from a portion of the coding regions of two separate and unlinked nuclear genes: (a) Elongation Factor 1-alpha (EF) and (b) Dopa Decarboxylase (DDC). Generation of novel DNA sequence was a three-tiered process: (A) genomic nucleic acid extraction; (B) amplification of the region of the genome of interest; and (C) sequencing of the bases comprising that amplified gene product.

#### A. Whole Nucleic Acid Extraction

Whole nucleic acids were obtained from insect tissue according to the SV Total RNA Isolation System (catalog no. Z3100, Technical Manual no. 048; Promega Corporation). While this kit was intended for extraction of RNA free of genomic DNA contamination, slight protocol modifications permitted precipitation of both genomic DNA and RNA from all samples (Otto, 1998). Extractions were conducted in batches of less than eight specimens, to ensure adequate attention was paid to each sample and to minimize opportunities for cross-contamination.

Specimen vials were removed from  $-80^{\circ}\text{C}$  storage to a wet ice bath, and allowed to equilibrate to ice temperature. Clean forceps were used to transfer the specimen from the ethanol preservative to a sterile disposable petri dish. A sterile disposable scalpel blade was used to section the specimen at the head, prothorax, and/or mesothorax, until approximately 10-30mg of tissue was obtained. Internal tissues were scraped out of these sectioned fragments, and antennae, ommatidia, the proboscis, and heavy chitinous structures (e.g., mandibles, tergites, proleg basal sclerites) were excluded. Ethanol-

moistened dissected tissue was air dried for several minutes before it was transferred to a 1.5mL eppendorf tube containing 178.5uL of SV RNA Lysis Buffer (4M guanidine thiocyanate, 0.01M tris, 0.97% beta-mercaptoethanol; pH7.5). Remaining unused specimen tissue was immediately returned to its original vial and refilled with fresh 100% ethanol for long-term storage at -80C.

Dissected tissue in Lysis Buffer was homogenized inside the eppendorf tube by pulverization using a pre-sterilized polypropylene pestle. Pestle pulverization on ice for 2-5 minutes yielded a brown/red homogenate with some insoluble chitin fragments. After all samples in a batch had been homogenized, 350uL of blue SV RNA Dilution Buffer (containing 25-50% guanidinium thiocyanate) was added to each tube and all tubes were inverted to mix contents gently without mechanically shearing genomic DNA macromolecules. Tubes were incubated in a 70C water bath for exactly 3 minutes, then centrifuged at 14,000g for 10 minutes in a fixed-angle rotor centrifuge (Eppendorf AG, model no. 5417C) to precipitate cellular debris. Supernatant containing dissolved whole nucleic acids was transferred to fresh 1.5mL eppendorf tubes, taking care not to disturb the debris pellet; when in doubt, supernatant was left behind rather than introducing contamination from a loose pellet. Exactly 200uL of 95% ethanol (containing 5% DEPC water) was added to this supernatant and all tubes were inverted to mix. The entire volume of fluid was loaded onto a labeled Promega Spin Column Assembly, and assemblies were spun at 14,000g for 60 seconds. Eluate was discarded, and 600uL of SV RNA Wash Solution (60mM potassium acetate, 10mM tris-hydrochloride, 60% ethanol; pH7.5) was loaded onto the dry spin column. After another centrifugation at 14,000g for 60 seconds, eluate was discarded and another 250uL of SV RNA Wash Solution was

added to the dry spin column. The manufacturer's protocol was modified at this stage in order to preserve genomic DNA bound to the spin column, as digestion of gDNA "contaminants" with DNase I was not performed. Centrifugation at 14,000g for 2 minutes completely flushed the SV RNA Wash Solution, and the dry spin column was transferred to the permanent 1.5mL eppendorf collection tube. Exactly 100uL of Promega Nuclease-Free Water (catalog no. P119E) was added to the dry spin column and allowed to incubate at room temperature for approximately five minutes. A final centrifugation at 14,000g for 60 seconds resulted in approximately 100uL of eluate containing dissolved whole nucleic acids (RNA & DNA), which was stored immediately at -80C until further processing.

To minimize the amount of sample manipulation and to conserve extract volume, aliquots were not loaded onto an agarose gel to assess the yield of RNA and DNA. Instead, extract quality was assessed indirectly through the success of downstream RT-PCR reactions.

## B.1 Reverse-Transcription Amplification

Products from the genomic whole nucleic acid extraction protocols described above served as template for selective amplification of target mRNA using the reverse transcription polymerase chain reaction (RT-PCR; Edwards *et al.* 1995; Larrick & Siebert 1995; Siebert 1999). This process entailed two stages: (i) hybridization of a single oligonucleotide primer to the 3' end of single-stranded mRNA actively transcribed *in vivo*, with subsequent reverse transcription (RT) *in vitro* of those mRNA transcripts into a double-stranded species; and (ii) polymerase-mediated synthesis of the strand

complementary to the cDNA, followed by annealing of two primers permitting selective amplification of target regions (PCR). For the purposes of this study, the key advantage of RT-PCR relative to direct PCR on genomic whole nucleic acid templates was the amplification of only coding regions. Because post-transcriptionally modified mRNA containing only spliced exons acts as template for cDNA synthesis and subsequent amplification, all amplicons generated in this study were free of intronic sequence and were readily translated to amino acids.

Oligonucleotide primers used in this study had been designed previously by members of the Regier Lab for use in amplifying both EF and DDC in taxa across Arthropoda (Regier & Shultz 1997; Cho *et al.* 1995; Fang *et al.* 1997, 2000; Friedlander *et al.* 1992, 1998, 2000; Mitchell 1998; Mitchell *et al.* 1997, 2000; Regier *et al.* 2000, 2002). Historically, amplification of EF had been trivial in these taxa and the primers and amplification strategies developed in the Regier Lab were correspondingly relatively standardized. In contrast, DDC amplification was technically much more problematic, and almost every primer developed for this gene had been redesigned multiple times, sometimes on a taxon-specific basis. A comprehensive review of all documented EF and DDC primers generated in the Regier Lab was undertaken to compile all known viable primer sites in the design of amplification strategies for each of these two genes.

Table 3 presents primer pairs used to amplify regions of EF in two studies from the Regier Lab: an investigation of the utility of this gene in resolving relationships across Arthropoda (Regier & Shultz 1997) and their original study employing EF to explore systematic relationships within Heliiothinae [Lepidoptera: Noctuoidea: Noctuidae] (Cho *et al.* 1995). Strategies developed in the arthropod work are currently

standard practice in the Regier Lab, and the four fragments labeled “p”, “A”, “E” and “C” were amplified in this study (Table 3). Figure 4 depicts the relative orientation of these primers along the mRNA molecule of the reference sequence from *Bombyx mori* [Bombycoidea: Bombycidae] (GenBank accession no. D13338; Kamiie *et al.* 1993). A single primer, m41.21rc, was used to generate cDNA the length of the desired EF fragment during the RT phase, with the terminal primer pair 30f/m41.21rc used for subsequent PCR amplification of that cDNA. Internal primer pairs were then used to generate smaller amplicons via nested PCR on the purified cDNA template.

Table 4 presents primer pairs used to amplify regions of DDC in four studies, as well as unpublished oligonucleotides currently used in the Regier Lab to amplify this gene. These primers are sorted by site along the DDC mRNA molecule, and different versions of a given primer are grouped together. Since the complete coding sequence of DDC for a sphingid, *Manduca sexta* (Bombycoidea: Sphingidae), had been published (GenBank accession no. U03909; Hiruma *et al.* 1995; Figure 5) and was used as the reference sequence for alignment of this gene, the most stringent (i.e., longest and least degenerate) primers were assayed first for utility in RT-PCR amplification of DDC from Sphingidae. In an ideal scenario, a single primer (7.5sR) was used to generate cDNA the entire length of DDC during the RT phase, and the terminal primer pair 1.0F/7.5sR was used to PCR amplify that cDNA. However, this primer did not yield adequate product for all taxa and in these cases a smaller cDNA fragment was generated by use of 4dnR or 4sR (two variants of a primer site upstream of 7.5sR) during the RT phase. Early attempts were made to evaluate the relative performance of alternative primer variants listed in Table 4 for both RT (especially [7.5R vs. 7.5sR]) and PCR (especially [1.0F vs.

1.1vF vs. 1.2F], [1.7F vs. 1.7dF vs. 1.7sF], [1.9dF vs. 1.9sF] and [3.2dF vs. 3.2sF]) phases by assessing amplification efficiency in ethidium-bromide stained agarose gels (data not shown). Primers eventually selected for use in this study are indicated with an asterisk (\*\* for RT primers) in Table 4 and are presented in their corresponding pairings in Table 5a. In contrast, primers preferred by the Regier Lab for amplification from non-sphingid taxa (Regier, pers. comm.) are labeled with a † (‡ for RT primers) in Table 4 and are presented in their corresponding pairings in Table 5b.

Reagent components and relative concentrations for RT reaction mixtures are presented in Table 6a. An individual RT reaction consisted of a 10uL volume, mixed in the order presented in the table. To help control for intersample variability in reaction success, the RT reagents were mixed as a “cocktail” consisting of the same ratio of components multiplied by a factor of (n+1), where n=the number of samples in a batch. This cocktail was then aliquotted into individual 0.2mL thin-walled reaction tubes prior to addition of genomic nucleic acid extract template to each. Magnesium Chloride ( $MgCl_2$ ; 25mM stock solution) and GeneAmp PCR Buffer II (10X stock solution; catalog no. N8080010) were obtained from Applied Biosystems. Reverse Transcriptase (50 units/uL stock; catalog no. N8080018) with accompanying RNase Inhibitor (20 units/uL; catalog no. N8080119) was also obtained from Applied Biosystems, and both reagents were stored at  $-20C$  until immediately before addition as the final components in the RT cocktail. A single oligonucleotide was included (stock 20uM) to hybridize with the 3' end of targeted mRNA. Water was obtained from Regier Lab stock and was DEPC-treated, deionized and autoclaved.

After aliquotting 9.9uL of RT cocktail into each reaction tube, individual nucleic acid extracts were retrieved from -80C storage and quick-thawed in a room-temperature water bath for less than 60 seconds. Exactly 0.1uL of raw extract was added to corresponding reaction tubes and the tubes were centrifuge-pulsed to gather contents into the bottom. Reaction tubes were loaded onto a precooled (4C) 48-well block of a DNA Engine thermal cycler (model no. PTC-200; MJ Research, Inc.) and incubated at 42C for 35 minutes, followed by 99C for 5 minutes. During this RT cycling, cocktails for PCR reactions were prepared so that time between RT and PCR reactions was minimized.

Reagent components and relative concentrations for the PCR reaction mixtures are presented in Table 6b. An individual PCR reaction consisted of a 50uL volume, 40uL of which was fresh "cocktail" added to the 10uL RT reaction immediately after RT thermal cycling was complete. Magnesium Chloride, PCR Buffer II and water were as above. AmpliTaq thermostable DNA polymerase was obtained from Applied Biosystems (5 units/uL stock; catalog no. N8080156), and was kept cold at -20C until addition to the cocktail as the last component. This AmpliTaq solution contained 0.07uM of TaqStart neutralizing monoclonal antibody (7uM stock; BD Biosciences Clontech, catalog no. 639251) to enable hot-start PCR by inhibiting AmpliTaq activity below 70C. In addition, two oligonucleotide primers (20uM stock each) bookending the fragment of interest were included to bind to the 3' ends of opposite strands in the cDNA synthesized during the RT reaction. No additional dNTP were added to the PCR cocktail.

Immediately upon completion of the RT cycle, samples were transferred to an ice bath and 40uL of PCR cocktail was added to each. Tubes were briefly shaken to mix, centrifuge-pulsed to gather contents in the bottom, and reincubated on a room-

temperature MJ DNA Engine block. Touchdown thermal cycling was employed in the PCR amplification of *in vitro* synthesized cDNA (Table 6c), in order to minimize amplification of competitively superior nontarget smaller amplicons (Don *et al.* 1991). For the first 25X cycles, annealing temperature was iteratively decreased by 0.4C per cycle, while extension time was iteratively increased by 2 seconds per cycle. After these 25X touchdown cycles, traditional PCR at a static annealing temperature was conducted for an additional 13X cycles, increasing the extension time by 3 seconds each cycle. A final extension at 72C for 10 minutes completed the thermal cycling, followed by indefinite incubation at 4C.

Amplification conditions for fragments of EF and DDC were very similar, but in consultation with Regier Lab personnel some modifications were introduced to accommodate the more troublesome DDC amplifications. All components of the RT phase were identical between genes, except that stringency was reduced for DDC by increasing the concentration of reverse primer from 2uM to 3uM. In the PCR phase, changes to the DDC protocol were more extensive: MgCl<sub>2</sub> concentration was increased from 2.5mM to 3.0mM; forward primer concentration was doubled from 0.5uM to 1.0uM; and reverse primer was increased by 50%, from 0.6uM to 0.9uM. These relaxations permitted more consistent RT-PCR amplification of DDC fragments from the same extracts as had been assayed for EF under more stringent conditions. In fact, because the extracts were never assayed via electrophoresis, presence/absence of EF amplicons through the above procedure served as a *de facto* check on the quality of the extraction procedure for a given sample.



Upon completion of the PCR phase, samples were transferred to ice and exactly 10uL of 60% glycerol loading dye (w/w in 1X TAE) containing trace bromophenol blue was added to each sample. After brief vortexing, 10uL of this sample was loaded onto a 1.4% agarose analytical gel (w/v in 1X TAE; Fisher DNA Grade High Melting Electrophoresis Grade, catalog no. BP164-500). This amounted to destructively sampling 15% of RT-PCR product at a final glycerol concentration of 10%(v/v). Samples were electrophoresed at approximately 120V for approximately 90 minutes, until the bromophenol dye band had traveled to approximately 2.5cm from the gel edge. Transillumination under UV light revealed whether viable RT-PCR product had been produced, and intensity of bands relative to known bands in a comigrating DNA ladder permitted rough quantification of product size and concentration.

## B.2 Gel Purification of RT-PCR Products

RT-PCR products, which themselves served as template for downstream nested PCR (see below), were gel purified to insure that the desired fragments and only the desired fragments were retained. Once analytical gel electrophoresis confirmed successful RT-PCR amplification, the remaining 50uL of product containing glycerol loading dye was loaded onto a large well of a 1.1% agarose purification gel (w/v in 1X TAE; Continental Lab Products AgarGel Low Melt Medium Fragment Agarose, catalog no. 5413.100). Samples were electrophoresed in fresh 1X TAE, in a cleaned gel apparatus covered with an opaque dark cloth to prevent UV damage from ambient light, at approximately 100V for approximately 2 hours. The entire gel was transferred on plastic wrap to a UV plate, and under brief UV illumination cubes containing the

fragment of interest were excised from the gel using an autoclaved steel spatula. Signature banding patterns for each sample in these purification gels were directly compared against the original RT-PCR analytical gel photos to verify that samples had not been crossed. These gel cubes were transferred to sterile 1.5mL eppendorf tubes and massed to quantify the amount of agarose containing the RT-PCR product of interest.

Double-stranded DNA within this excised gel slice was purified via the Promega Wizard PCR Preps DNA Purification System, exactly according to manufacturer suggested protocols (Promega Technical Bulletin No. 118). Instead of elution in TE, however, purified products were incubated at room temperature for approximately 5 minutes and eluted in 50uL of Promega Nuclease Free Water (part no. P119E). A 7.5uL aliquot of each purified eluate was transferred to a new eppendorf tube containing 2.5uL of 60% glycerol loading buffer (w/w in 1X ABI 10X PCR Buffer II and 2.5mM MgCl<sub>2</sub>) containing trace bromophenol blue. This loading buffer more closely mimicked background composition of all other amplification products run on agarose gels. All 10uL of the gel purification/loading buffer mixture was loaded onto a 1.4% agarose analytical gel; amounting to destructive sampling of 15% of gel-pure RT-PCR product at a final glycerol concentration of 15%(v/v). One or both of two DNA ladders was loaded into an adjacent well: (i) MBI Fermentas pUC Mix Marker 8 (catalog no. SM0302); or (ii) BioRad Precision Molecular Mass Standard (catalog no. 170-8207). Incorporation of these ladders permitted finer simultaneous assessment of both gel-purified fragment size and product concentration. The total mass of DNA in each band of the ladders was calculated under various loading volumes and used to calibrate an estimation of purified product concentration by comparing bands of similar intensity. In lieu of other

quantitation methods (e.g., spectrophotometry, fluorimetry), this approach permitted calculation of product concentration and tailoring of template amount contributed to downstream applications (i.e., nested PCR and direct sequencing).

### B.3 Nested PCR Amplification

In ideal cases, a primer binding to the 3' end of targeted mRNA (e.g., m41.21rc for EF; 7.5sR for DDC) yielded viable RT-PCR amplification through much of the gene's coding region. Because this product was large (>1kb) and often extremely weak in electrophoretic assays, a round of nested PCR amplification based on those purified RT-PCR templates was pursued to generate fragments of manageable lengths (approximately 500bp) at sufficiently high-copy number for direct DNA sequencing. Nested PCR provided a powerful technique to amplify desired subsequence from even extremely weak RT-PCR amplicons, because those products had been gel purified and were guaranteed to contain the sequence of interest if the RT-PCR had been at all effective.

Nested PCR was most often used to amplify subsequence from within larger RT-PCR products, using pairs of primers oriented approximately 500bp apart on the molecule (for EF, see Table 3 & Figure 4; for DDC, see Table 4 & Figure 5). Reagent compositions for nested PCR reactions are presented in Table 6d; contrary to conditions for RT-PCR, reagent compositions were identical between EF and DDC fragments. Ideally, nested PCR reactions received 1.0uL of template (2% of the final RT-PCR gel purification elution), but this amount was varied per sample to between 0.5-5.0uL for especially strong or weak RT-PCR templates, respectively. Thermal cycling parameters for nested PCR were very similar between the two genes, except that the annealing

temperature for EF was elevated 10C higher than for DDC; this higher annealing temperature created much more stringent binding conditions between the EF cDNA and nested primers, but with little reduction in yield.

A related reamplification strategy was used for smaller amplicons for which recovery of tangible nested PCR product had been difficult. All primers in this study incorporated 18bp M13 tails for compatibility with sequencing chemistry (see bottom of Tables 3 &4), so the termini of all nested PCR products were effectively end-labeled with M13. In cases where insufficient nested product was obtained from RT-PCR template for sequencing, gel purified nested PCR products were subjected to the same nested PCR conditions with M13 primers. Reactions of this type generated high copy numbers of entire nested fragments, and only failed when nested PCR had itself failed.

#### B.4 Gel Purification of Nested PCR Products

Subsequence amplification via nested PCR with internal primers or terminal M13 primers usually yielded amplification in high copy number. These products were gel purified using exactly the same protocol as detailed above for RT-PCR products. After electrophoretic concentration estimation, these products were submitted for direct DNA sequencing.

#### C. Automated Sequencing

Electrophoretic assay of purified PCR products against the mass ladders described above resulted in concentration estimates for every fragment, ranging from 0.67-

10.67ng/uL. DNA sequencing along both strands was performed on an Applied Biosystems DNA Sequencer (model 3100) at the UMBI CBR core sequencing facility. This facility recommended submission of 15uL of purified template at concentrations between 5-20ng/uL. Despite these guidelines, template concentrations estimated electrophoretically as low as 0.67ng/uL by the above method returned viable sequencing reactions. Templates spanning the range of concentrations were submitted to the core facility in trial reactions, and a correlation was drawn between template concentration and sequencing signal intensity for each of the four bases (data not shown). This permitted prediction of sequencing success on the basis of electrophoretic intensity, and confirmed that viable sequence could be obtained from 15uL of any template yielding a band comparable in intensity with even the lightest ladder bands.

#### D. Sequence Editing

Despite efficient base-calling algorithms in the ABI 3100 analysis software, each chromatogram was inspected visually to confirm proper translation of electrophoretic data into a nucleotide text string. Oddities during sequencing reactions or electrophoresis caused disturbances in the chromatograms which were remedied on a case-by-case basis. All raw ABI chromatogram files were imported into Sequencher (version 4.1.2; Gene Codes Corporation 2000) for alignment. Conflicting signal in a particular chromatogram (e.g., overlapping peaks) was assigned the appropriate binary IUPAC ambiguity code, and tertiary and quaternary ambiguities were assigned 'N'. Both forward and reverse strands of a given PCR product were edited independently in this way. Forward and reverse-complemented reverse sequences of a given fragment were then aligned at high

match percentage thresholds to generate a consensus "double stranded" sequence. Ambiguities were resolved where possible and ambiguity codes were preserved if the base could not be resolved. Any gaps inserted by Sequencher's alignment algorithms during comparison of forward and reverse strands were resolved by direct inspection of the opposing chromatograms, and were usually attributed to poor quality in one chromatogram (e.g., at the end of a sequence) which was readily resolved by the other. Sequencing single fragments in both directions provided a layer of redundancy which improved confidence in the deduced consensus sequences.

Gene contigs were assembled by aligning both forward and reverse strands of all fragments for a sample at high match threshold, anchoring both strands of a single fragment at regions of overlap with neighboring fragments. Any gaps inserted by Sequencher's alignment algorithms during contig assembly were resolved by direct inspection of overlapping chromatograms. Oligonucleotide primer motifs were tagged in each alignment, and primer sequence was deleted from all internal fragments to create a seamless consensus sequence. Terminal primer sites (30f and m41.21rc for EF; 1.0F and 7.5sR for DDC) were retained in the consensus only to provide bookend sequences for the bounds of mRNA investigated in this study. These primer sequences were truncated prior to phylogenetic analyses.

For EF, the same four fragments (p, A', E, C; Table 3 & Figure 4) were obtained from all 54 ingroup samples and contig assembly resulted in a consensus sequence of 1,274bp, including terminal primers. A single exception applied to *Neococytius cluentius* (UMD accession WJK-03-1949), for which viable purified RT-PCR and nested PCR

products were assayed electrophoretically, but for which every forward and reverse sequence was illegible due to uniformly and prohibitively high background noise.

For DDC, three fragments (X, Y, Z; Table 4 & Figure 5) were obtained from each of 42 ingroup samples and contig assembly resulted in a consensus sequence of 1,373bp, including terminal primers. Interestingly, *Neococytius cluentius* was among these “well-behaved” samples, indicating the intractable sequencing for EF in this sample was particular to that gene. For the remaining 12 samples, a fourth fragment (W; Table 4 & Figure 5) was sequenced to compensate for difficulty obtaining strong amplification in the middle of the DDC fragment. This strategy provided effective sequence through the entire range of a homologous DDC fragment for all 54 ingroup samples.

#### E. Sequence Alignment

The double stranded consensus sequence from each gene was aligned independently against an orthologous reference sequence obtained from *Bombyx mori* for EF (Figure 4; GenBank accession no. D13338; Kamiie *et al.* 1993) and from *Manduca sexta* for DDC (Figure 5; GenBank accession no. U03909; Hiruma *et al.* 1995).

Instances in which novel sphingid sequences contained gaps with respect to the reference sequences were interpreted as artifacts of the chromatogram editing process. In these cases, corresponding positions in the original chromatograms were re-examined under the null hypothesis that the reference sequence contained the “correct” number of bases. In all cases, reconciliation was possible on the basis of the chromatogram traces, so no artifactual N’s were introduced to achieve proper sequence length. While this procedure introduced an obvious bias toward the reference sequences, it was expected that in coding

regions of genes of such critical biochemical importance, insertions and deletions altering the entire reading frame for protein translation would be extremely improbable.

After each sample's consensus sequence had been aligned against the reference sequence, a final whole-family alignment across 54 samples was performed in Sequencher. This was a trivial procedure, as each sequence had already been standardized against the reference sequences and no gaps were inserted by Sequencher.

#### *Sequence Data Collection in silico*

In addition to original nucleotide sequence data collected for 54 novel sphingid samples described above, the National Center for Biotechnology Information (NCBI) Nucleotides Database (GenBank) was mined for all representatives of Lepidoptera for which orthologous nucleotide sequence fragments of both nuclear genes had been submitted. The set of results from each of several search strings submitted to the NCBI Entrez search engine on 06 April 2004 was downloaded and the union of all unique sequence accessions was compiled into a master list. This list was filtered for a nonredundant set of taxa containing both novel sphingid ingroup sequences and a range of potential outgroup candidates for phylogenetic analyses.

Kristensen (1999) established rigorous systematic hypotheses of monophyly for lepidopteran families based on analyses of morphological synapomorphies. While the monophyly of Sphingidae has been regarded as firmly established on morphological grounds (Lemaire & Minet 1999; Minet 1991, 1994), this study sought an independent test of that premise using molecular data and modern systematic methods. The aim of mining GenBank for lepidopteran sequences was to permit multiple phylogenetic



analyses conducted under different taxon samples. Of special interest was the robustness of a node depicting monophyletic Sphingidae in trees for which outgroups consisted of either all other available lepidopteran sequences or all non-sphingid bombycoid sequences. The classical concept of a monotypic superfamily Sphingoidea has been collapsed as a single family within superfamily Bombycoidea (Brock 1971; Common 1990; Minet 1986), suggesting the latter may be profitably explored for the sister lineages to Sphingidae.

Sampling variation in the GenBank Nucleotide Database prevented compilation of both EF and DDC sequences for a single broad set of lepidopteran taxa. Instead, sequences were compiled separately for each gene across as broad a taxon set as possible, according to the following choice hierarchy:

- (i) at least one EF and one DDC accession per subfamily across all Lepidoptera was selected;
- (ii) less than five accessions per gene per family were retained to avoid gross taxonomic overweighting and tree imbalance (especially for Noctuoidea: Noctuidae and Papilionoidea: Nymphalidae);
- (iii) one accession per tribe throughout Bombycoidea (Lemaire & Minet 1999; Minet 1991, 1994) was selected, these taxa being regarded as most closely related to the ingroup and representing the best outgroup candidates;
- (iv) any sequence from Sphingidae which did not exactly overlap species sequenced *de novo* in this study was retained;

- (v) accessions for which both EF and DDC sequences were derived from a single species or specimen were preferred, if possible, to accessions requiring sampling from multiple specimens or taxa;
- (vi) accessions containing nominate genera of any given tribe, subfamily or family were preferred over other taxa;
- (vii) GenBank accessions containing the longest unambiguous sequences were preferred to improve data richness;
- (viii) if all above criteria did not yield a single unambiguous choice, a GenBank accession was selected randomly from the remaining candidates.

Even after implementing criterion (vii) above, almost all retrieved GenBank sequences were shorter than the novel sequences generated in this study. All sequences were aligned against the *Bombyx* (EF) or *Manduca* (DDC) reference sequences under the same null hypothesis that the reference sequences contained the “correct” number of bases. Gaps suggested by Sequencher were inspected across all lepidopteran sequences and persistent indel events were marked with missing data characters (i.e., ‘N’ ambiguity codes). In addition, terminal ends of sequences were filled with missing characters until every sequence agreed in length with the reference sequences.

An exception to the above alignment strategy applied to the two DDC sequences from Nepticuloidea [Glossata: Heteroneura] (GenBank contained no EF sequences for this superfamily). These sequences aligned against each other and all other Lepidoptera only at very low match thresholds (approximately 60%). Alignment via the MATCHER utility of the European Molecular Biology Open Software Suite (EMBOSS) package through the Nationale Genomforschungsnetz (NGFN) web interface revealed numerous

gaps relative to all other Lepidoptera, as well as a multi-base indel event near DDC primer 3.3sF (Figure 5). While an intriguing finding, exploration of these alignment difficulties was beyond the scope of the current study, so both representatives of Nepticuloidea were excluded from phylogenetic analyses owing to their difficult homology assessment. Because sequence sampling from GenBank was an inherently biased process with broad fluctuations in breadth and depth of taxon sampling across the Lepidoptera, it was assumed that omission of these sequences would have miniscule effects on the inclusion of Lepidoptera outgroup sequences to address questions of Sphingidae monophyly.

#### *Data Matrix Construction*

Global alignments of consensus sequences were conducted for each gene, separately for ingroup Sphingidae (Table 8; 67 samples for EF, 65 samples for DDC) and outgroup Lepidoptera (Table 9; 51 samples for EF, 40 samples for DDC). These alignments were then combined into a single master Sequencher file for each gene, followed by a final round of inspection of suggested gaps. Upon completion, all sequences were exported into a NEXUS file (Maddison *et al.* 1997) in preparation for phylogenetic analyses in PAUP\* (version 4.0b10; Swofford 2003). In this way, three separate nucleotide matrices were assembled for phylogenetic analyses: (a) all EF data; (b) all DDC data; (c) combined EF&DDC data.

After these nucleotide matrices had been assembled, corresponding amino acid sequences were derived by conceptual translation in three forward frames using the standard genetic code. Terminal oligonucleotide sequences were trimmed from each

sequence and the resulting internal fragment was imported to the TRANSEQ utility of EMBOSS. Amino acid output was reimported into a parallel set of NEXUS files in PAUP\*.

### *Character Information Content*

Nucleotide data matrices were examined to determine the number of positions at which character states were invariant (constant) across taxa, were unique to only a single taxon (autapomorphic), or were suggestive of a taxon bipartition (parsimony informative). Values were tabulated for each gene individually and for the combined EF&DDC data matrix, and across four partitions by codon position (ntall, nt1, nt2, nt3). This operation was repeated separately for each of four taxon sets: (i) All Lepidoptera; (ii) All Bombycoidea; (iii) Ingroup Sphingidae only; and (iv) Sphingidae with two outgroups (Bombycidae and Saturniini; see below). This scheme was intended to provide a first approximation of agreement in the nature of character state change across different partitions and taxa sets.

Mean empirical nucleotide base frequencies, adjusted for missing data, were calculated in PAUP\* as a first step to investigate the potential that base composition bias could be responsible for perceived phylogenetic signal. Empirical base frequencies were calculated for every sequence to provide a direct assessment of base compositional bias. Counts of ambiguous (IUPAC codes) and missing ('N') data were also provided to gauge the variance in data content for each sequence, and was especially important for heterogeneous accessions obtained from GenBank.

### *Parsimony-Based Preliminary Analyses*

Analyses based on the criterion of Maximum Parsimony (MP) were conducted across all four taxon sets on each of four data partitions: (a) ntall for EF; (b) ntall for DDC; (c) ntall for combined EF&DDC, (d) nt1&nt2 for combined EF&DDC. EF and DDC data were analyzed separately to tease apart potentially subtle differences in phylogenetic signal contributed by each gene, as well as to shed light on the robustness of phylogenetic signal to minor changes in taxon sampling due to nonoverlapping taxa sampled from GenBank. For the combined data set, ntall versus nt1&nt2 partitions were analyzed separately to compare the effects of excluding hypervariable third codon positions, as advocated by Regier 2001. All MP analyses were conducted on unordered and equally weighted characters, with constant characters excluded (i.e., autapomorphies and parsimony informative sites both included).

#### A. PTP Test of Information Content

The Permutation Tail Probability (PTP) test as implemented in PAUP\* was conducted as a crude indicator of the presence of phylogenetic signal in each nucleotide data matrix (Faith 1991; Faith & Cranston 1991). Distribution of character states across taxa might be correlated due to either shared ancestry (i.e., phylogenesis has imposed order on the data) or stochasticity (i.e., order in the data is an artifact of random nucleotide substitutions independent of evolutionary history). The PTP test was designed to quantify the degree to which order in character state distributions has an evolutionary versus a stochastic basis.

Pseudoreplicate data matrices were constructed by randomly permuting character states within each nucleotide position across taxa. Using tree length as an indicator of phylogenetic structure in the fit of data to a topology, the length of the MP topology obtained under the empirical data was used as the test statistic. A null distribution was constructed by calculating the lengths of the MP trees recovered under each pseudoreplicate data set. Under the null hypothesis that character states in the empirical data matrix were correlated due to chance alone, it was expected that each randomly permuted data set would result in a tree length comparable to the original test statistic. The P value gave the proportion of all pseudoreplicated data matrices yielding an MP tree comparable in length. Small P values indicate that the structure in the empirical data is not a product of chance, refuting the null hypothesis of no phylogenetic structure. All PTP tests were calculated with at least 1,000 pseudoreplicates. In addition, the number of steps separating the original MP tree from the next most parsimonious tree derived from all permuted data was recorded as an indication of severity in parsimony penalty imposed by randomizing character states.

## B. Parsimony-Based Searches

Phylogenetic analysis under the criterion of Maximum Parsimony (MP) was conducted across four taxon sets for the four data partitions listed above. There are  $\Pi(2i-5)$  unrooted bifurcating trees depicting patterns of relatedness among  $T$  terminal taxa, where  $i$  varies from 3 to  $T$  (Swofford *et al.* 1996). For the number of taxa investigated in each data set in this study ( $n_{\text{tax}} \geq 64$ ), the number of possible topologies in treespace rendered exhaustive MP search algorithms untenable. Therefore, heuristic search

algorithms implemented in PAUP\* were employed to sample tree and data space for optimal topologies.

Starting topologies were computed heuristically via at least 1,000 furthest stepwise addition sequence replicates, holding 10 trees at each step (hold=5 for more computationally intensive analyses). These starting topologies were permuted via the tree-bisection-reconnection (TBR) branch-swapping algorithm, employing steepest descent. All minimal trees were saved (“MulTrees” option) and zero branch lengths were collapsed.

After each analysis, the set of saved trees was filtered for shortest length. In addition to tree length, number of MP trees recovered from each search and the number of islands encountered during the search was also recorded, as an indication of heterogeneity in data space (Maddison 1991; Page 1993). Existence of multiple islands of closely related topologies indicates a danger of becoming trapped on a local optimum when non-exhaustive search algorithms (e.g., heuristic search methods) are used. Small numbers of encountered islands were taken as a suggestion of uniformity in tree space pointing to a single globally optimal topology.

To explore the effects of tree space heterogeneity on the ability for heuristic algorithms to identify globally optimal topologies, four trials of identical heuristic searches (including the same random number seed) were launched differing only in number of replicates: 10, 100, 1,000 and 10,000. Results from each trial were filtered for topologies of shortest length, and the set of recovered trees compared across trials. Trials completing higher numbers of stepwise addition sequence replicates were expected to more adequately explore a highly stratified and complex tree space and be more likely to

locate globally optimal topologies. For simpler, more homogeneous tree space, trials completing only 10 or 100 heuristic search replicates were expected to perform equally well at locating globally optimal topologies.

### C. Nonparametric Bootstrap Analysis

Trees recovered from MP heuristic searches depicted taxon relatedness in a series of nested taxon bipartitions. Branch lengths of individual taxon bipartitions indicated the number of inferred synapomorphies supporting those relationships, but offered little information about the robustness of or confidence in the branches. Under the assumption that an empirical data matrix represents a finite sample from an underlying character space for the taxa being compared, nonparametric bootstrapping is a method developed to approximate the underlying distribution from which those data arose by random resampling with replacement from the empirical data (Felsenstein 1985; Harshman 1994; Sanderson 1989, 1995; Wilkinson 1996). Pseudoreplicate data matrices were constructed via bootstrap resampling and each was subjected to the same MP heuristic analysis (except only 10 or 100 random addition sequence replicates were conducted per bootstrap pseudoreplicate). Optimal trees derived from heuristic searches on each bootstrap pseudoreplicate were compared across pseudoreplicates and each taxon bipartition was assigned a percentage indicating the proportion of instances it was recovered. The resulting percentages do not represent strict confidence statements about the accuracy of the taxon bipartition, but indicate the relative degree of internal consistency in the data suggesting that bipartition.



At least 1,000 pseudoreplicates were constructed for each bootstrap analysis in an effort to increase the *precision* of the bootstrap proportion, although this had no impact the *accuracy* of the taxon bipartition (Felsenstein & Kishino 1993; Hillis & Bull 1993). Bootstrap values below 50% were interpreted as insufficient evidence for the inference method to make an assertion about a particular taxon bipartition given the data at hand. The number of internal branches in the topology receiving bootstrap support >50% was tabulated and compared to the total possible number of internal branches in a fully dichotomous rooted tree:  $(T-2)$ , where T is the number of terminal taxa.

#### D. Incongruence Length Difference (ILD) Test

Phylogenetic inferences were drawn from two separate sources of information (EF vs. DDC), whose patterns of evolutionary change may or may not be congruent. The Incongruence Length Difference (ILD; also called the partition homogeneity) test was implemented in PAUP\* in an attempt to explore interactions between phylogenetic information in these data (Darlu & Lecointre 2002; Downton & Austin 2002; Mason-Gamer & Kellogg 1996; Swofford 2003). The null hypothesis for the ILD test ignored the functional distinction between EF and DDC as separate genes, and assumed that both independent data partitions were derived from the same underlying pool of homogeneous characters. Assuming that EF and DDC data represent effectively random subpartitions of a single underlying distribution lead to the expectation that information regarding taxon relationships contained in both partitions would be fundamentally the same.

Assuming perfect agreement between partitions, the MP score of a tree derived from a combination of both genes into a single data set ( $L_{EF+DDC}$ ) should be

approximately equal to the sum of lengths of the two trees derived from each partition separately ( $L_{EF} + L_{DDC}$ ). In contrast, the MP score of a tree derived from a combination of two perfectly disagreeing genes should result in a tree much longer than the sum of their individual trees, since conflicting (homoplasious) signal will interact negatively to inflate overall length.

The original EF and DDC components of the combined EF & DDC data matrix were randomly repartitioned by scrambling characters between genes to produce two pseudoreplicate data matrices of the same size as the originals. The MP tree of each pseudoreplicate was determined heuristically and the tree length scores were added together ( $L_1 + L_2$ ). If this sum was no greater than the sum of MP trees derived from EF and DDC individually ( $L_{EF} + L_{DDC}$ ), then characters within each original partition were interpreted as not providing significantly conflicting signal. The proportion of pseudoreplicates for which random repartitions resulted in MP trees with a better sum of scores than the original was reported as the test's P value. Large P values suggest the ILD test failed to reject the null of partition homogeneity, suggesting the data partitions contain compatible phylogenetic signal. Small P values refute the null hypothesis, suggesting the two partitions are in significant conflict. Outcomes of the ILD test have been used as evidence to argue both for and against combining data into a single analysis (Bull *et al.* 1993; Chippindale & Wiens 1994; DeQueiroz *et al.* 1995; Huelsenbeck *et al.* 1996a; Mitchell *et al.* 2000; Olmstead & Sweere 1994; Weller *et al.* 1994; Wiens 1998).

ILD tests were conducted with at least 1,000 pseudoreplicates, each of which was subjected to 10 random stepwise addition replicates, holding 5 trees at each step and TBR branch swapping. The number of steps difference between the original ( $L_{EF} + L_{DDC}$ ) and

the best pseudoreplicate ( $L_1 + L_2$ ) was tabulated; negative values of this difference were taken as support for the null hypothesis of data homogeneity (i.e., some random repartitions generated *better* sums of MP tree scores), although the P value may not reflect this.

### *Evaluating Alternative Parsimony Topologies*

In addition to generating a strongly supported phylogenetic hypothesis of relationships within the Sphingidae ingroup, the preliminary parsimony analyses described above were also intended to pare down the broad range of potential outgroup taxa from the candidate lepidopteran sequences obtained from GenBank. Once a pair of appropriate outgroup sequences had been selected by the MP criterion, topologies consisting of the Sphingidae ingroup and 2 outgroups were then used to establish initial conditions for iterative parameter and topology estimation in Maximum Likelihood (ML) analyses. Employing a ML model-based approach to phylogenetic analysis was expected to more accurately reflect the underlying processes of nucleotide substitution producing the empirical patterns observed in the data matrices (Felsenstein 1973, 1981a; Fukami & Tateno 1989; Gaut & Lewis 1995; Goldman 1990; Huelsenbeck & Crandall 1997; Kishino & Hasegawa 1989; Rogers 1997; Saitou 1988, 1990). In addition, it has been demonstrated that ML-based phylogenetic analyses are both more appropriate than MP under a wide range of conditions and are also more robust than MP with respect to minor violations in their underlying models of sequence evolution (Felsenstein 1978, 1981b; Felsenstein & Sober 1986; Huelsenbeck 1995; Sober 1984; Tateno *et al.* 1993; Yang 1994, 1996).

MP analyses on each data matrix generated a set of equally optimal topologies, so selection of a single tree from among these alternatives was imperative to reduce the potential number of starting points from which computationally intensive ML searches would be launched. Each topology was assessed for congruence across data partitions according to the criterion of maximum parsimony, and the most universally compatible trees were selected as input starting topologies for maximum likelihood analyses. Using MP trees as input strongly biased the initial conditions of ML searches in the direction of MP tree space, but significantly reduced the range of taxon bipartition parameter space required for evaluation relative to ML searches starting from completely random topologies.

Character state changes inferred from MP for each partition were mapped onto all candidate topologies from each data set, and a set of parsimony metrics was calculated to describe the performance of that topology as an explanation of the character state distributions for that partition. Raw tree length provided a relative measure of the penalty imposed by forcing character state distributions from one data set onto another partition's MP tree. This penalty was also expressed as a percentage increase in tree length (%diff) relative to the shortest length score obtained for that partition across all candidate MP trees; thus, the topology yielding the lowest %diff averaged across all partitions was selected as the best MP tree for that data set. Similarly, consistency (ci) and retention (ri) indices (Farris 1989a,b; Kluge & Farris 1969) were calculated for each instance of character state mapping and the topology with highest mean ci and ri values across all partitions was selected as the best MP tree for that data set.

Those MP trees with lowest tree length & %diff, and high ci & ri averaged across all data partitions were selected as MP-optimal topologies upon which subsequent ML parameter estimation was conducted. Thus, three “best-guess” topologies were selected from results of MP analyses on EF, DDC and combined EF&DDC data for a 66-taxon set (iv) consisting of all 64 sphingid taxa shared between these genes as well as two selected bombycoid outgroup taxa.

#### *Selection of a Model of Nucleotide Substitution*

The key “disadvantage” of conducting phylogenetic analyses under the optimality criterion of maximum likelihood is decreased feasibility in computing tree scores when using parameter rich models of nucleotide substitution. At the expense of evaluating a broad range of more simplistic ML models which may have yielded equally viable topologies, the present study employed the most generalized and parameter rich model of nucleotide substitution for ML analysis of these data.

The general time reversible (GTR) model is founded upon a separate instantaneous relative rate parameter (expressed as number of substitutions per site per unit branch length) for each of the twelve possible transformations among the four character states (A,C,G,T) in these nuclear protein coding genes (Lanave *et al.* 1984; Rodriguez *et al.* 1990; Swofford *et al.* 1996). This model is time-reversible, however, so forward and backward transformations are assumed to occur at equal rates, reducing the total number of relative rate parameters to six. In addition, the GTR model assumes that the four nucleotide bases occur in the data matrix at separate equilibrium frequencies (i.e.,  $\pi_A \neq \pi_C \neq \pi_G \neq \pi_T$ ), and these frequencies remain unchanged over time. Probability of

change from nucleotide  $i$  to  $j$  is assumed to be a Markov process independent of  $i$ , and proportional to the equilibrium frequency of  $j$ .

This nucleotide substitution model makes no allowance for differences in patterns of character state change between independent sites along the molecule. For example, different portions of a gene may be subject to variable functional constraints, effectively altering the degree to which nucleotides in those positions are likely to change. An extreme example of such among-site rate heterogeneity is the special case where some sites are constrained to *never* vary. Ignoring the phenomenon that some sites may never change while others do effectively biases inference of character state change to underestimate branch lengths (Churchill *et al.* 1992; Hasegawa *et al.* 1985; Reeves 1992; Sidow *et al.* 1992). Therefore, a parameter was included in the GTR model to account for these invariant sites (I) by assigning a probability that any particular character is free to vary. Furthermore, characters which are assumed to vary may do so at different rates, and a parameter can be added to the model to account for these differences in the rates of character change. A discrete approximation to the gamma distribution provides a range of potential nucleotide change probabilities, conveniently defined by a single shape parameter (G). Addition of single shape parameter to the GTR model explicitly accounted for differences in the propensity for nucleotide change between presumably independent nucleotide positions along the molecule (Buckley *et al.* 2001; Felsenstein 1981a; Gaut & Lewis 1995; Gu *et al.* 1995; Hasegawa *et al.* 1991; Sorhannus & van Bell 1999; Steel 1993; Sullivan *et al.* 1999; Sullivan & Swofford 1997; Yang 1993, 1994).

Character states which are identical between taxa at a given site may have never changed in the time since those taxa diverged, or they may have changed repeatedly and

randomly converged on the same state. Incorporation of I and G parameters was intended to explicitly account for both scenarios generating observed nucleotide distributions. This highlighted a key distinction between MP and ML analyses, because likelihood-based inference engines were permitted to make use of all characters, even those which parsimony deems uninformative (i.e., constant and autapomorphic characters).

### *Likelihood-Based Analyses*

MP topologies selected from analyses of each data partition were used as independent starting hypotheses for estimation of GTR+I+G nucleotide substitution model parameters. The likelihood score for a fixed starting topology was calculated after parameters for a GTR model (5 relative rate parameters of a 6-class substitution matrix and 3 of the 4 equilibrium nucleotide frequencies), with assumed proportion of invariable sites (I) and among-site rate heterogeneity (G; i.e., the alpha shape parameter in a discrete approximation with 8 categories to the gamma distribution), were all estimated from the data. Initial branch lengths on the starting topology were estimated via the Rogers-Swofford approximation method suite of default options in PAUP\*. These initial ML parameter estimates were then fixed in the GTR+I+G model to permit calculation of likelihood scores during a heuristic search ('MulPars' option in effect, steepest descent off, collapsing branches with length less than or equal to  $10^{-8}$ ) employing TBR branch swapping based on the starting MP topology. This heuristic search resulted in a first-pass ML topology, the taxon bipartitions of which were then fixed in order to re-estimate model parameters. Re-estimated parameters were again fixed in a revised GTR+I+G

model used to calculate likelihood scores on trees generated during 10 random stepwise addition heuristic searches with SPR branch-swapping, holding 1 tree per step, with all other settings as above. The topology from these heuristic searches with highest likelihood (i.e., the second-pass ML topology) was then fixed for parameter re-estimation. This iterative parameter estimation / ML search cycle was continued through four passes, and GTR+I+G model parameter values were checked for convergence after each pass.

The ML search scheme detailed above was conducted nine times: for each of the three data sets (i.e., EF, DDC, combined EF&DDC) based on each of the three independently derived MP starting trees. Parameter values and ML topologies for a given data set derived after four iterations on each of the starting trees were then compared across starting trees to check for global convergence. The set of all unique ML topology/parameter values from a given data set was selected as the optimal ML estimate of relationships within Sphingidae.

Finally, in an attempt to select a single globally optimal topology of relatedness among sphingid genera, ML scores for every candidate MP and ML topology were calculated for each data set after convergent GTR+I+G model parameters particular to those data had been fixed. These likelihood score calculations were performed as above, except that the discrete approximation to the gamma distribution consisted of 16 categories.



## RESULTS

### *Taxon Sampling*

As of fall 2003, the UMD Lepidoptera Collections Database (FileMaker Pro, version 6.0) contained 3,608 records containing collections information for more than 5,600 specimens with known determination data across 34 superfamilies, 89 families, 945 genera and 1,477 species of Lepidoptera. A total of 350 specimens across all three subfamilies of Sphingidae was collected expressly for this research and accessioned into the UMD Lepidoptera Collections (Table 10). Of these freshly obtained specimens, 55 were processed for genomic nucleic acid extraction, RT-PCR amplification of EF and DDC fragments and sequencing (Table 8). One specimen [UMD accession number IJK-02-0107: *Compsulyx cochereaui* (Smerinthinae: Ambulycini)] failed to produce any viable RT-PCR products after multiple attempts at extraction from freshly dissected tissue. Failure to obtain amplification products from this specimen collected in New Caledonia in April 2001 was attributed to poor preservation conditions, as the detailed history for this specimen could not be verified. One other specimen [accession number WJK-03-1949: *Neococytius chuentius* (Sphinginae: Sphingini)] yielded exceptionally strong RT-PCR products for both EF and DDC, but failed to produce clean sequence for any EF fragment despite multiple rounds of gel purification; DDC sequence for this specimen was excellent.

In addition to the 54 ingroup Sphingidae sequenced *de novo* in this study, EF sequence for another 14 species and DDC sequence for another 11 species was obtained from the NCBI GenBank nucleotides database. Almost all of these (13 species for EF, 10 species for DDC) were obtained from the Regier 2001 pilot study. The *Manduca sexta*

(Sphinginae: Sphingini) DDC sequence from Regier 2001 was replaced by GenBank accession number U03909 (Hiruma *et al.* 1995) and used as the reference sequence against which all others were aligned. Sequences for the remaining three species in Regier 2001 [*Hyles lineata* (Macroglossinae: Macroglossini: Choerocampina), *Paonias myops* (Smerinthinae: Ambulycini), *Lapara coniferarum* (Sphinginae: Sphingini)] were generated *de novo* in this work because original specimens from which the sequences had been derived could not be verified. Finally, EF sequence for *Proserpinus clarkiae* (Macroglossinae: Macroglossini: Macroglossina) was obtained from Caterino *et al.* (2001), but comparable DDC sequence from the same species could not be obtained.

Sphingid genera sampled in this study are marked in Table 2, distributed across the complete genus-level classification scheme provided by Kitching & Cadiou (2000). Forty-eight (24%) of the 201 recognized genera in Sphingidae were sampled, distributed heterogeneously across the family. In Smerinthinae 11 (14%) of 78 genera were sampled overall: 8 genera (14%) inside the Smerinthini, 2 genera (20%) from Ambulycini and a single genus (*Hopliocnema*) from Sphingulini. Sampling was much more dense inside Sphinginae, where 13 (34%) of 38 genera were sampled overall: 10 genera (30%) inside the Sphingini and 3 genera (60%) from Acherontiini. For the most diverse subfamily, Macroglossinae, 24 (28%) of 85 genera were sampled overall: 12 genera (46%) from Dilophonotini, 5 genera (12%) from Macroglossina (Macroglossini), 6 genera (40%) from Choerocampina (Macroglossini) and a single genus (*Eumorpha*) from Philampelini.

Homologous sequences from outgroup taxa were obtained by mining the NCBI GenBank Nucleotides Database under the search parameters and selection criteria described above. Table 7 presents the number of hits and their distribution across

taxonomic levels within Lepidoptera for several similar search strings targeting both EF and DDC sequence. For EF, a single search string (“*elongat\** AND *lepidopt\*[organism]*”) yielded the most inclusive set of 419 hits distributed across only 9 (20%) of the 46 lepidopteran superfamilies. Many other permutations of “<gene> AND <taxon>” search strings were attempted, but none retrieved any hits not already captured by this top query (data not shown). Two examples are given to demonstrate that subtle changes in text strings submitted to the Entrez Browser can have substantial impacts on the extent of database space explored by the search engine. For example, the slightly more specific query “*elong\* fact\* AND lepidopt\*[organism]*” returned all but two hits from the original 419. In contrast, a relatively simple search string “EF AND *lepidopt\*[organism]*” returned only 259 (62%) of the hits from the original 419. Similar results were observed for DDC, for which a single search string (“*dopa AND lepidopt\*[organism]*”) returned the most inclusive set of 238 hits distributed across 13 (28%) of the 46 lepidopteran superfamilies. No other DDC search strings were found to return hits not already subsumed by this original query.

Accessions in GenBank for EF and DDC in Lepidoptera were extremely sparsely distributed across the 46 superfamilies. Table 11 illustrates this distribution by assigning the number of hits for EF and DDC to each family within a classification of Lepidoptera compiled from multiple sources (Arnett 2000; Borror 1989; Kristensen 1999; Scoble 1992; Wagner 2001). While there were 76% more accessions for EF than DDC (419 vs. 238), those hits were concentrated in 4 fewer superfamilies. In fact, 89% of all EF lepidopteran accessions were concentrated in only three superfamilies: 165 (39%) of the 419 hits inside the Papilionoidea (106 in the Nymphalidae alone), 113 (27%) in the

Bombycoidea, and 94 (22%) in the Noctuoidea. DDC accessions were distributed across a wider range of superfamilies, especially the ancestral lineages (see top of Table 11), but 75% of all DDC lepidopteran accessions were concentrated in only two superfamilies: 103 (43%) of the 238 hits inside the Noctuoidea (91 in the Noctuidae alone), and 76 (32%) in the Bombycoidea.

Obtaining a broad cross-section of Lepidoptera for which EF and DDC sequences had both been sampled was challenging, a consequence of the patchy distribution of GenBank accessions for these markers across superfamilies. This finding was especially important for outgroup analyses in this study, and was illustrated by the paucity of superfamilies (5 of 46) and families (12 of 125) for which hits were registered in both EF and DDC columns in Table 11. Thus, while EF and DDC sequences could be obtained for 20% and 28% of superfamilies and 16% and 21% of families, respectively, the intersection of taxa for which both genes were available was only 11% of superfamilies and 10% of families. This resulted in a significant decrease in taxonomic diversity available for the combined EF&DDC data set (see below), but was not unexpected given the wide sampling variance in nucleotide databases such as GenBank.

Working from the master lists used to compile Tables 7 and 11, selection criteria were applied as described above and resulted in collection of 51 potential outgroups for EF and 40 potential outgroups for DDC (Table 9). Not surprisingly, 31% (16) of EF outgroups came from the Noctuoidea, 24% (12) from the Papilionoidea and 22% (11) from the Bombycoidea. Similarly, 40% (16) of DDC outgroups came from the Noctuoidea and 20% (8) from the Bombycoidea. Also as expected, DDC outgroups covered a wider range superfamilies (11) than EF (9), but both sequences could be

compiled for members of only 5 superfamilies. Also of interest was that 40 (57%) of the 70 taxa for which at least one sequence was collected had been submitted to GenBank by the Regier Lab (see all taxa for which specimen collection information was available in Table 9).

### *Data Matrix Construction*

GenBank accession numbers for all publicly available EF and DDC sequences used in this study are presented in Tables 8 and 9. Alignment of both nuclear protein coding genes against the reference sequences and against all other taxa was unambiguous: no insertions, deletions or hypervariable regions were detected in either gene. Introns were neither detected nor expected, as all of the novel sequences and many of the publicly available sequences were synthesized via reverse-transcription from native mRNA. Variation in sequence length for GenBank accessions necessitated filling the ends of almost every GenBank sequence with missing data characters ('N') to standardize length across the matrix. For EF, all 14 ingroup and 50 of 51 outgroup sequences collected from GenBank were shorter than the novel sequences generated in this study (1,223bp and 1,136bp average lengths were 4% and 11% shorter for ingroups and outgroups, respectively). For DDC, 10 of 11 ingroup and 39 of 40 outgroup GenBank sequences were shorter than the final matrix length (805bp and 697bp average lengths were 41% and 49% shorter for ingroups and outgroups, respectively).

Final assembly resulted in three nucleotide data matrices for phylogenetic analyses with the following dimensions in [number of nucleotides] x [number of taxa]: (a) EF: [1,274nt] x [118 taxa]; (b) DDC: [1,373nt] x [105 taxa]; and (c) combined

EF&DDC: [2,647nt] x [91 taxa]. The combined nucleotide matrix represented the strict intersection of taxa for which both EF and DDC sequences had been gathered, and was obtained by deleting 27 and 14 taxa from the EF and DDC data matrices, respectively. This represented a significant loss in taxon density (23% reduction for EF; 13% reduction for DDC), but provided the largest taxon set for which both markers could be concatenated into a single analysis.

Prior to amino acid translation and all nucleotide-based phylogenetic analyses, terminal primer sequences were stricken from the matrices (for EF, see Table 3 & Figure 4; for DDC, see Table 4 & Figure 5). This reduced the total number of nucleotides to 1,228 for EF, 1,329 for DDC and 2,557 for the combined data set. Conceptual translation to amino acids produced three protein data matrices: (a) EF: [409aa] x [118 taxa]; (b) DDC: [443aa] x [105 taxa]; and (c) combined EF&DDC: [852aa] x [91 taxa].

### *Information Content*

Table 12 itemizes the number (and percentage) of nucleotide positions at which character states were constant, autapomorphic or parsimony informative, as well as the mean nucleotide base frequencies for all three matrices: (a) EF; (b) DDC; and (c) combined EF&DDC. These calculations were repeated for four taxon sets within each matrix: (i) all Lepidoptera; (ii) all Bombycoidea (i.e., entire Sphingidae ingroup with all bombycoid outgroups); (iii) all Sphingidae (i.e., ingroup only); and (iv) Sphingidae&2OG (i.e., 66-taxon final set). This last taxon set included all 64 Sphingidae ingroup taxa for which EF and DDC sequence had both been collected, plus two bombycoid outgroups: “Bombycidae” (*Bombyx mori*) and “Saturniini” (*Saturnia*

*albofasciata* for EF and *S. naessigi* for DDC). Values in Table 12 are raw uncorrected measures of variation, which ignore the possibility that multiple substitutions may have occurred at a given site. Thus, these values underestimate actual amount of evolutionary change which may have occurred in these markers across the taxa sampled.

Echoing the findings of Regier 2001, the vast majority of nucleotide variability (autapomorphic *and* parsimony informative changes) in both genes was harbored in the third codon position. In the EF matrix, 85.9%, 78.0%, 60.2% and 64.6% of nt3 were parsimony informative in taxon sets (i), (ii), (iii) and (iv), respectively. This accounted for 90% (352nt3/393allnt), 92% (320nt3/349allnt), 92% (247nt3/269allnt) and 92% (265nt3/287allnt) of all parsimony informative character state change in these taxon sets for EF. This trend in high indices of nt3 change was robust across taxon sets, lending support to Regier *et al.*'s (2001) assertion that nt3 in these data were saturated and might be productively ignored for the purposes of phylogenetic analysis. Also echoing a pattern uncovered in the Regier 2001 pilot data, nt1 were approximately three times as parsimony informative as nt2 for EF. Looking across taxon sets within EF, the percentage of parsimony informative character state changes increased and the percentage of invariant character states decreased with increasing taxonomic depth, as more ancestral Lepidoptera were added. Autapomorphic character state change was consistently approximately 5% across taxon sets, although nt3 autapomorphies increased from 5.4% to 15.1% from sets (i) to (iii).

The proportion of parsimony informative characters in DDC was approximately 50% greater than within EF, but a similar trend in excessive nt3 variation was observed. For example, 95.5%, 95.3%, 94.4% and 95.0% of nt3 were parsimony informative in

taxon sets (i), (ii), (iii) and (iv), respectively. This accounted for 67% (423nt3/649allnt), 73% (422nt3/576allnt), 77% (418nt3/544allnt) and 76% (421nt3/557allnt) of all parsimony informative character state change in these taxon sets for DDC. Similarly, there were approximately twice as many parsimony informative nt1 characters as there were for nt2 in DDC. As with EF, the percentage of parsimony informative character state changes in DDC increased and the percentage of invariant character states decreased with increasing taxonomic depth. Autapomorphic character state change in DDC was consistently approximately 5% across taxon sets, similar to EF, however nt3 autapomorphies were more consistent (~1%).

Similar trends were observed in the combined data set constructed by concatenating EF and DDC sequences for the set of taxa possessing both sequences. One difference between this study and the pilot work of Regier 2001 was that the novel DDC fragment (1,329bp) sequenced across Sphingidae in this study was 620bp longer than the fragment in Regier 2001 and 101bp longer than the EF fragment. Thus, while the contribution of characters from each gene to the combined matrix was balanced (48% EF vs. 52% DDC), the systemic increased nucleotide variation in DDC relative to EF may have shifted the relative contribution of information from each gene in this study from that in Regier 2001.

Relative nucleotide variability between the genes was also reflected in proportions of variable amino acids observed after conceptual translation. For EF, 12.2%, 6.1%, 3.9% and 4.4% of amino acids were variable (parsimony informative or autapomorphic) in taxon sets (i), (ii), (iii) and (iv), respectively. These values were much higher for DDC: 42.2%, 31.1%, 25.7% and 28.9% variable amino acids in taxon sets (i), (ii), (iii)



and (iv), respectively. Alignment of all variable amino acid characters for EF are presented in Table 13 and for DDC in Table 14. Contrasting patterns of variation between EF and DDC could be observed by searching for common “amino acid haplotypes” in the alignments in Tables 13 and 14. Across all 105 taxa in DDC matrix (i), 104 amino acid sequences were unique, and 64 of 65 Sphingidae sequences were unique (both *Cautethia* sequences were identical). In contrast, only 81 of 118 EF amino acid sequences were unique across all Lepidoptera, and 34 of 67 EF amino acid sequences were unique across Sphingidae. Even after reducing matrix sizes by culling duplicate EF haplotypes, MP phylogenetic analyses via random addition heuristic searches on amino acid data across these taxa proved too computationally intensive and could not be completed.

Mean empirical base frequencies averaged across all codon positions and adjusted for missing data hovered between 20-30% for each nucleotide across genes and taxon sets (Table 12). For EF ntall, frequencies ranged from: A(.2478-.2526), C(.2852-.2935), G(.2510-.2548), T(.2039-.2112) across taxon sets. For DDC ntall, frequencies ranged from: A(.2499-.2555), C(.2245-.2309), G(.2521-.2579), T(.2613-.2681) across taxon sets. This apparent base composition homogeneity was deconstructed by inspecting EF and DDC codon positions individually. For example, taxon set Sphingidae (iii) within the EF matrix harbored extreme fluctuations in base composition: nt1 ranged from 14.94% for T vs. 37.61% for G; nt2 ranged from 15.84% for G vs. 32.52% for A; nt3 ranged from 12.79% for A vs. 44.61% for C. Such base composition heterogeneity was less pronounced in every nucleotide position for the Sphingidae taxon set (iii) in DDC: nt1

ranged from 20.58% for T vs. 34.56% for G; nt2 ranged from 19.73% for G vs. 29.66% for T; nt3 ranged from 21.34% for G vs. 30.18% for T.

Tables 15 (Ingroup) and 16 (Outgroups) present raw empirical base frequencies calculated for all codon positions across every sequence collected in this study, including percentage of missing or ambiguous character states. As expected from above, because these values combined data from codon positions, base composition homogeneity appeared to hold as a working assumption within these genes. For example, base composition across all ingroup taxa for EF ranged from: A(.1971-.2598), C(.2288-.3143), G(.2174-.2622), T(.1669-.2182), with standard deviations of .0078(A), .0125(C), .0054(G), .0090(T) [see Table 15]. For DDC, comparable values ranged from: A(.1272-.2694), C(.1106-.2476), G(.1362-.2603), T(.1362-.2852), with standard deviations of .0418(A), .0342(C), .0362(G), .0427(T) [see Table 15]. In contrast, base composition across all outgroup taxa for EF extended over much broader ranges: A(.0969-.2826), C(.1189-.3021), G(.0993-.2630), T(.0717-.2492), with standard deviations of .0334(A), .0364(C), .0277(G), .0321(T) [see Table 16]. For DDC, comparable values ranged from: A(.0429-.2536), C(.0504-.2340), G(.0451-.2521), T(.0459-.2724), with standard deviations of .0403(A), .0336(C), .0374(G), .0438(T) [see Table 16]. While these contrasts in minimum and maximum mean base frequencies revealed no systematic trend toward base composition bias in these genes, frequencies in Tables 12, 15 & 16 highlighted two phenomena evident in these data: (a) inspection of all codon positions as a single data set suggested only minor fluctuations around base composition homogeneity; (b) inspection of individual codon positions revealed more extreme base composition heterogeneity; and (c) quantitative differences in patterns of base

composition between EF and DDC across all taxon sets may be expected to affect patterns of observed nucleotide change in these genes.

Pairwise distance matrices calculated in PAUP\* based on raw uncorrected pairwise divergence estimates from amino acids and separately for the three nucleotide codon positions across EF and DDC are presented in Tables 17 and 18, respectively.

### *Parsimony-Based Preliminary Analyses*

Results of preliminary parsimony analyses contributing to conclusions below are compiled in Table 19. Results from only a single series of analyses from each matrix are presented in Figures 6, 7 & 8.

#### A. Testing for Information Content

All four PTP tests conducted separately on EF and DDC returned extremely low P values, implying significant rejection of the null hypothesis that observed character state distributions in taxon sets of both matrices were the result of purely stochastic processes. For the EF matrix, 1,125 PTP replicates were completed on the ingroup Sphingidae taxon set (iii), returning a P value of 0.000889 and the next most parsimonious tree 871 steps longer than the MP tree (length=1,525 steps). In addition, 1,316 PTP replicates were completed on the Sphingidae&2OG taxon set (iv), returning a P value of 0.00076 and the next MP tree 898 steps longer than the MP tree (length=1,736 steps). For the DDC matrix, 3,821 PTP replicates were completed on the Sphingidae taxon set (iii), returning a P value of 0.000262 and the next MP tree 3,305 steps longer than the MP tree

(length=4,117 steps). In addition, 3,984 PTP replicates were completed on the Sphingidae&2OG taxon set (iv), returning a P value of 0.000251 and the next MP tree 3,336 steps longer than the MP tree (length=4,566 steps). These results were taken as evidence of phylogenetic structure within both EF and DDC, as interpreted via the maximum parsimony criterion. PTP tests were not conducted on the combined EF&DDC data matrix.

## B. Parsimony Searches

The first MP analyses conducted were heuristic searches on the EF, DDC and combined EF&DDC data matrices for the All Lepidoptera (i) taxon set. These trial exploratory searches were intended primarily to pare down the list of potential outgroups in Table 9, not to generate viable hypotheses of relationships among all Lepidoptera. Two hundred random sequence addition replicates on EF data yielded 680 equally parsimonious trees confined to a single island, the strict consensus of which displayed excellent resolution in non-sphingid groups but produced many polytomies in the Sphingidae. Similarly, one thousand replicates on DDC data yielded 240 equally parsimonious trees across two islands, the strict consensus of which displayed excellent resolution throughout both ingroup and outgroups. One thousand replicates on combined EF&DDC data yielded 2 equally parsimonious trees on a single island, differing only in the relative placement of subfamilies within Noctuidae. Finally, codon position nt3 was excluded from matrix EF&DDC and taxa with identical EF amino acid haplotypes were deleted; 421 replicates on the resulting matrix returned 243 MP trees distributed across

43 islands, the strict consensus of which suggested an almost completely unresolved but monophyletic Sphingidae.

Many taxon bipartitions from the initial MP analyses agreed with well-established morphological taxonomic hypotheses, while others were nonsensical. For example, the EF MP tree suggested a polyphyletic Bombycoidea, and placed a papilionoid (Lycaenidae: Polyommatainae) next to the base of the tree with Micropterigoidea. The DDC MP tree also suggested a polyphyletic Bombycoidea and paired Papilionoidea with Gracillarioidea. Bootstrap support across all trees was very poor. Importantly, all three of these searches generated trees containing a monophyletic Sphingidae with modest bootstrap support, and all analyses suggested at least some combination of macrolepidopteran taxa as sister lineages to Sphingidae.

In an attempt to reduce heuristic search computation time, all non-bombycoid taxa were pruned from the three matrices and the above analyses repeated. All analyses again yielded trees with a monophyletic Sphingidae supported by moderate bootstrap values, but they differed in their suggestion of the most basal sphingid lineages, those most closely recently derived from the bombycoid outgroups. As with the Lepidoptera taxon set, EF data across All Bombycoidea (ii) yielded the largest set of equally parsimonious trees (n=280) and the least resolution in strict consensus. In contrast, DDC returned a manageable number of MP trees (n=20) and the combined EF&DDC matrix returned a single optimal topology.

These preliminary analyses confirmed that the sphingid taxa sampled in this study probably comprised a monophyletic group and that some members of Macrolepidoptera, usually Bombycoidea, were the most closely related outgroup(s). For this reason, an

effort was made to further decrease computation time by minimizing the number of taxa required to be informative about sphingid ingroup. The list of potential outgroups was pruned down to two ('Bombycidae' and 'Saturniini' in Table 9) to provide a means of rooting a tree of the 64 Sphingidae for which DDC and EF sequences had both been obtained. This resulted in the 66-taxon set Sphingidae&2OG (iv), on which further MP analyses for the EF, DDC and EF&DDC matrices was based. These outgroups were selected because they had demonstrated a "near-sister" relationship with the sphingid ingroup in all analyses based on the Lepidoptera (i) and Bombycoidea (ii) taxon sets, and because these two sequences collected *in silico* had the least number of missing characters relative to the 1,228bp of EF and 1,329bp of DDC sequences collected *de novo*. The EF sequence for 'Bombycidae' was in fact complete and had served as the reference sequence during all EF alignments.

Parallel MP analyses of the original nonoverlapping EF and DDC matrices tested the effects of adding three (ProserpinusGB, PachysphinxGB, PaoniasGB) and one (Neococytius1949) ingroup taxa to the Sphingidae&2OG (iv) analyses, respectively (see Table 8). Results of these analyses were unremarkable in the sense that inclusion of a few additional taxa had very little impact on global topological arrangements (data not shown). Supplementary EF sequences in the Regier 2001 pilot study from the smerinthine genera *Pachysphinx* and *Paonias* paired with their newly sequenced congeners (Pachysphinx1528 and Paonias1540, respectively) with extremely strong bootstrap support in all EF trees. While genus monophyly was preserved, however, inclusion of these taxa did impact the basal intergenus relationships in a clade consisting of *Smerinthus*, *Paonias* and *Pachysphinx*. The EF sequence for the macroglossine genus

*Proserpinus* (Caterino *et al.* 2001) consistently formed a clade with *Sphecodina* in analyses of the EF matrix, confirming their close orientation in Kitching & Cadiou's (2000) classification (see Table 2). Similarly, the novel DDC sequence obtained for *Neococytius* consistently proved most closely related to *Cocytius*, confirming a grouping explicitly predicted by Kitching & Cadiou (see vertical bar joining these taxa in Table 2).

The occasionally large number of equally parsimonious trees distributed across many islands encountered by the trial heuristic searches suggested the possibility of significant heterogeneity in the data space for the Bombycoidea taxon set (iii). Under these conditions, the heuristic search strategy (even with many random addition sequence replicates followed by TBR) may have had difficulty locating globally optimal topologies. To explore this phenomenon, a series of four heuristic searches with identical starting conditions (including random seed) but differing in number of replicates was performed for each of the three matrices (Table 19). As the number of random addition sequence replicates was increased, the heuristic search algorithms investigated more rearrangements and continued to find more equally MP trees distributed across more and more islands. However, when a filter was applied to retain only those topologies with optimal score, the same set of MP trees across the same few islands was retained regardless of the number of replicates. This suggested that the heuristic search settings (starting from a random addition sequence, employing TBR, with MulPars active, holding 10 trees at each step and steepest descent on) in this study generated a high-performance algorithm capable of identifying optimal solutions, in many cases even with just 10 replicates.

### C. Nonparametric Bootstrap Analysis

Maximum parsimony nonparametric bootstrap analyses across all taxon sets and data matrices revealed significant variation in internal consistency for these data. Majority rule bootstrap consensus topologies consistently included moderate bootstrap proportions (i.e., greater than or equal to 50%) for a small percentage of internal nodes discussed below. EF&DDC analyzed without nt3 consistently resulted in the weakest bootstrap support measures, probably a result of the relatively low number of parsimony informative characters in this partition.

### D. ILD Test

A single test was performed to evaluate homogeneity of phylogenetic signals from EF vs. DDC across all nucleotides for just the ingroup Sphingidae taxon set (iii). The ILD test implemented in PAUP\* (1,164 replicates) revealed statistically significant heterogeneity in signal between these genes within Sphingidae ( $P=0.000859$ ), suggesting that the two genes were contributing conflicting phylogenetic signal. To test whether intergene conflict was a consequence of the extremely high variability and possible saturation in nt3, an attempt was made to repeat this test with only nt1&2. However, the progress of computations prevented accumulation of enough replicates to make a robust inference about statistically significant heterogeneity between the genes when nt3 was eliminated from the analysis.



### *Evaluating Alternative Parsimony Topologies*

Having settled on a standard taxon set (Sphingidae&2OG, ntax=66), all three matrices were analyzed according to the criterion of maximum parsimony with the aim of selecting a single optimal MP topology from each for use in seeding iterative model parameter estimation / heuristic searches under the criterion of maximum likelihood.

For the Sphingidae&2OG taxon set (iv), MP analyses on the EF matrix resulted in 161 equally parsimonious trees distributed across three islands. The strict consensus of these equally viable trees was a poorly resolved topology retaining just 43 (67%) of a possible 64 nodes in a rooted, fully bifurcating tree with 66 taxa. Because the iterative ML parameter estimation / heuristic search strategy required as input a fully resolved (bifurcating) starting topology, it was important to determine a way to select a single tree from among the 161 MP alternatives. A much less stringent consensus tree building algorithm, the 50% majority rule, was employed to generate a more well-resolved topology consisting of 61 (95%) nodes. This topology was imported as a constraint tree, and filtering the original set of 161 MP trees for compatibility with it resulted in retention of only 2 MP trees. The strict consensus of these two trees was selected for input into ML analyses, with the understanding that starting tree algorithms in PAUP\* would randomly resolves polytomies to produce a fully bifurcating topology. Both trees were also evaluated more rigorously according to the parsimony-based selection criteria described below.

MP analyses on the DDC matrix were much less difficult to interpret and resulted in only 10 equally parsimonious trees confined to a single island. The strict consensus of these equally viable trees was well-resolved, retaining 61 (95%) of a possible 64 nodes.

Polytomies were confined to two terminal groups: [Ceratomia1870, CeratomiaGB, Paratreia1939] and [Lapara1670, Sphinx1532, SphinxGB, Sphinx1938]. MP analyses on the combined EF&DDC matrix yielded only 3 equally parsimonious trees confined to a single island. The strict consensus of these trees was also well-resolved, retaining 62 (97%) of a possible 64 nodes, with all polytomies confined to a single clade, Dilophonotina: [Aellopos2399, AelloposGB, Nyceryx2378, Perigonia2191, Callionima0966, Erinnyis1542, Isognathus1646, Pachylia1644].

Table 20 itemizes the parsimony scores obtained by mapping each data matrix's character state distribution onto every candidate MP topology recovered by independent heuristic searches across the separate matrices. Parsimony penalty incurred by constraining one data set onto a suboptimal topology was assessed by increase in length (expressed as % of the original), CI and RI, and mean values of each measure averaged across all data matrices for a given topology were used to select the optimal candidate MP tree for each data matrix. For example, of the 161MP trees generated from analyses of the EF matrix for the Sphingidae&2OG taxon set, 2 MP trees (i, ii; length=1705, CI=0.300, RI=0.549) were retained after filtering for compatibility with the 50% majority rule consensus topology. When DDC data and combined EF&DDC data were mapped onto each of these topologies, topology (ii) had a lower mean % increase in parsimony score (%diff=3.31), while both topologies had identical mean CI (0.261) and mean RI (0.565) when averaged across all three data matrices. On this basis, tree (ii) was chosen as the optimal topology generated from the EF data (marked with a \* in Table 20 and shown in Figure 6). Neither topology could be distinguished on the basis of these criteria when the same cross-mapping exercise was performed after excluding nt3.

In similar fashion, topology (v) was chosen as the optimal candidate from among the 10 MP trees (i-x; length=4484, CI=0.249, RI=0.611) produced by the MP analyses of DDC data matrix (see \* in Table 20 and Figure 7). When EF data and combined EF&DDC data were mapped onto each of these topologies, topology (v) had the lowest mean % increase in parsimony score (%diff=1.83) and one of the four highest RI (0.571), while all ten topologies had identical mean CI (0.264) when averaged across all three data matrices. In addition to tree (v), trees (vi) and (ix) emerged as equally optimal choices when nt3 was excluded from cross-mapping exercises.

Finally, topology (i) was chosen as the optimal candidate from among the 3 MP trees (i,ii,iii; length=6280, CI=0.259, RI=0.588) produced by the combined EF&DDC data matrix (see \* in Table 20 and Figure 8). When EF data were mapped onto each of these topologies, topology (ii) was one step shorter than the original EF tree, while this same topology was one step longer than the DDC tree when DDC data were mapped. All three indices (%diff, CI, RI) were similarly unconvincing, so topology (i) was selected randomly. None of the three topologies could be distinguished by these criteria when nt3 was excluded from the cross-mapping.

#### *Qualification of Parsimony-Based Topologies*

The optimal topology selected from MP analyses of EF for the Sphingidae&2OG taxon set is presented in Figure 6. Two subfamilies (Sphinginae and Macroglossinae) were recovered as monophyletic, though neither had bootstrap support greater than 50%, nor were they supported by many synapomorphies (4 and 6, respectively). The phylogram illustrates how widely branch lengths varied both between and within clades,

raising concern over artifacts stemming from long branch attraction (Felsenstein 1978; Hendy & Penny 1989). For example, one of the shortest branches in the tree (7 synapomorphies) separated the ingroup from the sister outgroup lineages. Since the most basal sphingid (*Marumba*0118) and both bombycoid outgroups have accumulated at least ten times as many autapomorphies as the branch separating them, the position of *Marumba* as the most ancestral sphingid must be interpreted cautiously. In addition, only 32 (50%) of 64 internal nodes had bootstrap support greater than 50%, with 19 of those nodes consisting of sister terminal lineages. In other words, bootstrap support for internal nodes was extremely poor and this topology can be considered only suggestive of relationships among super-generic taxonomic groups within the Sphingidae. Despite this, EF seemed efficient at placing taxa in proper subfamilial orientation, rendering only Smerinthinae paraphyletic and inserting monophyletic Ambulycini between Sphinginae and Macroglossinae.

The optimal topology selected from MP analyses of DDC is presented in Figure 7. Two subfamilies (Sphinginae and Smerinthinae) were recovered as monophyletic, with excellent and modest bootstrap support, respectively. Both subfamilies were also supported by many synapomorphies (57 and 93, respectively), and all of the deep branches within the family were longer than the more derived lineages. Derived groups within the Sphinginae and Macroglossinae formed clusters of especially short branches, highlighting potential hotspots for accelerated evolution among those lineages (e.g., *Sphinx*, *Xylophanes*). As with EF, branch lengths varied widely across the tree, but generally became shorter from the root toward the tips. One glaring exception was the branch separating ingroup from outgroup (13 synapomorphies), again suggesting long

branch attraction may have resulted in an artifactual placement of the [*Hemaris*, *Cephonodes*] clade as the most basal sphingid lineages. As with EF, the branch leading to this most basal sphingid clade and both terminal branches of the bombycoid outgroups had accumulated at least ten times as many autapomorphies as the branch separating them, suggesting the interpretation of [*Hemaris*, *Cephonodes*] as the most ancestral sphingid may be incorrect. Bootstrap support for the DDC tree was more impressive than for EF, with 46 (72%) of 64 internal nodes receiving bootstrap support greater than 50%, and 17 of those nodes uniting sister terminal lineages. In an absolute sense, bootstrap support was again extremely poor and this topology can be considered only suggestive of relationships among super-generic taxonomic groups within the Sphingidae. However, like EF, DDC retained proper expected subfamilial orientations, rendering only Macroglossinae paraphyletic and inserting *Hopliocnema* between Sphinginae and other Smerinthinae.

Not unexpectedly, the optimal topology selected from MP analyses of the combined EF&DDC data set contained elements found in both the EF and DDC trees (Figure 8). The same two subfamilies (Sphinginae and Macroglossinae) were recovered as monophyletic as for EF, this time with excellent and modest bootstrap support, respectively. Both subfamilies were also supported by many synapomorphies (59 and 110, respectively), and like the DDC tree the deep branches within the family were generally longer than the more derived lineages (with the exception of some macroglossines). Derived groups within the Sphinginae and Macroglossinae (e.g., *Sphinx*, *Xylophanes*, respectively) again formed clusters of especially short branches, but many of these also received modest bootstrap support. Interpretation of the root suffered

from the same potential long branch attraction pitfall, as the branch separating ingroup from outgroup was supported by only 23 synapomorphies. Consistent with the EF data, *Marumba* reassumed the role of most basal sphingid, with the most basal sphingids from DDC analyses (*Cephonodes* and *Hemaris*) instead constituting a very long branch nested terminally within a monophyletic Macroglossinae. Bootstrap support for the combined tree was as poor as for EF, with only 31 (48%) of 64 internal nodes receiving bootstrap support greater than 50%, and 18 of those nodes uniting sister terminal lineages. This lack of internal consistency was surprising, given that heuristic searches settled on only very few MP trees, in stark contrast to heuristic searches on the EF data. Such weak bootstrap support suggests that resolution of deeper relationships among sphingid genera will continue to be only speculative when relying on phylogenetic analysis of these markers under the criterion of maximum parsimony.

Despite poor bootstrap support, a few themes emerged consistently across the suite of parsimony analyses described above. A monophyletic Sphinginae was recovered by all three analyses, with strong bootstrap support from DDC and the combined EF&DDC data. In addition, the sister group to Sphinginae in all analyses was *Hopliocnema*, the sole representative of the smerinthine tribe Sphingulini. This unexpected result was supported by very high bootstrap proportions in the DDC and combined trees. The sphingine tribe Acherontiini was also recovered with strong support, however the position of *Coelonia* was malleable across trees. Despite the paraphyly of Smerinthinae in the EF and combined trees, all three analyses returned an extremely strongly supported monophyletic smerinthine tribe Ambulycini. Similarly, Macroglossinae was rendered paraphyletic in EF and combined analyses, yet several of

its subgroups were consistently retained with high support. Section Choerocampina and its sister relationship with *Darapsa* was very highly supported in all analyses. Section Hemarina was also consistently recovered at high support values. Some form of section Dilophonotina was also consistently recovered in all analyses, although the positions of *Cautethia*, *Enyo*, *Spheredina* and *Unzela* were extremely unstable and occasionally rendered the tribe polyphyletic. In addition, the tribe Philampelini (represented by only three *Eumorpha* species) was consistently nested within the dilophonotine assemblage. Finally, the majority of congeneric samples did in fact form monophyletic groups. Exceptions occurred in the three hyperdiverse sphingid genera for which four species each were included in this study: (a) while the four included species of *Sphinx* (56 species worldwide) were consistently monophyletic, the single representative of *Lapara* (4 species worldwide) was always inserted among them; (b) the four included species of *Manduca* (88 species worldwide) were monophyletic in all trees except EF, but in every case the monotypic *Dolba* was always inserted among them; (c) the four included species of *Xylophanes* (96 species worldwide) were monophyletic in every MP tree, but for DDC and the combined analyses one of two sampled species of *Darapsa* (*Darapsa1778*) was inserted among them.

#### *Likelihood-Based Parameter Estimation*

The three MP topologies selected and described above (\* in Table 20) and depicted in Figures 6, 7 & 8 were used as starting topologies for estimating nucleotide substitution model parameters for the Sphingidae&2OG taxon set (ntax=66). Maximum likelihood scores of these initial trees were estimated under the GTR+I+G model, and

resulting parameter estimates were used to heuristically search for an ML tree via branch swapping on the initial MP tree. Iterative parameter re-estimation and ML heuristic searches resulted in convergence to equilibrium parameter values in most cases after only the second of four iterations. Table 21 presents the results from every iteration for likelihood estimation of every data matrix on every starting topology. Rapid convergence to equilibrium parameter values (see boldface lines in Table 21) was taken to indicate relative simplicity of the likelihood surface and high accuracy in parameter estimates. In the fourth and final iteration of each analysis, converged parameter values were fixed and more extensive heuristic searches with more replicates were launched to locate the globally ML tree.

Of special interest was not only the efficient parameter convergence within a given series of iterations of one data matrix on any given starting topology, but the global convergence of parameter values for a given data matrix across all three starting topologies. Table 21 demonstrates that for the EF and DDC data matrices, starting topology had an effect on the rapidity of parameter convergence but *not* on the final parameter values themselves. The EF data converged after only two iterations when the EF MP tree was used to seed the iterative searches; these same data converged after three iterations when the combined EF&DDC MP tree was the start topology, and after four iterations when the DDC MP tree was the start topology. In contrast, the DDC data converged to stable parameter values after only two iterations regardless of the starting topology. The combined EF&DDC data behaved slightly differently, converging to identical sets of parameter values after two iterations on the DDC starting topology and after three iterations on the EF starting topology. However, likelihood optimization of



the same data on the EF&DDC MP tree resulted in convergence after two iterations to a *different* set of parameters. While very similar, these values varied enough that the iterative ML searches on the EF&DDC data based on the EF&DDC MP starting topology produced a ML tree of slightly different topology and slightly higher likelihood than when EF or DDC starting topologies were used.

Equilibrium base frequencies estimated under the GTR+I+G model (Table 21) deviated slightly from base composition homogeneity (i.e.,  $\pi_A = \pi_C = \pi_G = \pi_T \approx 0.25$ ), reflecting the trend of empirical base frequencies in the three original data matrices (Tables 12, 15 & 16). For EF, globally convergent base frequency parameters suggested a slight excess in adenine and deficiency in guanine: 27.2%(A), 26.1%(C), 22.4%(G), 24.3%(T). Globally convergent base frequency parameters revealed a more symmetrical and greater AT bias in DDC than for EF: 27.4%(A), 21.9%(C), 21.6%(G), 29.1%(T). The greatest differences between gene base composition was in proportions of C (4.2% greater in EF) and T (4.8% greater in DDC), and not unexpectedly the convergent parameter values for the combined EF&DDC data set reflected this with intermediate values for these bases (Table 21).

Global relative rate parameter estimates of the 6-class GTR substitution model revealed a stark contrast in molecular evolution of these two genes. Relative rate parameters for EF were extremely varied across substitution classes, with an enormous excess in transitions (AG: 13.998, CT: 25.062) and transversion rates which varied fivefold between classes (AC: 2.262, AT: 5.386, CG: 2.310, GT: 1.0). In contrast, relative rate parameters for DDC were of both lower magnitude and greater homogeneity across classes. DDC revealed a more modest excess in transition substitutions (AG:

5.571, CT: 6.839) with more homogeneous transversion rates across classes (AC: 1.503, AT: 1.333, CG: 1.151, GT: 1.0). Given the widely differing pictures these values suggested about molecular evolution of EF and DDC, it was perhaps not unexpected that the convergent relative rate parameter values for the combined data set could not be predicted from the two genes independently (Table 21).

Two parameters of the nucleotide substitution model augmenting the 6-class GTR framework were the proportion of sites assumed to be invariant (I) during evolution and the one-parameter descriptor of the gamma distribution (G) describing among-site rate heterogeneity along each molecule. Values of I varied from 0.616 for EF and 0.510 for DDC to 0.574 for the combined data. These values were each lower than the empirical proportion of invariant sites calculated in Table 12, demonstrating the deviation from observation often encountered when likelihood parameters are optimized to an explicit model of nucleotide substitution. While this value suggested DDC is a slightly more variable and perhaps less evolutionarily constrained molecule than EF, the magnitude of invariant sites between them did not in itself suggest these genes are evolving under grossly different regimes. In contrast, there was a two-fold difference in alpha shape parameter of the gamma distribution between these genes ( $G=0.680$  for EF,  $G=1.400$  for DDC). A difference of this magnitude indicated gamma distributions with very different shapes against which the substitution model for each gene assumed independent sites were likely to vary, suggesting strongly that these two genes have accumulated variation under very different evolutionary scenarios. The value of the gamma shape parameter for the combined EF&DDC data ( $G=1.039-1.044$ ) was intermediate between these two extremes, suggesting that concatenation of data caused the model to effectively average

the patterns of two separate genes experiencing very different regimes of among-site rate heterogeneity.

### *Evaluating Topologies from Likelihood Analyses*

In addition to providing a means of efficient convergence to stable nucleotide substitution model parameter values, the ML iterative estimation / search routine discussed above was also very effective at identifying convergent topologies optimized under the criterion of maximum likelihood. Individual trees were saved after each iteration and the topologies compared for concordance after the analysis was complete. Identical topologies are indicated in Table 21 with shared symbols under the ‘Tree’ column. Similar to results of parameter estimation, ML topologies not only converged within iterations of a given analysis but converged globally across all analyses for a given data matrix. Optimizing the GTR+I+G substitution model for the EF data matrix on the starting topology derived from the MP EF analyses resulted in four identical trees across all iterations. This tree also matched those derived from the last two and last three iterations when the EF data was fit to the DDC and EF&DDC MP starting trees, respectively (Figure 9). Global convergence to a single ML topology was even more impressive for the DDC data set, for which every ML tree across every iteration was identical (Figure 10). For the combined data, EF and DDC MP starting topologies resulted in convergence to the same tree (‘c1’,  $-\ln L = 31221.47311$ ). However, when the EF&DDC MP tree was used as the starting topology, a slightly different topology was found to be optimal (‘c2’,  $-\ln L = 31221.29642$ ). These two topologies differed only in arrangements within the [*Paonias*, *Pachysphinx*, *Smerinthus*] clade, mirroring results of

MP analyses under nonoverlapping taxon sampling. Strictly speaking, topology 'c2' was selected as the optimal tree because it had higher likelihood (Figure 11).

Analyses based on the EF data matrix produced a ML tree which retained only a single subfamily (Macroglossinae) as monophyletic. Similar to MP analyses for this gene, super-generic groups within this subfamily were preserved, including Hemarina, Choerocampina and Dilophonotina with nested Philampelini. Smerinthinae was rendered paraphyletic because Ambulycini was suggested as the sister lineage to the macroglossines, with a monophyletic Smerinthini the sister lineage to that group. Members of the Sphinginae were the among the most basal lineages in the family, with the smerinthine *Hopliocnema* assuming the most basal position. In contrast to the MP analyses, the length of the branch separating outgroup from ingroup was the longest internode in the entire tree, with extremely long terminal branches for each outgroup taxon. After the *Hopliocnema* split, branch lengths throughout the remainder of the ingroup appeared to become longer toward more derived taxa and almost every terminal branch was longer than the internode from which it arose.

Analyses based on the DDC data matrix produced a ML tree much more appealing from a taxonomic point of view, as all three subfamilies were retained as monophyletic. Two exceptions included: (a) *Hopliocnema*, oriented as sister to Sphinginae, with the remaining smerinthines sister to that lineage; and (b) the sphingine *Coelonia* was embedded on a long branch inside Macroglossinae. The same super-generic groups within all subfamilies were also preserved, except that only a subset of Dilophonotina remained monophyletic. Branch lengths within and between subfamilies were heterogeneous, with no global trends like those in the EF ML tree. Sphinginae

branches were more often short, Macroglossinae branches were more often long, and Smerinthinae branches were intermediate. Unlike the EF ML tree, not every terminal branch was longer than the internode from which it arose. Similar to the EF ML tree, the length of the branch separating outgroup from ingroup was the longest internode in the entire tree, with extremely long terminal branches for each outgroup taxon. Because all three subfamilies were monophyletic, the DDC ML tree permitted the first assessment of genealogical relationships among subfamilies. Macroglossinae was the most diverse and most basal subfamily in the tree, with the sister lineages Sphinginae and Smerinthinae more derived.

Analyses of the combined EF&DDC data matrix produced a ML tree globally similar to the DDC ML tree, with some extensive differences in fine structure. All three subfamilies were again retained as monophyletic in the same orientation: [Macroglossinae,(Sphinginae, Smerinthinae)], with *Hopliocnema* and *Coelonia* the same two exceptions. A broader monophyletic Dilophonotina consistent with the EF ML tree was retained. Unlike either single-gene analysis, Smerinthinae was broken into two monophyletic sister tribes Ambulycini and Smerinthini. Branch lengths within and between subfamilies were heterogeneous: Sphinginae branches were often short, Macroglossinae branches were often long, and Smerinthinae branches were intermediate. Every terminal branch was longer than in the DDC tree, though not always longer than the internode from which it arose. Finally, consistent with both individual gene trees, the branch separating outgroup from ingroup and the terminal branches of both outgroup taxa were the longest in the entire tree.

### *Evaluating the Likelihood of All Candidate Topologies*

Table 22 presents the results of ML cross-calculations obtained after fixing both the model parameters optimized for each data set and each candidate topology recovered from MP and ML analyses. Four distinct versions of the GTR+I+G model of nucleotide sequence evolution were evaluated, corresponding to the globally convergent parameter values presented in Table 21d. For each unique GTR+I+G model, corresponding data were fit to every MP and ML candidate topology presented in Tables 20 & 21. Comparison of likelihood scores across topologies within a given data & model parameter set (i.e., down each column of Table 22) provided a probabilistic evaluation of the relative effectiveness of each topology at explaining the observed distribution of character states, in the context of the assumed underlying model of nucleotide sequence evolution.

Among the four alternative ML topologies presented in Table 21, likelihood scores under the EF GTR+I+G model were optimal for the EF ML topology and worst for the DDC ML topology (-lnL difference = 197.47847). The converse was true for the DDC GTR+I+G model (-lnL difference = 515.23907), underscoring the trend toward discordant phylogenetic information between the EF and DDC data sets. Interestingly, likelihood scores under both combined EF&DDC GTR+I+G models were slightly better for ML topology 'c2' than for 'c1' in Table 21 (mean -lnL difference = 0.16639), and in both cases were worst for the EF ML topology (-lnL difference = 361.24008).

Among the fifteen alternative MP topologies presented in Table 20, likelihood scores under the EF GTR+I+G model were optimal for the EF MP topology presented in Figure 6 and were worst for the DDC MP topologies (max -lnL difference = 161.07546).

For all other GTR+I+G models, likelihood scores were optimal for the second MP topology derived from combined EF&DDC data, and in every case were worst for the first EF MP topology (mean  $-\ln L$  difference = 425.04928).

When the fifteen MP topologies and four ML topologies were pooled into a single set of alternative hypotheses, the ML topologies had superior likelihood scores under all four sets of GTR+I+G model parameters. For the EF model, the EF ML topology was better than the MP tree with highest likelihood ( $-\ln L$  difference = 24.2507), but both EF MP topologies were better than the three other ML topologies. In contrast, under the DDC model, the MP tree with highest likelihood was worse than three of the four ML topologies (mean  $-\ln L$  difference = 25.581). The same held true when MP and ML trees were compared under both combined EF&DDC models.

## DISCUSSION

Building on pilot work of Regier *et al.* (2001), the present study offered some important contributions in the next phase toward more fully resolving the phylogeny of the Bombycoidea and using those phylogenetic hypotheses to interpret life history evolution in this diverse group of Lepidoptera. Confirming earlier findings in studies employing EF and DDC in phylogenetic resolution of macrolepidopteran groups (Cho *et al.* 1995; Fang *et al.* 1997, 2000; Friedlander *et al.* 1992, 1998, 2000; Mitchell 1998; Mitchell *et al.* 1997, 2000; Regier *et al.* 2000, 2002), the present work demonstrated that EF and DDC, both separately and in combination, harbored significant phylogenetic information for the resolution of relationships among genera of Sphingidae. However, both genes differed in signatures of variation and in the phylogenetic hypotheses drawn

from them, providing distinct glimpses into the molecular evolutionary history of Sphingidae.

The vast majority of nucleotide variation in both genes was concentrated in the third codon position, and of the remaining variation nt1 was thrice and twice as variable as nt2 in EF and DDC, respectively. Nucleotides in DDC were approximately 50% more variable than in EF, an observation paralleled by an ML estimate of invariant sites approximately 20% lower for DDC than EF. Amino acids in DDC were several fold more variable than the protein sequences for EF. Differences in nucleotide base composition between these genes were more subtle, but both empirical nucleotide frequencies and maximum-likelihood estimates of equilibrium base composition suggested that EF harbored an excess of adenine (27.2%) with a deficiency in guanine (22.4%), while DDC demonstrated a more classic signature of AT bias (27.4% and 29.1%, respectively, versus 21.9% C and 21.6% G).

Maximum likelihood estimates of nucleotide substitution relative rate parameters also provided a powerful means to contrast the differences in molecular evolution between these two genes. The estimated increase in rates of transition versus transversion substitutions was much higher for EF (14.0 purine transitions and 25.1 pyrimidine transitions, versus 2.7 average transversion rate) than for DDC (5.6 purine transitions and 6.8 pyrimidine transitions, versus 1.2 average transversion rate), as was the degree of variation in rates of change among the 6 substitution classes (standard deviation in rate parameters: 9.5 for EF and 2.6 for DDC). The twofold difference (DDC: 1.4 > EF: 0.7) in ML estimates of the shape parameter for a gamma distribution modeling among-site rate heterogeneity also revealed striking differences in patterns of substitution



between these genes. While the amount of data, in number of nucleotides, contributed by each gene in this study was balanced (48.1% EF and 51.9% DDC), taken together the above observations suggested strongly that patterns of nucleotide substitution and resulting information content of both genes seemed to be strongly heterogeneous.

Differences between EF and DDC in signatures of molecular evolution were mirrored by differences in phylogenetic information content from each of these genes. Parsimony-based permutation tail probability (PTP) tests revealed highly significant phylogenetic structure for both genes, confirming their utility in phylogenetic studies in insect groups. This was not surprising, given that their utility had already been demonstrated experimentally in previous studies employing one or both genes in resolution of lepidopteran groups (Cho *et al.* 1995; Fang *et al.* 1997, 2000; Friedlander *et al.* 1992, 1998, 2000; Mitchell 1998; Mitchell *et al.* 1997, 2000; Regier *et al.* 2000, 2002). However, despite their proven utility in phylogenetic analyses, consistent generation of congruent gene trees from EF and DDC had not been conclusively demonstrated. In this study, across all taxon samples, data partitions, optimality criteria and methods of analysis, the phylogenetic hypotheses inferred from EF and DDC were strikingly discordant. Disagreement in suggested relationships extended across all taxonomic levels, including monophyly and relative orientation of the three subfamilies, monophyly and relative composition of individual tribes and sections, and even patterns of relatedness among congeneric species. Consistent and reliable phylogenetic patterns from analyses of one gene were seldom both consistently and reliably recovered from analyses of the other gene. Thus, distillation of a universal genus-based family

phylogeny from these two divergent individual gene phylogenies was a formidable challenge.

Broad discordance in phylogenetic hypotheses drawn from EF and DDC simultaneously increased the relevance of a whole-data approach (i.e., constructing a phylogenetic estimate from a combined data set), and also challenged the notion that concatenation of two such conflicting genes into a single analysis was theoretically justified (Bull *et al.* 1993; Chippindale & Wiens 1994; DeQueiroz *et al.* 1995; Huelsenbeck *et al.* 1996; Mitchell *et al.* 2000; Olmstead & Sweere 1994; Weller *et al.* 1994; Wiens 1998). MP analyses on the combined data matrices in this study were noticeably more analytically efficient and less ambiguous than for either gene separately, generating fewer equally parsimonious trees in shorter computation times. Results from these analyses incorporated elements of both EF and DDC topologies, as well as novel rearrangements not viewed in either independent tree. At the deepest levels, the topology in Figure 8 suggested a sister relationship between Sphinginae and Macroglossinae, consistent with the EF MP tree. However, Figure 8 also placed Ambulycini as the most derived lineage within a paraphyletic Smerinthinae grade, more consistent with smerinthine monophyly illustrated by the DDC tree. At terminal levels, the combined EF&DDC tree demonstrated greater fidelity to the DDC MP topology, especially in relationships among species of the three included hyperdiverse genera: *Manduca*, *Sphinx* and *Xylophanes*.

Difficulty interpreting the stark differences in suggested genealogical relatedness among sphingid lineages stemming from these two independent markers was diminished somewhat when viewed in the context of support for individual nodes in each topology.

Nonparametric bootstrapping, a technique designed to quantify the internal consistency of the data on the basis of individual taxon bipartitions, was the prime means of assessing node support in this study. Bootstrap values on all three parsimony trees suggested strongly that these data alone were grossly insufficient to establish strongly supported, phylogenetically robust nodes against which existing taxonomic hypotheses could be rigorously evaluated. EF, DDC and combined EF&DDC data were able to generate topologies with only 50%, 72% and 48% of all possible nodes receiving even moderate (i.e., values greater than or equal to 50%) bootstrap support, respectively. Even more telling was that the majority of the sparse bootstrap support was concentrated among relatively “obvious” terminal nodes, for example, those uniting congeneric species into a single monophyletic genus. The most critical nodes for a systematic study of the family, those deep nodes describing the interrelationships between sections, tribes and subfamilies, were in fact the most weakly supported. While there were consistent patterns to be gleaned from MP analyses (see below), results of this study made it clear that EF and DDC in conjunction provided insufficient information to adequately and robustly resolve the phylogeny of the Sphingidae. While improved taxon sampling beyond that employed here remains a viable possibility to extract more robust phylogenetic hypotheses from these markers, pursuit of other independently evolving gene sequences seems a justified and promising line of further research for this group.

Given the poor performance of these genes to produce strongly support nodes under the criterion of maximum parsimony, pursuit of optimal topologies according to the criterion of maximum likelihood proved productive. Discordance between the three MP trees in Figures 6, 7 & 8 became an asset in a sense, as these topologies expanded the

range of treespace used to seed three independent cycles of maximum likelihood parameter estimation and heuristic searches. Using the MP trees as initial conditions biased the likelihood search toward taxon bipartitions recovered in MP analyses, but permitted more efficient model parameter estimation than would have been possible if starting from random trees. For all three data sets, convergence to a stable set of model parameters was striking for two reasons. First, parameters converged to stable values after only the second iteration in 6 out of 9 estimation/search cycles listed in Table 21. This demonstrated the efficacy of MP topologies as starting points to launch ML searches determining model parameters and globally optimal topologies. Second, in all but one case, parameter values converged globally for a given data set regardless of the MP starting topology used to seed the searches. This suggested that, while discordant in relationships among subgroups, the differences among the three MP starting topologies were not so vast as to extend the ML searches into widely dispersed areas of parameter and tree space. Alternatively, global convergence of this sort suggested a relatively smooth likelihood surface efficiently traversed by SPR branch swapping in the heuristic search algorithm.

It was not clear why the combined EF&DDC data globally converged to parameter values when seeded by the EF or DDC MP trees, but converged to a distinct set of parameters when the combined EF&DDC MP tree was the seed topology. While both sets of parameters were similar in absolute values, the latter set resulted in a ML tree with slightly higher likelihood (Figure 11 and Tree 'c2' in Table 21). This topology differed from that obtained by seeding with the EF or DDC MP trees in the orientation of a single terminal lineage: the smerinthine clade [*Paonias*, *Pachysphinx*, *Smerinthus*].

Minor rearrangements among these genera (though each remained monophyletic) were encountered throughout every analysis using both optimality criteria, demonstrating these relationships have yet to be adequately defined and suggesting an area in which increased taxon sampling may be warranted.

Exploration of topological differences between trees derived from a given data set via maximum likelihood versus maximum parsimony provided a glimpse into the ways these data were differentially interpreted under different optimality criteria. Most noticeably, ML analyses incorporating an underlying model of nucleotide substitution did a much better job of reconstructing a reasonable scenario between Sphingidae and their bombycid and saturniid outgroups. While MP trees separated these outgroups from basal sphingid lineages (*Marumba* or Hemarina) by short internal and long terminal branches, ML trees reconstructed outgroup branches as the longest in the entire tree, with a comparably long branch leading to the monophyletic Sphingidae. This stark difference provided another empirical example of the ability for maximum likelihood to more reasonably reconstruct evolutionary history in scenarios of long-branch attraction when maximum parsimony could be positively misleading (Felsenstein 1978, 1985). Another consistent difference between MP and ML trees was relocation of the root from within a paraphyletic assemblage (in MP) to the base of a monophyletic assemblage (in ML). In every case, this had dramatic consequences on the overall tree structure and especially on interpretation of relationships among the three subfamilies. In fact, only the ML trees in Figures 10 and 11 suggested concepts of three strictly monophyletic subfamilies, in the orientation [Macroglossinae, (Smerinthinae, Sphinginae)]. All three MP analyses and even the EF ML analysis rendered at least one subfamily as a basal paraphyletic grade

leading to a sister relationship between the other two subfamilies. Interestingly, at some point in all six trees presented in Figure 6-11 every subfamily assumed that basal paraphyletic position! Given the vast disagreement between trees regarding an issue as basic as subfamily relatedness, the trees presented in this study should be viewed as a new set of phylogenetic hypotheses derived from molecular data, subject to further testing through collection of novel data and implementation of novel analytical techniques.

Despite the fundamental discordance between trees, there were a few areas of agreement which gained some strong support in this study. First, all trees except one (the EF ML topology) suggested a monophyletic Sphinginae whose closest relative was *Hopliocnema*, a single taxon from the smerinthine tribe Sphingulini. The consistency with which this hypothesis recurred suggested the assignment of Sphingulini to the Smerinthinae warrants further scrutiny. However, because this finding was based on sampling a single species, future studies should focus on including several sphingulines before a taxonomic revision is undertaken. Second, the sphingine tribe Acherontiini was reconstructed as monophyletic in every analysis. However, of the three genera sampled in this study, *Coelonia* was part of the tribe only in the EF analyses and switched subfamilies (to Macroglossinae) in analyses involving DDC. Third, the smerinthine tribe Ambulycini was recovered as a monophyletic pair of sister genera in every analysis. However, the position of this tribe relative to other smerinthines was malleable, and its placement often rendered the tribe Smerinthini and/or the entire subfamily Smerinthinae paraphyletic. Fourth, the macroglossine tribe Philampelini, sampled for three species of only one genus (*Eumorpha*), was recovered as monophyletic in every analysis. This was

in fact the only tribe in Macroglossinae supported by phylogenetic analysis in this study. While members of Dilophonotini and Macroglossini consistently clustered together, they never formed monophyletic clades. The dilophonotine section Hemarina was recovered within every analysis, and large portions of Dilophonotina were often recovered, but these were never in a sister relationship. The most stable assemblage in Macroglossinae was section Choerocampina, recovered in every analysis. Interestingly, taxa in this section are characterized by a morphological synapomorphy involving development of functionally viable sound detection apparatus on their mouthparts (Roeder 1972; Roeder *et al.* 1968, 1970; Roeder & Treat 1970). The other macroglossine section, Macroglossina, was never recovered as a monophyletic group in any analysis, echoing findings from the Regier 2001 study and calling into question its taxonomic legitimacy. Finally, with the exception of *Darapsa*, all congeneric species sampled in this study grouped together in monophyletic assemblages in almost every analysis. While *Darapsa* was reconstructed as monophyletic in EF, all analyses involving DDC not only embedded *Darapsa*1778 within *Xylophanes* (i.e., in a different section), but consistently separated it from its congener and a sample sequenced in Regier 2001, *Darapsa*GB. Given this extreme behavior, a reidentification of specimen GS-02-1778 and clarification of the specimen(s) used in Regier 2001 seems warranted.

In addition to redefining and solidifying the classically recognized taxonomic groups in the Sphingidae, Kitchin & Cadious's (2000) classification provided a handful of finer grain hypotheses of relationships among sphingid genera (see vertical bars in Table 2). Of sixteen such hypotheses, nine were testable given the taxon sample used in this study and six provisional support by analyses from all three data matrices:

- a. within Smerinthini: (*Pachysphinx*, *Smerinthus*, *Paonias*), but see above for difficulty interpreting the arrangement among these genera;
- b. within Ambulycini: (*Protambulyx*, *Adhemarius*), as discussed above;
- c. within Acherontiini: (*Agrius*, *Acherontia*), with confusing placements of *Coelonia*, as discussed above;
- d. within Dilophonotina: (*Nyceryx*, *Perigonia*, *Aellopos*);
- e. Hemarina, within Dilophonotini: (*Hemaris*, *Cephonodes*), as discussed above;
- f. Choerocampina, within Macroglossini, as discussed above.

Kitching & Cadiou's (2000) larger assemblage within Dilophonotina received support with all analyses involving DDC, but EF trees also included *Unzela*, *Cautethia* and Philampelini (*Eumorpha*) in this clade, rendering such a delimitation too restrictive. As with many groupings, the two markers sampled in this study were discordant with respect to this group, so it warrants further investigation.

## DIRECTIONS FOR FURTHER ANALYSIS

The suite of analyses in this study represented only a sample of the available analytical tools which could use the EF and DDC data to shed new light on phylogenetic relatedness within the Sphingidae. Other approaches which might be productively applied to these data include:

- (1) A comprehensive molecular evolutionary analysis of nucleotide substitution in these genes. Corrected estimates of transition vs. transversion and synonymous vs. nonsynonymous nucleotide changes would help refine relative rate parameter estimates. In addition, model-based distance corrections would permit pairwise



- divergence plots to assess degree of saturation across all codon positions in a quantitative fashion.
- (2) Differences in empirical base frequencies and uncorrected empirical information content between codon positions suggest they may evolve at different rates. ML relative rate parameter estimates and topology searches could be conducted for each codon position separately as another way to assess the congruence and reliability of phylogenetic signal from each partition.
  - (3) Topologies derived from ML analyses suffered for having no rigorous assessment of robustness for taxon bipartitions. Convergent model parameters could be fixed and used to generate simulated data sets for use in parametric bootstrapping (Huelsenbeck *et al.* 1996b).
  - (4) ML estimates of relative rate parameters could be converted to a step matrix for use in 6-parameter parsimony, capitalizing on the differences between optimality criteria and analytical methods to strengthen each approach.
  - (5) Increased diversity in starting topologies input for ML iterative parameter estimation/searching. Corrected distance-based topologies, morphological hypotheses, and a broader range of MP trees would seed ML analyses in more extensive areas of tree space and permit more exhaustive exploration of the dependence of parameter estimate convergence on initial conditions.
  - (6) Application of the likelihood ratio tests to assess partition incongruence between various data partitions, especially EF vs. DDC and nt1 vs. nt2 vs. nt3, and combinations thereof.

(7) Expansion of taxon and character sampling, through continued collection of rare sphingid taxa and selection of novel nuclear coding genes informative at lepidopteran family levels.

## REFERENCES

- Arnett, Jr., R.H. 2000. *American Insects: A Handbook of the Insects of America North of Mexico*. Second Edition. CRC Press LLC, Boca Raton, FL.
- Bartholomew, G.A. and T.M. Casey. 1978. Oxygen consumption of moths during rest, pre-flight warm-up, and flight in relation to body size and wing morphology. *Journal of Experimental Biology*, 76: 11-25.
- Batra, S.W.T. 1983. Establishment of *Hyles euphorbiae* (L.) (Lepidoptera: Sphingidae) in the United States for control of the weedy spurge *Euphorbia esula* L. and *E.cyparissias* L.. *New York Entomological Society*, 91(4): 304-311.
- Bernays, E.A. and D.H. Janzen. 1988. Saturniid and sphingid caterpillars: two ways to eat leaves. *Ecology*, 69(4): 1153-1160.
- Borror, D.J., C.A. Triplehorn and N.F. Johnson. 1980. *An Introduction to the Study of Insects*. Saunders College Publishing.
- Brock, J.P. 1971. A contribution towards the understanding of the morphology and phylogeny of the Ditrysian Lepidoptera. *Journal of Natural History*, 5: 29-102.
- Brown, J.M., O. Pellmyr, J.N. Thompson and R.G. Harrison. 1994. Phylogeny of *Greya* (Lepidoptera: Prodoxidae), based on nucleotide sequence variation in mitochondrial cytochrome oxidase I and II: congruence with morphological data. *Molecular Biology and Evolution*, 11(1): 128-141.
- Buckley, T.R., C. Simon and G.K. Chambers. 2001. Exploring among-site rate variation models in a maximum likelihood framework using empirical data: effects of model assumptions on estimates of topology, branch lengths, and bootstrap support. *Systematic Biology*, 50(1): 67-86.
- Bull, J.J., J.P. Huelsenbeck, C.W. Cunningham, D.L. Swofford and P.J. Waddell. 1993. Partitioning and combining data in phylogenetic analysis. *Systematic Biology*, 42(3): 384-397.
- Bullock, S.H. and A. Pescador. 1983. Wings and proboscis dimensions in a sphingid fauna from western Mexico. *Biotropica*, 15(4): 292-294.
- Buttiker, W., H.W. Krenn and J.F. Putterill. 1996. The proboscis of eye-frequenting and piercing Lepidoptera (Insecta). *Zoomorphology*, 116: 77-83.
- Casey, T.M. 1976. Flight energetics of sphinx moths: power input during hovering flight. *Journal of Experimental Biology*, 64: 529-543.

- Caterino M.S., R.D. Reed, M.M. Kuo and F.A. Sperling. 2001. A partitioned likelihood analysis of swallowtail butterfly phylogeny (Lepidoptera: Papilionidae). *Systematic Biology*, 50(1): 106-127.
- Chippindale, P.T. and J.J. Wiens. 1994. Weighting, partitioning and combining characters in phylogenetic analysis. *Systematic Biology*, 43: 278-287.
- Cho, S., A. Mitchell, J.C. Regier, C. Mitter, R.W. Poole, T.P. Friedlander and S. Zhao. 1995. A highly conserved nuclear gene for low-level phylogenetics: Elongation Factor-1a recovers morphology-based tree for Heliothine moths. *Molecular Biology and Evolution*, 12(4): 650-656.
- Coffelt, M.A. and P.B. Schultz. 1993. Quantification of an aesthetic injury level and threshold for an urban pest management program against orangestriped oakworm (Lepidoptera: Saturniidae). *Journal of Economic Entomology*, 86(5): 1512-1515.
- Coffelt, M.A. and P.B. Schultz. 1991. Citizen attitudes toward orangestriped oakworm: impact, control, host aesthetics, and IPM practices. *Journal of Arboriculture*, 17(11): 298-302.
- Coffelt, M.A. and P.B. Schultz. 1990. Development of an aesthetic injury level to decrease pesticide use against orangestriped oakworm (Lepidoptera: Saturniidae) in an urban pest management project. *Journal of Economic Entomology*, 83(5): 2044-2049.
- Common, I.F.B. 1990. *Moths of Australia*. Melbourne University Press, Carlton, Victoria.
- Costa, J.T., J.H. McDonald and N.E. Pierce. 1996. The effect of ant association on the population genetics of the Australian butterfly *Jalmenus evagoras* (Lepidoptera: Lycaenidae). *Biological Journal of the Linnean Society*, 58: 287-306.
- Cunningham, C.W. 1997. Is congruence between data partitions a reliable predictor of phylogenetic accuracy? Empirically testing an iterative procedure for choosing among phylogenetic methods. *Systematic Biology*, 46(3): 464-478.
- Darlu, P. and G. Lecointre. 2002. When does the incongruence length difference test fail?. *Molecular Biology and Evolution*, 19(4): 432-437.
- Darwin, C. 1862. *On the Various Contrivances by which British and Foreign Orchids are Fertilised by Insects, and On the Good Effects of Intercrossing*. John Murray, London, England.
- de Queiroz, A., M.J. Donoghue and J. Kim. 1995. Separate versus combined analysis of phylogenetic evidence. *Annual Review of Ecology and Systematics*, 26: 657-681.

- Dessauer, H.C., C.J. Cole and M.S. Hafner. 1996. Collection and storage of tissues. Chapter 3, pp. 29-47 in Hillis, D.M., C. Moritz and B.K. Mable (Editors), *Molecular Systematics*. Second Edition. Sinauer Associates, Inc., Sunderland, MA.
- Dillon, P.M., S. Lowrie and D. McKey. 1983. Disarming the "Evil Woman": petiole constriction by a sphingid larva circumvents mechanical defenses of its host plant, *Cnidoscolus urens* (Euphorbiaceae). *Journal of the Lepidopterists' Society*, 24(4): 267-270.
- Dobler, S. and B.D. Farrell. 1999. Host use evolution in *Chrysochus* milkweed beetles: evidence from behaviour, population genetics and phylogeny. *Molecular Ecology*, 8: 1297-1307.
- Don, R.H., P.T. Cox, B.J. Wainwright, K. Baker and J.S. Mattick. 1991. 'Touchdown' PCR to circumvent spurious priming during gene amplification. *Nucleic Acids Research*, 19(14): 4008.
- Dowton, M. and A.D. Austin. 2002. Increased congruence does not necessarily indicate increased phylogenetic accuracy: the behavior of the incongruence length difference test in mixed-model analyses. *Systematic Biology*, 51(1): 19-31.
- Dyer, L.A. 1995. Tasty generalists and nasty specialists? Antipredator mechanisms in tropical lepidopteran larvae. *Ecology*, 76(5): 1483-1496.
- Edwards, J.B.D.M., P. Ravassard, C. Icard-Liepkalns and J. Mallet. 1995. cDNA cloning by RT-PCR. Chapter 6, pp. 89-118 in McPherson, M.J., B.D. Hames and G.R. Taylor (Editors), *PCR2: A Practical Approach*. Oxford University Press, Oxford, England.
- Eernisse, D.J. and A.G. Kluge. 1993. Taxonomic congruence versus total evidence, and amniote phylogeny inferred from fossils, molecules, and morphology. *Molecular Biology and Evolution*, 10(6): 1170-1195.
- Eisikowitch, D. and J. Galil. 1971. Effect of wind on the pollination of *Pancratium maritimum* L. (Amaryllidaceae) by hawkmoths (Lepidoptera: Sphingidae). *Journal of Animal Ecology*, 40: 673-678.
- Faith, D.P. 1991. Cladistic permutation tests for monophyly and nonmonophyly. *Systematic Zoology*, 40(3): 366-375.
- Faith, D.P. and P.S. Cranston. 1991. Could a cladogram this short have arisen by chance alone?: Permutation tests for cladistic structure. *Cladistics*, 7: 1-28.
- Fang, Q.Q., A. Mitchell, J.C. Regier, C. Mitter, T.P. Friedlander and R.W. Poole. 2000. Phylogenetic utility of the nuclear gene Dopa Decarboxylase in Noctuid moths (Insecta: Lepidoptera: Noctuoidea). *Molecular Phylogenetics and Evolution*, 15(3): 473-486.

- Fang, Q.Q., S. Cho, J.C. Regier, C. Mitter, M. Matthews, R.W. Poole, T.P. Friedlander and S. Zhao. 1997. A new nuclear gene for insect phylogenetics: Dopa Decarboxylase is informative of relationships within Heliiothinae (Lepidoptera: Noctuidae). *Systematic Biology*, 46(2): 269-283.
- Fanger, H. 1999. Comparative morphology of tergal phragmata occurring in the dorsal thoraco-abdominal junction of ditrysian Lepidoptera (Insecta). *Zoomorphology*, 119: 163-183.
- Farrell, B.D. 2001. Evolutionary assembly of the milkweed fauna: cytochrome oxidase I and the age of *Tetraopes* beetles. *Molecular Phylogenetics and Evolution*, 18(1): -.
- Farrell, B.D. 1998. "Inordinate Fondness" explained: why are there so many beetles?. *Science*, 281: 555-559.
- Farrell, B.D. 1993. Phylogenetic determinants of insect/plant community diversity. In Ricklefs, R.E. and D. Schluter (Editors). *Species Diversity in Ecological Communities: Historical and Geographical Perspectives*. University of Chicago Press, Chicago, IL.
- Farrell, B.D., A. Sequeira, B. O'Meara, B. Normark, J. Chung and B. Jordal. 2001. The evolution of agriculture in beetles (Curculionidae: Scolytinae and Platypodinae). *Evolution*, 55(10): 2011-2027.
- Farrell, B.D. and C. Mitter. 1994. Adaptive radiation in insects and plants: time and opportunity. *American Zoologist*, 34: 57-69.
- Farrell, B.D. and C. Mitter. 1990. Phylogenesis of insect/plant interactions: have *Phyllobrotica* leaf beetles (Chrysomelidae) and the Lamiales diversified in parallel?. *Evolution*, 44(6): 1389-1403.
- Farrell, B.D., C. Mitter and D.J. Futuyma. 1992. Diversification at the insect-plant interface: insights from phylogenetics. *Bioscience*, 42(1): 34-42.
- Farris, J.S. 1989a. The retention index and homoplasy excess. *Systematic Biology*, 38: 406-407.
- Farris, J.S. 1989b. The retention index and the rescaled consistency index. *Cladistics*, 5: 417-419.
- Felsenstein, J. 1973. Maximum likelihood and minimum-steps methods for estimating evolutionary trees from data on discrete characters. *Systematic Zoology*, 22: 240-249.
- Felsenstein, J. 1978. Cases in which parsimony or compatibility methods will be positively misleading. *Systematic Zoology*, 27: 401-410.

- Felsenstein, J. 1981a. A likelihood approach to character weighting and what it tells us about parsimony and compatibility. *Biological Journal of the Linnean Society*, 16: 183-196.
- Felsenstein, J. 1981b. Evolutionary trees from DNA sequences: a maximum likelihood approach. *Journal of Molecular Evolution*, 17: 368-376.
- Felsenstein, J. 1985. Confidence limits on phylogenies: an approach using the bootstrap. *Evolution*, 39(4): 783-791.
- Felsenstein, J. and E. Sober. 1986. Parsimony and likelihood: an exchange. *Systematic Zoology*, 35(4): 617-626.
- Felsenstein, J. and H. Kishino. 1993. Is there something wrong with the bootstrap on phylogenies? A reply to Hillis and Bull. *Systematic Biology*, 42: 193-200.
- Fink, L.S. 1995. Foodplant effects on colour morphs of *Eumorpha fasciata* (Lepidoptera: Sphingidae). *Journal of the Linnaean Society*, 56(3): 423-437.
- Fleming, R.C. 1968. Head musculature of sphinx moths (Lepidoptera: Sphingidae). *Contributions of the American Entomological Institute*, 3(3): 1-32.
- Friedlander, T.P., J.C. Regier and C. Mitter. 1992. Nuclear gene sequences for higher phylogenetic analysis: 14 promising candidates. *Systematic Biology*, 41(4): 483-490.
- Friedlander, T.P., J.C. Regier, C. Mitter and D.L. Wagner. 2000. Evolution of heteroneuran Lepidoptera (Insecta) and the utility of dopa decarboxylase for Cretaceous-age phylogenetics. *Zoological Journal of the Linnean Society*, 130: 213-234.
- Friedlander, T.P., K.R. Horst, J.C. Regier, C. Mitter, R.S. Piegler and Q.Q. Fang. 1998. Two nuclear genes yield concordant relationships within Attacini (Lepidoptera: Saturniidae). *Molecular Phylogenetics and Evolution*, 9(1): 131-140.
- Fukami, K. and Y. Tateno. 1989. On the maximum likelihood method for estimating molecular trees: uniqueness of the likelihood point. *Journal of Molecular Evolution*, 28: 460-464.
- Fullard, J.H. and J.E. Yack. 1993. The evolutionary biology of insect hearing. *Trends in Ecology and Evolution*, 8(7): 248-252.
- Funk, D.J., L. Helbling, J.J. Wernegreen and N.A. Moran. 2000. Intraspecific phylogenetic congruence among multiple symbiont genomes. *Proceedings of the Royal Society of London, Series B Biological Sciences*, 267: 2517-2521.
- Gaut, B.S. and P.O. Lewis. 1995. Success of maximum likelihood phylogeny inference in the four-taxon case. *Molecular Biology and Evolution*, 12(1): 152-162.

- Ghiradella, H. 1998. Hairs, Bristles, and Scales. Chapter 11, pp. 257-287 in Harrison, F.W. and M. Locke (Editors), *Microscopic Anatomy of Invertebrates. Volume 11A: Insecta*. Wiley-Liss, Inc., New York, NY.
- Goldman, N. 1990. Maximum likelihood inference of phylogenetic trees, with special reference to a poisson process model of DNA substitution and to parsimony analyses. *Systematic Zoology*, 39: 345-361.
- Goldsmith, M.R. and A.S. Wilkins. 1995. *Molecular Model Systems in the Lepidoptera*. Cambridge University Press, Cambridge, England.
- Gopfert, M.C., A. Surlykke and L.T. Wasserthal. 2002. Tympanal and atympanal 'mouth-ears' in hawkmoths (Sphingidae). *Proceedings of the Royal Society of London, Series B Biological Sciences*, 269: 89-95.
- Gopfert, M.C. and L.T. Wasserthal. 1999a. Auditory sensory cells in hawkmoths: identification, physiology and structure. *Journal of Experimental Biology*, 202: 1579-1587.
- Gopfert, M.C. and L.T. Wasserthal. 1999b. Hearing with the mouthparts: behavioural responses and the structural basis of ultrasound perception in acheloniine hawkmoths. *Journal of Experimental Biology*, 202: 909-918.
- Grant, V. 1983. The systematic and geographical distribution of hawkmoth flowers in the temperate North American fauna. *Botanical Gazette*, 144(3): 439-449.
- Grant, V. and K.A. Grant. 1983a. Behavior of hawkmoths on flowers of *Datura meteloides*. *Botanical Gazette*, 144(2): 280-284.
- Grant, V. and K.A. Grant. 1983b. Hawkmoth pollination of *Mirabilis longiflora* (Nyctaginaceae). *Proceedings of the National Academy of Sciences*, 80: 1298-1299.
- Grant, G.G. and J.L. Eaton. 1973. Scent brushes of the male tobacco hornworm *Manduca sexta* (Lepidoptera: Sphingidae). *Annals of the Entomological Society of America*, 66(4): 901-904.
- Grodnitsky, D.L. 1999. Wing morphology and evolution in the Amphiesmenoptera. Chapter 4.2, pp. 125-143 in Grodnitsky, D.L. (Editor), *Form and Function of Insect Wings: The Evolution of Biological Structures*. The Johns Hopkins University Press, Baltimore, MD.
- Gu, X., Y.-X. Fu and W.-H. Li. 1995. Maximum likelihood estimation of the heterogeneity of substitution rate among nucleotide sites. *Molecular Biology and Evolution*, 12: 546-557.
- Haber, W.A. 1984. Pollination by deceit in a mass-flowering tropical tree *Plumeria rubra* L. (Apocynaceae). *Biotropica*, 16(4): 269-275.



- Haber, W.A. and G.W. Frankie. 1989. A tropical hawkmoth community: Costa Rican dry forest Sphingidae. *Biotropica*, 21(2): 155-172.
- Haber, W.A. and G.W. Frankie. 1982. Pollination of *Luehea* (Tiliaceae) in Costa Rican deciduous forest. *Ecology*, 63(6): 1740-1750.
- Harshman, J. 1994. The effect of irrelevant characters on bootstrap values. *Systematic Biology*, 43(3): 419-424.
- Harvey, P.H. and M.D. Pagel. 1991. *The Comparative Method in Evolutionary Biology*. Oxford Press, Oxford, England.
- Hasegawa, M., H. Kishino and N. Saitou. 1991. On the maximum likelihood method in molecular phylogenetics. *Journal of Molecular Evolution*, 32: 443-445.
- Hasegawa, M., H. Kishino and T. Yano. 1985. Dating of the human-ape splitting by a molecular clock of mitochondrial DNA. *Journal of Molecular Evolution*, 22: 160-174.
- Hatzopoulos, A.K. and J.C. Regier. 1987. Evolutionary changes in the developmental expression of silkworm chorion genes and their morphological consequences. *Proceedings of the National Academy of Sciences*, 84: 479-483.
- Hawthorne, D.J. and S. Via. 2001. Genetic linkage of ecological specialization and reproductive isolation in pea aphids. *Nature*, 412: 904-907.
- Heinrich, B. 1971a. Temperature regulation of sphinx moth, *Manduca sexta*. 1. Flight energetics and body temperature during free and tethered flight. *Journal of Experimental Biology*, 54(1): 141-.
- Heinrich, B. 1971b. Temperature regulation of sphinx moth, *Manduca sexta*. 2. Regulation of heat loss by control of blood circulation. *Journal of Experimental Biology*, 54(1): 153-.
- Heinrich, B. and G.A. Bartholo. 1971. Analysis of pre-flight warm-up in sphinx moth, *Manduca sexta*. *Journal of Experimental Biology*, 55(1): 223.
- Hendy, M.D. and D. Penny. 1989. A framework for the quantitative study of evolutionary trees. *Systematic Zoology*, 38(4): 297-309.
- Hillis, D.M., C. Moritz and B.K. Mable (Editors). 1996. *Molecular Systematics*. Second Edition. Sinauer Associates, Inc., Sunderland, MA.
- Hillis, D.M. and J.J. Bull. 1993. An empirical test of bootstrapping as a method for assessing confidence in phylogenetic analysis. *Systematic Biology*, 42(2): 182-192.

- Hiruma, K., M.S. Carter and L.M. Riddiford. 1995. Characterization of the Dopa Decarboxylase gene of *Manduca sexta* and its suppression by 20-hydroxyecdysone. *Developmental Biology*, 169: 195-209.
- Hodges, R.W. 1971. *The Moths of North America North of Mexico. Fascicle 21: Sphingoidea (Hawkmoths)*. E.W. Classey Limited & R.B.D. Publications, Inc., London, England.
- Hovemann, B., S. Richter, U. Walldorf and C. Cziepluch. 1988. Two genes encode related cytoplasmic elongation factors 1alpha (EF-1alpha) in *Drosophila melanogaster* with continuous and stage specific expression. *Nucleic Acids Research*, 16(8): 3175-3194.
- Huelsenbeck, J.P. 1995. The robustness of two phylogenetic methods: four-taxon simulations reveal a slight superiority of maximum likelihood over neighbor joining. *Molecular Biology and Evolution*, 12: 843-849.
- Huelsenbeck, J.P. and K.A. Crandall. 1997. Phylogeny estimation and hypothesis testing using maximum likelihood. *Annual Review of Ecology and Systematics*, 28: 437-466.
- Huelsenbeck, J.P., D.M. Hillis and R. Jones. 1996. Parametric bootstrapping in molecular phylogenetics: applications and performance. Chapter 2, pp. 19-45 in Ferraris, J.D. and S.R. Palumbi (Editors), *Molecular Zoology: Advances, Strategies, and Protocols*. Wiley-Liss, Inc., New York, NY.
- Huelsenbeck, J.P., J.J. Bull and C.W. Cunningham. 1996. Combining data in phylogenetic analysis. *Trends in Ecology and Evolution*, 11(4): 152-157.
- Hufbauer, R.A. and S. Via. 1999. Evolution on an aphid-parasitoid interaction: variation in resistance to parasitism among aphid populations specialized on different plants. *Evolution*, 53(5): 1435-1445.
- Janzen, D.H. 1988. Ecological characterization of a Costa Rican dry forest caterpillar fauna. *Biotropica*, 20(2): 120-135.
- Janzen, D.H. 1984. Two ways to be a tropical big moth: Santa Rosa saturniids and sphingids. Pp. 85-140 in Dawkins, R. and M. Ridley (Editors), *Oxford Surveys in Evolutionary Biology*. Volume 1. Oxford University Press, Oxford, England.
- Janzen, D.H. 1981. Patterns of herbivory in a tropical deciduous forest. *Biotropica*, 13(4): 271-282.
- Janzen, D.H. and P.G. Waterman. 1984. A seasonal census of phenolics, fibre and alkaloids in foliage of forest trees in Costa Rica: some factors influencing their distribution and relation to host selection by Sphingidae and Saturniidae. *Journal of the Linnaean Society*, 21(4): 439-454.

- Kamiie, K., H. Taira, H. Ooura, A. Kakuta, S. Matsumoto, S. Ejiri and T. Katsumata. 1993. Nucleotide sequence of the cDNA encoding silk gland elongation factor 1a. *Nucleic Acids Research*, 21(3): 742-742.
- Kelley, S.T., B.D. Farrell and J.B. Mitton. 2000. Effects of specialization on genetic differentiation in sister species of bark beetles. *Heredity*, 84: 218-227.
- Kelley, S.T. and B.D. Farrell. 1998. Is specialization a dead end? The phylogeny of host use in *Dendroctonus* bark beetles (Scolytidae). *Evolution*, 52(6): 1731-1743.
- Kishino, H. and H. Hasegawa. 1989. Evaluation of the maximum likelihood estimate of the evolutionary tree topologies from DNA sequence data, and the branching order in Hominoidea. *Journal of Molecular Evolution*, 29: 170-179.
- Kitching, I.J. 2002. The phylogenetic relationships of Morgan's Sphinx, *Xanthopan morgani* (Walker), the tribe Acherontiini, and allied long-tongued hawkmoths (Lepidoptera: Sphingidae, Sphinginae). *Zoological Journal of the Linnean Society*, 135: 471-527.
- Kitching, I.J. and J.-M. Cadiou. 2000. *Hawkmoths of the World: An Annotated and Illustrated Revisionary Checklist (Lepidoptera: Sphingidae)*. The Natural History Museum, London, England.
- Kluge, A.G. and J.S. Farris. 1969. Quantitative phyletics and the evolution of anurans. *Systematic Zoology*, 18: 1-32.
- Krenn, H.W. 2000. Proboscis musculature in the butterfly *Vanessa cardui* (Nymphalidae, Lepidoptera): settling the proboscis recoiling controversy. *Acta Zoologica*, 81: 259-266.
- Krenn, H.W. 1998. Proboscis sensilla in *Vanessa cardui* (Lepidoptera: Nymphalidae): functional morphology and significance in flower-probing. *Zoomorphology*, 118: 23-30.
- Krenn, H.W. 1997. Proboscis assembly in butterflies: a once in a lifetime sequence of events. *European Journal of Entomology*, 94: 495-501.
- Krenn, H.W. 1990. Functional morphology and movements of the proboscis of Lepidoptera (Insecta). *Zoomorphology*, 110: 105-114.
- Krenn, H.W. and N.P. Kristensen. 2000. Early evolution of the proboscis of Lepidoptera (Insecta): external morphology of the galea in basal glossotan moths lineages, with remarks on the origin of the pilifers. *Zoologischer Anzeiger*, 239: 179-196.
- Kristensen, N.P. (Editor). *Lepidoptera, Moths and Butterflies, Volume 1: Evolution, Systematics, and Biogeography*. In M. Fischer (Ed.), *Handbook of Zoology: A Natural History of the Phyla of the Animal Kingdom, Volume IV Arthropoda: Insecta*, Part 35. Walter de Gruyter, Inc., Hawthorne, NY.

- Kritsky, G. 1991. Darwin's Madagascan hawkmoth prediction. *American Entomologist*, 37: 206-210.
- Lanave, C., G. Preparata, C. Saccone and G. Serio. 1984. A new method for calculating evolutionary substitution rates. *Journal of Molecular Evolution*, 20: 86-93.
- LeClerc, R.F. and J.C. Regier. 1993. Choriogenesis in Lepidoptera: morphogenesis, protein synthesis, specific mRNA accumulation and primary structure of a chorion cDNA from the gypsy moth. *Developmental Biology*, 160(1): 28-38.
- Lemaire, C. and J. Minet. 1999. The Bombycoidea and their Relatives. Chapter 14, pp. 321-353 in Kristensen, N.P. (Editor), *Lepidoptera, Moths and Butterflies, Volume 1: Evolution, Systematics, and Biogeography*. Walter de Gruyter, Inc., Hawthorne, NY.
- Liu, H., C.P. Ellington, K. Kawachi, C. Van den Berg and A.P. Willmott. 1998. A computational fluid dynamic study of hawkmoth hovering. *Journal of Experimental Biology*, 201(4): 461-477.
- Mabberley, D.J. 1997. *The Plant Book: A Portable Dictionary of the Vascular Plants*. Second Edition. Cambridge University Press, Cambridge, England.
- Maddison, D.R. 1991. The discovery and importance of multiple islands of most-parsimonious trees. *Systematic Zoology*, 40(3): 315-328.
- Maddison, D.R., D.L. Swofford and W.P. Maddison. 1997. NEXUS: An extensible file format for systematic information. *Systematic Biology*, 46(4): 590-621.
- Mason-Gamer, R.J. and E.A. Kellogg. 1996. Testing for conflict among molecular data sets in the tribe Triticeae (Gramineae). *Systematic Biology*, 45(4): 524-545.
- Mazur, G.D., J.C. Regier and F.C. Kafatos. 1989. Morphogenesis of silkmoth chorion: sequential modification of an early helicoidal framework through expansion and densification. *Tissue and Cell*, 21: 227-242.
- Mickevich, M.F. and J.S. Farris. 1981. The implications of congruence in *Menidia*. *Systematic Zoology*, 30(3): 351-370.
- Miller, R.B. 1981. Hawkmoths and the geographic patterns of floral variation in *Aquilegia caerulea*. *Evolution*, 35(4): 763-774.
- Miller, W.E. 1997a. Body weight as related to wing measure in hawkmoths (Sphingidae). *Journal of the Lepidopterists' Society*, 51(1): 91-92.
- Miller, W.E. 1997b. Diversity and evolution of tongue length in hawkmoths (Sphingidae). *Journal of the Lepidopterists' Society*, 51(1): 9-31.
- Miller, W.E. 1996. Population behavior and adult feeding capability in Lepidoptera. *Environmental Entomology*, 25(2): 213-226.

- Minet, J. 1994. The Bombycoidea: phylogeny and higher classification (Lepidoptera: Glossata). *Entomologica Scandinavica*, 25: 63-88.
- Minet, J. 1991. Tentative reconstruction of the ditrysian phylogeny (Lepidoptera: Glossata). *Entomologica Scandinavica*, 22: 69-95.
- Minet, J. 1986. Ebauche d'une classification moderne de l'ordre des Lepidopteres. *Alexanor*, 14: 291-313.
- Mitchell, A., C. Mitter and J.C. Regier. 2000. More taxa or more characters revisited: combining data from nuclear protein-encoding genes for phylogenetic analyses of Noctuoidea (Insecta: Lepidoptera). *Systematic Biology*, 49(2): 202-224.
- Mitchell, A., S. Cho, J.C. Regier, C. Mitter, R.W. Poole and M. Matthews. 1997. Phylogenetic utility of Elongation Factor-1a in Noctuoidea (Insecta: Lepidoptera): the limits of synonymous substitution. *Molecular Biology and Evolution*, 14(4): 381-390.
- Mitter, C.M. and B.D. Farrell. 1991. Macroevolutionary aspects of insect-plant relationships. Chapter 2, pp. 35-78 in Bernays, E. (Editor), *Insect Plant Interactions*, Volume 3. CRC Press, Boca Raton, FL.
- Mitter, C., B.D. Farrell and D.J. Futuyma. 1991. Phylogenetic studies of insect-plant interactions: insights into the genesis of diversity. *Trends in Ecology and Evolution*, 6(9): 290-293.
- Mitter, C., B.D. Farrell and B. Wiegmann. 1988. The phylogenetic study of adaptive zones: has phytophagy promoted insect diversification?. *American Naturalist*, 132(1): 107-128.
- Miyamoto, M.M. and W.M. Fitch. 1995. Testing species phylogenies and phylogenetic methods with congruence. *Systematic Biology*, 44(1): 64-76.
- Nilsson, L.A. 1998. Deep flowers for long tongues. *Trends in Ecology and Evolution*, 13(11): 259-260.
- Nilsson, L.A. 1988. The evolution of flowers with deep corolla tubes. *Nature*, 334: 147-149.
- Nilsson, L.A., L. Jonsson, L. Ralison and E. Randrianjohany. 1987. Angraecoid orchids and hawkmoths in central Madagascar: specialized pollination systems and generalist foragers. *Biotropica*, 19(4): 310-318.
- Nilsson, L.A., L. Jonsson, L. Rason and E. Randrianjohany. 1985. Monophily and pollination mechanisms in *Angraecum arachnites* Schltr. (Orchidaceae) in a guild of long-tongued hawk-moths (Sphingidae) in Madagascar. *Biological Journal of the Linnaean Society*, 26: 1-19.

- O'Brien, D. 1999. Fuel use in flight and its dependence on nectar feeding in the hawkmoth *Amphion floridensis*. *Journal of Experimental Biology*, 202: 441-451.
- O'Brien, D.M. and R.K. Suarez. 2001. Fuel use in hawkmoth (*Amphion floridensis*) flight muscle: enzyme activities and flux rates. *Journal of Experimental Zoology*, 290: 108-114.
- O'Brien, D.M., D.P. Schrag and C. Martinez del Rio. 2000. Allocation to reproduction in a hawkmoth: a quantitative analysis using stable isotopes. *Ecology*, 81(10): 2822-2831.
- Ojeda-Avila, T., H.A. Woods and R.A. Raguso. 2003. Effects of dietary variation on growth, composition, and maturation of *Manduca sexta* (Sphingidae : Lepidoptera). *Journal of Insect Physiology*, 49(4): 293-306.
- Ojeda-Avila, T., H.A. Woods and R.A. Raguso. 2001. Effects of dietary variation on growth, composition, and maturation of *Manduca sexta*. *American Zoologist*, 41(6): 1545-1545.
- Olmstead, R.G. and J.A. Sweere. 1994. Combining data in phylogenetic systematics: An empirical approach using three molecular data sets in the Solanaceae. *Systematic Biology*, 43(4): 467-481.
- Otto, P., D. Kephart and R. Bitner. 1998. Separate isolation of genomic DNA and total RNA from single samples using the SV Total RNA Isolation System. *Promega Notes*, 69: 19-24.
- Page, R. D. M. 1993. On islands of trees and the efficacy of different methods of branch swapping in finding most-parsimonious trees. *Systematic Biology*, 42: 200-210.
- Paige, R.T. and T.G. Whitham. 1985. Individual and population shifts in flower color by scarlet gilia: a mechanism for pollinator tracking. *Science*, 227: 315-317.
- Penny, D. and M.D. Hendy. 1986. Estimating the reliability of evolutionary trees. *Molecular Biology and Evolution*, 3: 403-417.
- Pierce, N.E. 1995. Predatory and parasitic Lepidoptera: carnivores living on plants. *Journal of the Lepidopterists' Society*, 49(4): 412-453.
- Pierce, N.E. 1987. The evolution and biogeography of associations between lycaenid butterflies and ants. Pp. 89-116 in Harvey, P. and L. Partridge (Editors), *Oxford Surveys in Evolutionary Biology*. Volume 4. Oxford University Press, Oxford, England.
- Post, R.J., P.K. Flook and A.L. Millest. 1993. Methods for the preservation of insects for DNA studies. *Biochemical Systematics and Ecology*, 21(1): 85-92.

- Powell, J.A., C. Mitter and B.D. Farrell. 1999. Evolution of Larval Food Preferences in Lepidoptera. Chapter 20, pp. 403-422 in Kristensen, N.P. (Editor), *Lepidoptera, Moths and Butterflies, Volume 1: Evolution, Systematics, and Biogeography*. Walter de Gruyter, Inc., Hawthorne, NY.
- Price, P.W. 1997. *Insect Ecology*. Third Edition. John Wiley & Sons, New York, NY.
- Raguso, R.A and M.A. Willis. 2002. Synergy between visual and olfactory cues in nectar feeding by naive hawkmoths, *Manduca sexta*. *Animal Behavior*, 64: 685-695.
- Raguso, R.A and D.M. Light. 1998. Electroantennogram responses of male *Sphinx perelegans* hawkmoths to floral and 'green-leaf volatiles'. *Entomologia Experimentalis et Applicata*, 86(3): 287-293.
- Raguso, R.A., D.M. Light and E. Pickersky. 1996. Electroantennogram responses of *Hyles lineata* (Sphingidae: Lepidoptera) to volatile compounds from *Clarkia breweri* (Onagraceae) and other moth-pollinated flowers. *Journal of Chemical Ecology*, 22(10): 1735-1766.
- Reeves, J.H. 1992. Heterogeneity in the substitution process of amino acid sites of proteins coded for by mitochondrial DNA. *Journal of Molecular Evolution*, 35: 17-31.
- Regier, J.C., C. Mitter, R.S. Piegler and T.P. Friedlander. 2002. Monophyly, composition, and relationships within Saturniinae (Lepidoptera: Saturniidae): evidence from two nuclear genes. *Insect Systematics and Evolution*, 33(1): 9-21.
- Regier, J.C., C. Mitter, T.P. Friedlander and R.S. Peigler. 2001. Phylogenetic relationships in Sphingidae (Insecta: Lepidoptera): initial evidence from two nuclear genes. *Molecular Phylogenetics and Evolution*, 20(2): 311-325.
- Regier, J.C., C. Mitter, R.S. Piegler and T.P. Friedlander. 2000. Phylogenetic relationships in Lasiocampidae (Lepidoptera): initial evidence from elongation factor 1-alpha sequences. *Insect Systematics and Evolution*, 31(2): 179-186.
- Regier, J.C. and J.W. Shultz. 1997. Molecular phylogeny of the major arthropod groups indicates polyphyly of crustaceans and a new hypothesis for the origin of hexapods. *Molecular Biology and Evolution*, 14(9): 902-913.
- Regier, J.C., T.P. Friedlander, R.F. Leclerc, C. Mitter and B. Wiegmann. 1995. Lepidopteran phylogeny and applications to comparative studies of development. Chapter 4, pp. 107-137 in Goldsmith, M.R. and A.S. Wilkins (Editors), *Molecular Model Systems in the Lepidoptera*. Cambridge University Press, Cambridge, England.
- Regier, J.C., C. Cole and R.F. LeClerc. 1993. Cell specific expression in the silkworm follicle: developmental characterization of a major chorion protein, its mRNA and gene. *Developmental Biology*, 160: 236-245.

- Regier, J.C. and F.C. Kafatos. 1991. Molecular genetics in the study of development and evolution: the insect chorion. Pp. 98-132 in Vinson, S.B. and R.L. Metcalf (Editors), *Entomology Serving Society: Emerging Technologies and Challenges*. Entomological Society of America, Lanham, MD.
- Robinson, G.S. and H.S. Robinson. 1972. Genital stridulation in male *Psilogramma jordana* Bethune-Baker (Lepidoptera, Sphingidae). *The Entomologist's Record and Journal of Variation*, 84: 212-215.
- Rodriguez, F., J.L. Olizer, A. Marin and J.R. Medina. 1990. The general stochastic model of nucleotide substitution. *Journal of Theoretical Biology*, 142: 485-501.
- Roeder, K.D. 1972. Acoustic and mechanical sensitivity of the distal lobe of the pilifer in choerocampine hawkmoths. *Journal of Insect Physiology*, 18: 1249-1264.
- Roeder, K.D., A.E. Treat and J.S. Vandeberg. 1970. Distal lobe of the pilifer: an ultrasonic receptor in choerocampine hawkmoths. *Science*, 170: 1098-1099.
- Roeder, K.D. and A.E. Treat. 1970. An acoustic sense in some hawkmoths (Choerocampinae). *Journal of Insect Physiology*, 16: 1069-1086.
- Roeder, K.D., A.E. Treat and J.S. Vandeberg. 1968. Auditory sense in certain sphingid moths. *Science*, 159: 331-333.
- Rogers, J.S. 1997. On the consistency of maximum likelihood estimation of phylogenetic trees from nucleotide sequences. *Systematic Biology*, 46(2): 354-357.
- Rothschild, L.W. and K. Jordan. 1903. A revision of the lepidopterous family Sphingidae. *Novitates Zoologicae*, 9: 1-972.
- Saitou, N. 1990. Maximum likelihood methods. *Methods in Enzymology*, 183: 584-598.
- Saitou, N. 1988. Property and efficiency of the maximum likelihood method for molecular phylogeny. *Journal of Molecular Evolution*, 183: 261-273.
- Sanderson, M.J. 1995. Objections to bootstrapping phylogenies: A critique. *Systematic Biology*, 44(3): 299-320.
- Sanderson, M.J. 1989. Confidence limits on phylogenies: the bootstrap revisited. *Cladistics*, 5: 113-129.
- Schmitz, A. and L.T. Wasserthal. 1999. Comparative morphology of the spiracles of the Papilionidae, Sphingidae, and Saturniidae (Insecta: Lepidoptera). *International Journal of Insect Morphology*, 28: 13-26.
- Scoble, M.J. 1992. *The Lepidoptera. Form, Function and Diversity*. Oxford University Press, Oxford, England.



- Scriber, J.M. 1979. Effects of leaf water supplementation upon post-ingestive nutritional indices of forb-, shrub-, vine-, and tree-feeding Lepidoptera. *Entomologia Experimentalis et Applicata*, 25: 240-252.
- Sequeira, A., B.B. Normark and B.D. Farrell. 2000. Evolutionary assembly of the conifer fauna: distinguishing ancient from recent associations in bark beetles. *Proceedings of the Royal Society of London, Series B Biological Sciences*, 267: 2359-2366.
- Shaw, K.L. 1996a. Polygenic inheritance of a behavioral phenotype: interspecific genetics of song in the Hawaiian cricket genus *Laupala*. *Evolution*, 50(1): 256-266.
- Shaw, K.L. 1996b. Sequential radiations and patterns of speciation in the Hawaiian cricket genus *Laupala* inferred from DNA sequences. *Evolution*, 50(1): 237-255.
- Sidow, A., T. Nguyen and T.P. Speed. 1992. Estimating the fraction of invariable codons with a capture-recapture method. *Journal of Molecular Evolution*, 35: 253-260.
- Siebert, P.D. 1999. Quantitative RT-PCR. Chapter 4, pp. 61-85 in Kochanowski, B. and U. Reischl (Editors), *Quantitative PCR Protocols*. Humana Press, Totowa, NJ.
- Siebert, P.D. and J.W. Larrick. 1995. Introduction and Overview. Chapter 1, pp. 1-20 in Larrick, J.W. and P.D. Siebert (Editors), *Reverse Transcriptase PCR*. Ellis Horwood, Ltd., London, England.
- Sober, E. 1984. A likelihood justification of parsimony. *Cladistics*, 1: 209-233.
- Sorhannus, U. and C. Van Bell. 1999. Testing for equality of molecular evolutionary rates: a comparison between a relative-rate test and a likelihood ratio test. *Molecular Biology and Evolution*, 16(6): 849-855.
- Stamp, N.E. and T.M. Casey. 1993. *Caterpillars: Ecological and Evolutionary Constraints on Foraging*. Chapman & Hall Press, New York, NY.
- Steel, M.A., L. Szekely, P.L. Erdos and P.J. Waddell. 1993. A complete family of phylogenetic invariants for any number of taxa under Kimura's 3ST model. *New Zealand Journal of Botany*, 31: 289-296.
- Sullivan, J., D.L. Swofford and G.J.P. Naylor. 1999. The effect of taxon sampling on estimating rate heterogeneity parameters of maximum-likelihood models. *Molecular Biology and Evolution*, 16(10): 1347-1356.
- Sullivan, J. and D.L. Swofford. 1997. Are guinea pigs rodents? The importance of adequate models in molecular phylogenies. *Journal of Mammalian Evolution*, 4(2): 77-86.

- Swofford, D.L. 2003. *PAUP\*: Phylogenetic Analysis Using Parsimony (\* and Other Methods)*. Version 4.0b10. Sinauer Associates, Inc., Sunderland, MA.
- Swofford, D.L., G.J. Olsen, P.J. Waddell and D.M. Hillis. 1996. Phylogenetic Inference. Chapter 11, pp. 407-514 in Hillis, D.M., C. Moritz and B.K. Mable (Editors), *Molecular Systematics*. Second Edition. Sinauer Associates, Inc., Sunderland, MA.
- Tatarenkov, A., J. Kwiatowski, D. Skarecky, E. Barrio and F.J. Ayala. 1999. On the evolution of Dopa Decarboxylase (Ddc) and Drosophila systematics. *Journal of Molecular Evolution*, 48: 445-462.
- Tateno Y, Takezaki N, Nei M. 1993. Relative efficiencies of the maximum likelihood, maximum parsimony, and neighbor-joining methods for estimating protein phylogeny. *Molecular Phylogenetics and Evolution*, 2: 1-5.
- Wagner, D.L. 2001. Moths. Pp. 249-270 in *Encyclopedia of Biodiversity*. Volume 4 Academic Press, London, England.
- Wannenmacher, G. and L.T. Wasserthal. 2003. Contribution of the maxillary muscles to proboscis movement in hawkmoths (Lepidoptera : Sphingidae) - an electrophysiological study. *Journal of Insect Physiology*, 49(8): 765-776.
- Wasserthal, L.T. 2001. Flight-motor-driven respiratory air flow in the hawkmoth *Manduca sexta*. *Journal of Experimental Biology*, 204(13): 2209-2220.
- Wasserthal, L.T. 1998. Deep flowers for long tongues. *Trends in Ecology and Evolution*, 13(11): 459-460.
- Wasserthal, L.T. 1997. The pollinators of the Malagasy star orchids *Angraecum sesquipedale*, *A.sororium* and *A.compactum* and the evolution of extremely long spurs by pollinator shift. *Botanica Acta*, 110: 343-359.
- Weller, S.J., D.P. Pashley, J.A. Martin and J.L. Constable. 1994. Phylogeny of noctuid moths and the utility of combining independent nuclear and mitochondrial genes. *Systematic Biology*, 43(2): 194-211.
- White, R.H., R.D. Stevenson, R.R. Bennet, D.E. Cutler and W.A. Haber. 1994. Wavelength discrimination and the role of ultraviolet vision in the feeding behavior of hawkmoths. *Biotropica*, 26(4): 427-435.
- Wiegmann, B.M., C. Mitter and B.D. Farrell. 1993. Diversification of carnivorous parasitic insects: extraordinary radiation or specialized dead end? *American Naturalist*, 142(5): 737-754.
- Wiens, J.J. 1998. Combining data sets with different phylogenetic histories. *Systematic Biology*, 47(4): 568-581.

- Wilkinson, M. 1996. Majority-rule reduced consensus trees and their use in bootstrapping. *Molecular Biology and Evolution*, 13(3): 437-444.
- Willmott A.P. and C.P. Ellington. 1997a. The mechanics of flight in the hawkmoth *Manduca sexta* .1. Kinematics of hovering and forward flight. *Journal of Experimental Biology*, 200(21): 2705-2722.
- Willmott A.P. and C.P. Ellington. 1997b. The mechanics of flight in the hawkmoth *Manduca sexta* .2. Aerodynamic consequences of kinematic and morphological variation. *Journal of Experimental Biology*, 200(21): 2723-2745.
- Willmott A.P., C.P. Ellington and A.L.R. Thomas. 1997. Flow visualization and unsteady aerodynamics in the flight of the hawkmoth, *Manduca sexta*. *Philosophical Transactions of the Royal Society of London, Biology*, 352(1351): 303-316.
- Winder, J.A. 1976. Ecology and control of *Erinnyis ello* and *E.alope*, important insect pests in the new world. *PANS*, 22(4): 449-466.
- Yack, J.E. and J.H. Fullard. 2000. Ultrasonic hearing in nocturnal butterflies. *Nature*, 403: 265-266.
- Yack, J.E. and J.H. Fullard. 1993a. Proprioceptive activity of the wing-hinge stretch receptor in *Maduca sexta* and other atympanate moths: a study of the noctuid moth ear B cell homologue. *Journal of Comparative Physiology*, 173: 301-307.
- Yack, J.E. and J.H. Fullard. 1993b. What is an insect ear?. *Annals of the Entomological Society of America*, 86(6): 677-682.
- Yang, Z. 1996. Phylogenetic analysis using parsimony and likelihood. *Journal of Molecular Evolution*, 42: 294-307.
- Yang, Z. 1994. Statistical properties of the maximum likelihood method of phylogenetic estimation and comparison with distance matrix methods. *Systematic Biology*, 43: 329-342.
- Yang, Z. 1993. Maximum-likelihood estimation of phylogeny from DNA sequences when substitution rates differ over sites. *Molecular Biology and Evolution*, 10(6): 1396-1401.
- Yeates, D.K. and B.M. Wiegmann. 1999. Congruence and controversy: toward a higher-level phylogeny of Diptera. *Annual Review of Entomology*, 44: 397-428.
- Young, A.M. 1972. Notes on a community ecology of adult sphinx moths in Costa Rican lowland tropical rain forest. *Caribbean Journal of Science*, 12(34): 151-163.

**Table 1. Selected life history contrasts between Sphingidae and Saturniidae (Lepidoptera: Bombycoidea).** Compiled from observations cited in Janzen (1984) and Bernays & Janzen (1988). Members of Smerinthinae generally share many life history traits with Saturniidae, despite strong morphological evidence for their inclusion in Sphingidae.

<i>Life History Parameter</i>	<b>SPHINGIDAE (Sphinginae&amp;Macroglossinae)</b>	<b>SATURNIIDAE &amp; SPHINGIDAE (Smerinthinae)</b>
<i>adult foraging &amp; feeding</i>	- constant diet of nectar and water (male & female)	- no adult feeding; nutrition from larval fat and water reserves
<i>proboscis</i>	- functional	- vestigial
<i>neural capacity</i>	- large head and eyes - memory	- small head and eyes
<i>adult lifespan</i>	- weeks	- days
<i>adult flight</i>	- streamlined wing shape - powerful, agile, sustained flight - speed dash escape behavior - seasonal migration - diurnal, matinal, crepuscular, nocturnal	- broad ornate wing shape - weak flight - varied avoidance maneuvers - no seasonal migration - crepuscular, nocturnal
<i>adult coloration</i>	- crypsis - hindwing flash coloration	- crypsis - mimetic & aposematic coloration
<i>intra/interspecific polymorphism</i>	- low (color, size, wing shape)	- high (color, size, wing shape)
<i>adult sexual dimorphism (size &amp; behavior)</i>	- reduced - female larger at eclosion, weights eventually equalize	- pronounced - female larger at eclosion and throughout development
<i>attraction to light</i>	- females arrive all night - male & female loosely attracted, stray - 10 males : 1 female	- females arrive before midnight - male and female tightly attracted, sessile - >100 males : 1 female
<i>mating</i>	- courtship & female choice mediated by male secondary sex organs - multiple female matings, days after female eclosion	- indiscriminate mating  - single female mating, immediately after eclosion
<i>egg maturation in female</i>	- continuous maturation - eggs 3X smaller than saturniids	- full complement at eclosion - eggs 3X larger than sphingids
<i>oviposition</i>	- single egg per oviposition event - weeks/months	- large egg clutch per oviposition - approx. 50% egg load in first night; remainder within 1 week
<i>time to egg hatch</i>	- fast: 4-8 days	- slow: 6-15 days
<i>larval development</i>	- fast: 2-5 weeks	- slow: 4-10 weeks
<i>larval defense</i>	- crypsis - eyespot mimicry - no sequestration	- crypsis - aposematic coloration - urticating spines and urticator mimicry
<i>larval mandibles</i>	- intricate morphology - masticating action	- simple morphology - snipping action
<i>larval relative head mass</i>	- twice that of saturniids	- half that of sphingids
<i>larval gut contents</i>	- intense processing of little material - heterogeneous, macerated particles - effectively digested into slurry	- light processing of ample material - large, homogeneous, intact particles - only edges effectively digested
<i>larval diet breadth</i>	- oligophagous - diverse range of growth forms	- polyphagous - few growth forms, especially trees
<i>larval hostplant syndrome</i>	- low density, low apparency - small, immature - high nutrition and water content - small toxic qualitative defensive chemicals	- high density, high apparency - large, mature - low nutrition and water content - large nontoxic quantitative defensive chemicals

**Table 2. Taxonomic classification and phylogenetic sequence of genera in SpHINGidae (Lepidoptera: Bombycoidea) presented by Kitching & Cadiou (2000).** Order of genera is approximately phylogenetic and matches that reported in Kitching & Cadiou 2000 (pp. 16-19); putative clades advocated by these authors indicated by nested vertical bars to the left of the genus name. Number of worldwide recognized species units within each genus, including distinct subspecies, indicated in 'ssp' column; single species names given for monotypic genera only. Genera for which specimens have been accessioned in the UMD Lepidoptera Collections and are available for molecular sequence collection marked with 'X' in the 'Coll' column. Genera for which EF and DDC sequence have been obtained indicated in the 'EF' and 'DDC' columns: asterisks mark sequences collected de novo in this study; 'R' marks sequences submitted to GenBank by Regier, et al. (2001); 'C' marks the sequence submitted to GenBank by Caterino, et al. (2001). Genera containing species which occur in North America (not necessarily endemics) are shaded, and were determined by consulting Hodges (1971) and Ferguson & Opler (1999).

Taxonomy	ssp	Genus	species	Genus Author	Synonyms	Coll	EF	DDC
Lepidoptera>Heteroneura>Ditrysia>Apoditrysia>Obtectomera>Macrolepidoptera>Bombycoidea>SPHINGIDAE								
SMERINTHINAE								
Smerinthini								
	4	<i>Langia</i>		Moore, 1872				
	8	<i>Laothoe</i>		Fabricius, 1807	Amorpha	X	*	*
	4	<i>Pachysphinx</i>		Rothschild & Jordan, 1903		X	*	*
	12	<i>Smerinthus</i>		Latreille, [1802]	Bebroptera,Bellia,Bellinca,Copi-smerinthus,Daddia,Dilina,Eurmer-inthus,Merinthus,Nicholsonia,Niia Calasymbolas	X	*R	*R
	5	<i>Paonias</i>		Hubner, [1819]		X	*R	*R
	1	<i>Poliodes</i>	<i>roseicornis</i>	Rothschild & Jordan, 1903				
	1	<i>Xenosphingia</i>	<i>jansel</i>	Jordan, 1920				
	3	<i>Ceridia</i>		Rothschild & Jordan, 1903				
	2	<i>Craspedortha</i>		Mell, 1922				
	1	<i>Parum</i>	<i>colligata</i>	Rothschild & Jordan, 1903				
	1	<i>Anambulyx</i>	<i>elwesi</i>	Rothschild & Jordan, 1903				
	38	<i>Marumba</i>		Moore, [1882]	Burrowsia,Kayeia,Sichia	X	*	*
	2	<i>Daphnusa</i>		Walker, 1856	Allodaphnusa			
	6	<i>Gynoeryx</i>		Carcasson, 1968				
	2	<i>Likoma</i>		Rothschild & Jordan, 1903				
	2	<i>Phyllosphingia</i>		Swinhoe, 1897	Clarkia,Clarkunella			
	1	<i>Amorpha</i>	<i>juglandis</i>	Hubner, [1819]	Cressonia	X	*	*
	2	<i>Mimas</i>		Hubner, [1819]	Lucena	X	*	*
	4	<i>Lophostethus</i>		Butler, 1876	Euclea			
	3	<i>Andriasa</i>		Walker, 1856	Devitzia,Pseudosmerinthus	X		
	1	<i>Microclanis</i>	<i>ertlangeri</i>	Carcasson, 1968				
	4	<i>Falcatula</i>		Carcasson, 1968				
	2	<i>Chloroclanis</i>		Carcasson, 1968		X		
	8	<i>Platysphinx</i>		Rothschild & Jordan, 1903				
	1	<i>Neoclanis</i>	<i>basalis</i>	Carcasson, 1968				
	1	<i>Afrosphinx</i>	<i>amabilis</i>	Carcasson, 1968				
	1	<i>Viriclanis</i>	<i>kingstoni</i>	Aarvik, 1999				
	7	<i>Rufoclanis</i>		Carcasson, 1968				
	2	<i>Coequosa</i>		Walker, 1856	Metamimas			
	2	<i>Rhodambulyx</i>		Mell, 1939				
	6	<i>Rhodoprasina</i>		Rothschild & Jordan, 1903				
	1	<i>Cypoides</i>	<i>chinensis</i>	Matsumura, 1921	Amorphulus			
	13	<i>Cypa</i>		Walker, [1865]				
	7	<i>Smerinthulus</i>		Huwe, 1895				
	2	<i>Degmaptera</i>		Hampson, 1896				
	1	<i>Grillotius</i>	<i>bergeri</i>	Rougeot, 1973				
	1	<i>Opistoclanis</i>	<i>hawkeri</i>	Jordan, 1929				
	2	<i>Agnosia</i>		Rothschild & Jordan, 1903				
	11	<i>Callambulyx</i>		Rothschild & Jordan, 1903				
	6	<i>Sataspes</i>		Moore, [1858]	Myodezia			
	1	<i>Afrosataspes</i>	<i>galleyi</i>	Basquin & Cadiou, 1986				
	1	<i>Pseudopolyptychus</i>	<i>foliaceus</i>	Carcasson, 1968				
	2	<i>Afroclanis</i>		Carcasson, 1968				
	2	<i>Malgassoclanis</i>		Carcasson, 1968				
	1	<i>Pseudandriasa</i>	<i>mutata</i>	Carcasson, 1968				
	2	<i>Rhadinopasa</i>		Karsch, 1891				
	5	<i>Leucophebia</i>		Westwood, 1847	Rasphele			
	1	<i>Leptoclanis</i>	<i>pulchra</i>	Rothschild & Jordan, 1903				
	10	<i>Phylloxiphia</i>		Rothschild & Jordan, 1903	Acentropoclanis,Libyoclanis, Typhosia			
	18	<i>Clanis</i>		Hubner, [1819]	Basiana,Metagates			
	1	<i>Clanidopsis</i>	<i>exusta</i>	Rothschild & Jordan, 1903				
	1	<i>Acanthosphinx</i>	<i>guessfeldti</i>	Aurivillius, 1891				
	10	<i>Neopolyptychus</i>		Carcasson, 1968				
	18	<i>Pseudoclanis</i>		Rothschild, 1894	Larunda	X	*	*
	7	<i>Polyptychoides</i>		Carcasson, 1968		X		
	44	<i>Polyptychus</i>		Hubner, [1819]		X		
	3	<i>Polyptychopsis</i>		Carcasson, 1968				
	1	<i>Lycosphingia</i>	<i>hamatus</i>	Rothschild & Jordan, 1903				
	1	<i>Avinoffia</i>	<i>hollandi</i>	Clark, 1929				

Table 2. (continued)

Taxonomy	ssp	Genus	species	Genus Author	Synonyms	Coll	EF	DDC	
Sphingulini	1	<i>Synoecha</i>	<i>marmorata</i>	Rothschild & Jordan, 1903					
	1	<i>Coenotes</i>	<i>eremophilae</i>	Rothschild & Jordan, 1903					
	1	<i>Hoplocnema</i>	<i>brachycera</i>	Rothschild & Jordan, 1903		X	*	*	
	1	<i>Tetrachroa</i>	<i>edwardsi</i>	Rothschild & Jordan, 1903					
	3	<i>Pentateucha</i>		Swinhoe, 1908					
	3	<i>Kentrochrysalis</i>		Staudinger, 1887	Centrochrysalis				
	7	<i>Dolbina</i>		Staudinger, 1877	Dolbinopsis, Elegodolba				
	1	<i>Sphingulus</i>	<i>mus</i>	Staudinger, 1887					
	1	<i>Monarda</i>	<i>oryx</i>	Druce, 1896					
	Ambulycini	63	<i>Ambulyx</i>		Westwood, 1847	Oxyambulyx			
1		<i>Barbourion</i>	<i>lemaii</i>	Clark, 1934					
6		<i>Amplapterus</i>		Hubner, [1819]	Calymnia, Compsogene				
1		<i>Compsulyx</i>	<i>cochereaui</i>	Holloway, 1979		X			
1		<i>Akbesia</i>	<i>davidi</i>	Rothschild & Jordan, 1903					
6		<i>Batocnema</i>		Rothschild & Jordan, 1903					
8		<i>Protambulyx</i>		Rothschild & Jordan, 1903	Ambulyx	X	*	*	
5		<i>Orecta</i>		Rothschild & Jordan, 1903					
16		<i>Adhemarius</i>		Oiticica Filho, 1939		X	*	*	
1		<i>Trogolegnum</i>	<i>pseudambulyx</i>	Rothschild & Jordan, 1903					
SPHINGINAE									
Sphingini	1	<i>Sagenosoma</i>	<i>elsa</i>	Jordan, 1946	Dictyosoma				
	2	<i>Dolbogone</i>		Rothschild & Jordan, 1903					
	1	<i>Dolba</i>	<i>hyloeus</i>	Walker, 1856		X	R	R	
	7	<i>Ceratonia</i>		Harris, 1839	Autogramma, Daremna, Isogramma	X	*R	*R	
	1	<i>Paratreia</i>	<i>plebeja</i>	Grote, 1903	Atreides, Atreus	X	*	*	
	56	<i>Sphinx</i>		Linnaeus, 1758	Gargantua, Herse, Hyloecus, Lethia, Lintneria, Mesosphinx, Spectrum	X	*R	*R	
	1	<i>Thamnoecha</i>	<i>uniformis</i>	Rothschild & Jordan, 1903					
	4	<i>Lapara</i>		Walker, 1856	Ellena, Exedrium	X	*R	*R	
	1	<i>Isoparce</i>	<i>cupressi</i>	Rothschild & Jordan, 1903					
	3	<i>Nannoparce</i>		Rothschild & Jordan, 1903					
	9	<i>Neogene</i>		Rothschild & Jordan, 1903					
	88	<i>Manduca</i>		Hubner, [1807]	Chlaenogramma, Diludia, Macroslita, Phlegethontius, Protoparce, Svzyzia	X	*R	*R	
	8	<i>Euryglottis</i>		Boisduval, [1875]		X	*	*	
	1	<i>Apocalypsis</i>	<i>velox</i>	Rothschild & Jordan, 1903					
	3	<i>Pseudodolbina</i>		Rothschild, 1894					
	3	<i>Praedora</i>		Rothschild & Jordan, 1903					
	1	<i>Ellenbeckia</i>	<i>monospila</i>	Rothschild & Jordan, 1903					
	1	<i>Litosphingia</i>	<i>corticea</i>	Jordan, 1920					
	2	<i>Hoplistopus</i>		Rothschild & Jordan, 1903					
	1	<i>Oligographa</i>	<i>juniperi</i>	Rothschild & Jordan, 1903					
	2	<i>Dovania</i>		Rothschild & Jordan, 1903		X			
	1	<i>Lomocyma</i>	<i>oegrapha</i>	Rothschild & Jordan, 1903					
	4	<i>Panogena</i>		Rothschild & Jordan, 1903					
	6	<i>Macropoliana</i>		Carcasson, 1968					
	5	<i>Poliana</i>		Rothschild & Jordan, 1903	Taboribia				
	14	<i>Meganoton</i>		Boisduval, [1875]					
	5	<i>Psilogramma</i>		Rothschild & Jordan, 1903		X	*	*	
	1	<i>Leucomonia</i>	<i>bethia</i>	Rothschild & Jordan, 1903					
	3	<i>Pantophaea</i>		Jordan, 1946					
	2	<i>Xanthopon</i>		Rothschild & Jordan, 1903					
	1	<i>Amphimoea</i>	<i>walkeri</i>	Rothschild & Jordan, 1903					
	1	<i>Neococytius</i>	<i>cluentius</i>	Hodges, 1971		X		*	
	6	<i>Cocytius</i>		Hubner, [1819]	Amphonyx, Ancistrognathus	X	*	*	
	Acherontini	2	<i>Megacorma</i>		Rothschild & Jordan, 1903				
		6	<i>Agrius</i>		Hubner, [1819]	Timoria	X	*	*
		1	<i>Callosphingia</i>	<i>circe</i>	Rothschild & Jordan, 1916				
		5	<i>Coelonia</i>		Rothschild & Jordan, 1903		X	*	*
		4	<i>Acherontia</i>		[Laspeyres], 1809	Atropos, Brachyglossa, Manduca	X	*	*
	MACROGLOSSINAE								
	Dilophonotini	Dilophonotina	9	<i>Cautethia</i>		Grote, 1865	Braesia, Oenosanda	X	*
1			<i>Himantoides</i>	<i>undata</i>	Butler, 1876				
7			<i>Pachygonidia</i>		Fletcher, 1982	Pachygonia			
11			<i>Enyo</i>		Hubner, [1819]	Epister, Triptogon	X	*	*
7			<i>Aleuron</i>		Boisduval, 1870	Callenyo, Gonenyo, Tylognathus			
4			<i>Unzela</i>		Walker, 1856	Comipalpus	X	*	*
15			<i>Callionima</i>		Lucas, 1857	Callionima, Euecheryx	X	*	*
7			<i>Madoryx</i>		Boisduval, [1875]				
2			<i>Stolidoptera</i>		Rothschild & Jordan, 1903				
1			<i>Protaleuron</i>	<i>rhodogaster</i>	Rothschild & Jordan, 1903				
4			<i>Pachylia</i>		Walker, 1856		X	*	*
1			<i>Kloneus</i>	<i>babayaga</i>	Skinner, 1923	Oberthuerion			
1			<i>Pachylioides</i>	<i>resumens</i>	Hodges, 1971				
2			<i>Oryba</i>		Walker, 1856				
4			<i>Hemeroplanes</i>		Hubner, [1819]	Leucorhampha			

Table 2. (continued)

Taxonomy	ssp	Genus	species	Genus Author	Synonyms	Coll	EF	DDC
Hemarina	21	<i>Nyceryx</i>		Boisduval, [1875]		X	*	*
	1	<i>Baniwa</i>	<i>yavitensis</i>	Lichy, 1981				
	16	<i>Perigonia</i>		Herrich-Schäffer, [1854]	Stenolophia	X	*	*
	3	<i>Eupyrhroglossum</i>		Grote, 1865				
	9	<i>Aelopus</i>		Hubner, [1819]		X	*R	*R
	1	<i>Pseudosphinx</i>	<i>tetrio</i>	Burmeister, 1855	Macrosila			
	18	<i>Isognathus</i>		Felder & Felder, 1862	Tatoglossum	X	*	*
	16	<i>Erinnys</i>		Hubner, [1819]	Anceryx, Dilophonota	X	*	*
	1	<i>Phryxus</i>	<i>caicus</i>	Hubner, [1819]	Grammodia			
	20	<i>Hemaris</i>		Dalman, 1816	Aege, Chamaesesia, Cochrania, Haemorrhagia, Hemaria, Jilinga, Mandarina, Saundersia	X	*R	*R
	24	<i>Cephonodes</i>		Hubner, [1819]	Potidaca	X	*	*
Philampelini	32	<i>Eumorpha</i>		Hubner, [1807]	Argaea, Dupo, Philampelus, Pholus	X	*R	*R
	1	<i>Tinostoma</i>	<i>smaragditi</i>	Rothschild & Jordan, 1903				
Macroglossini								
Macroglossina	2	<i>Sphecodina</i>		Blanchard, 1840	Brachynota, Maredus, Thyreus	X	R	R
	7	<i>Proserpinus</i>		Hubner, [1819]	Dienees, Lepisiesia, Pogocolon, Pteroxon, Pteropoxon	X	C	
	1	<i>Amphion</i>	<i>floridensis</i>	Hubner, [1819]				
	1	<i>Arctonotus</i>	<i>lucidus</i>	Boisduval, 1852				
	3	<i>Euproserpinus</i>		Grote & Robinson, 1865				
	7	<i>Neogurelca</i>		Hogenes & Treadaway, 1993				
	8	<i>Sphingonaepiopsis</i>		Wallengren, 1858	Pterodonta			
	1	<i>Microsphinx</i>	<i>pumilum</i>	Rothschild & Jordan, 1903				
	2	<i>Odontosida</i>		Rothschild & Jordan, 1903				
	9	<i>Antinephele</i>		Holland, 1889				
	4	<i>Hypaedalea</i>		Butler, 1877				
	1	<i>Pseudenyo</i>	<i>benitensis</i>	Holland, 1889				
	72	<i>Temnora</i>		Walker, 1856	Aspledon, Diodosida, Eulophura, Gurelca, Lophura, Lophuron, Ocvton	X		
	1	<i>Temnoripais</i>	<i>lasti</i>	Rothschild & Jordan, 1903				
	26	<i>Nephele</i>		Hubner, [1819]	Omeus, Zonilia	X		
	3	<i>Maassenia</i>		Sallmuller, 1884				
	5	<i>Angonyx</i>		Boisduval, [1875]				
	8	<i>Rethera</i>		Rothschild & Jordan, 1903	Borshomia			
	2	<i>Cizara</i>		Walker, 1856	Abrisa, Microlophia			
	2	<i>Hayesiana</i>		Fletcher, 1982	Rhodossoma			
	7	<i>Eurypteryx</i>		R. Felder, [1874]	Indiana			
	1	<i>Giganteopalpus</i>	<i>mirabilis</i>	Huwe, 1895				
	6	<i>Gnathothlibus</i>		Wallengren, 1858	Chromus			
	1	<i>Philodila</i>	<i>astyanor</i>	Rothschild & Jordan, 1903				
	14	<i>Daphnis</i>		Hubner, [1819]	Histriosphinx, Regia	X	*	*
	5	<i>Ampelophaga</i>		Bremer & Grey, 1853				
	2	<i>Clarina</i>		Tutt, 1903	Berutana			
	4	<i>Darapsa</i>		Walker, 1856	Ampeloeca, Otus	X	*R	*R
	30	<i>Eupanacra</i>		Cadiou & Holloway, 1989				
	3	<i>Enpinanga</i>		Rothschild & Jordan, 1903				
	2	<i>Elibia</i>		Walker, 1856				
	1	<i>Acosmerycoides</i>	<i>harterti</i>	Mell, 1922				
	1	<i>Deidamia</i>	<i>inscriptum</i>	Clemens, 1859	Tricholon			
	16	<i>Acosmeryx</i>		Boisduval, [1875]				
	1	<i>Micracosmeryx</i>	<i>chaochauensis</i>	Mell, 1922				
	1	<i>Lepchina</i>	<i>tridens</i>	Oberthur, 1904				
	1	<i>Thibetia</i>	<i>niphaphylla</i>	Joicey & Kaye, 1917				
	6	<i>Gehlenia</i>		Bryk, 1944				
	1	<i>Dahira</i>	<i>rubiginosa</i>	Moore, 1888				
	1	<i>Atemnora</i>	<i>westermanni</i>	Rothschild & Jordan, 1903				
	111	<i>Macroglossum</i>		Scopoli, 1777	Bombylia, Macroglossa, Psithyros, Rhamphoschisma, Rhamphopsveche	X	*	*
	2	<i>Leucostrophus</i>		Rothschild & Jordan, 1903				
Choerocampina	96	<i>Xylophanes</i>		Hubner, [1819]	Deilonche, Dilonche, Isoples	X	*R	*R
	1	<i>Phanoxyta</i>	<i>hystrix</i>	Rothschild & Jordan, 1903				
	42	<i>Hyles</i>		Hubner, [1819]	Celerio, Danneria, Eremohyles, Hawaiina, Hippohyles, Rommeliana, Surholtia, Thaumias, Tumeria, Weismannia	X	*R	*R
	2	<i>Rhodaфра</i>		Rothschild & Jordan, 1903				
	5	<i>Deilephila</i>		[Laspeyres], 1809	Choerocampa, Cinogon, Dilephila, Elpenor, Eumorpha, Metopsilus	X	*	*
	5	<i>Basiothia</i>		Walker, 1856		X	*	*
	4	<i>Chaerocina</i>		Rothschild & Jordan, 1903		X		
	3	<i>Euchloron</i>		Boisduval, [1875]	Chlorina	X		
	43	<i>Hippotion</i>		Hubner, [1819]	Lilina, Panacra	X	*	*
	2	<i>Centroctena</i>		Rothschild & Jordan, 1903				
	1	<i>Pergesa</i>	<i>acteus</i>	Walker, 1856	Rhyncholaba			
	59	<i>Theretra</i>		Hubner, [1819]	Florina, Gnathostypis, Hathia, Oreus	X	*	*
	2	<i>Griseosphinx</i>		Cadiou & Kitching, 1990				
	19	<i>Rhagastis</i>		Rothschild & Jordan, 1903				
	11	<i>Cechenena</i>		Rothschild & Jordan, 1903				

**Table 3. Elongation Factor 1-alpha (EF) Primers.** Compilation of select oligonucleotide primers developed in the Regier Lab and used to amplify EF (i) across Arthropoda and (ii) within Lepidoptera. Primers are grouped into pairs generating overlapping fragments which have been successfully assembled to obtain continuous sequence for this gene. 'f' suffix in the Primer Name denotes forward primer, which anneals to the antisense strand and promotes synthesis of the sense strand. 'rc' prefix or suffix in the Primer Name denotes reverse primer, which anneals to the sense strand and promotes synthesis of the antisense strand. First four primer pairs were used in this study (abbreviated p, A', E and C), nested within purified templates obtained by reverse transcription with m41.21rc (marked with an asterisk). (iii) lists the forward and reverse M13 primers used in sequencing reactions. 'Position in Figure 4' denotes coordinate of the 5' end of the primer relative to the sense strand in the *Bombyx mori* EF reference sequence shown in Figure 4; coordinate '1' corresponds to the 66<sup>th</sup> nucleotide in the original GenBank accession D13338. Oligonucleotide primer sequence is written 5' to 3', irrespective of orientation in Figure 4 (i.e., reverse primers can be oriented by taking their reverse complement). 'Notes': (a) 30f is a more degenerate version of M3; (b) replacing m40.71f with m40.6f generates an amplicon 42 bp longer; (c) m52f is a more degenerate version of M51.9.

Primer Name	Sequence (5' ⇒ 3')	Primer Length	Position in Figure 4	Note	Fragment Size
(i) Regier & Shultz (1997)					
30f	CAY ATY AAY ATH GTS GTI ATH GG	23	1	a	449 (p)
m45.71rc	TCC ATY TTR TTN CAN SCN AC	20	449		
m40.6f	ATY GAR AAR TTY GAR AAR GAR GC	23	97	b	656 (A')
m52rc	CCD ATY TTR TAN ACR TCY TG	20	752		
m45.71f	GTN GSN GTN AAY AAR ATG GA	20	430		656 (E)
m53.5rc	ATR TGV GMN GTR TGR CAR TC	20	1085		
m52f	CAR GAY GTN TAY AAR ATH GG	20	733	c	542 (C)
*m41.21rc	TGY CTC ATR TCD CGV ACR GCR AA	23	1274		
m40.71f	TCN TTY AAR TAY GCN TGG GT	20	139	b	na
m52.4f	TCN GTN GAR ATG CAY CAY G	19	853		
(ii) Cho, <i>et al.</i> (1995)					
M3	CAC ATY AAC ATT GTC GTS ATY GG	23	1	a	282
rcM44.9	CTT GAT GAA ATC YCT GTG TCC	21	282		
M44.1	GCT GAG CGY GAR CGT GGT ATC AC	23	175		411
rcM51.1	CAT RTT GTC KCC GTG CCA KCC	21	585		
M46.1	GAG GAA ATY AAR AAG GAA G	19	484		392
rcM52.6	GCY TCG TGG TGC ATY TCS AC	20	875		
M51.9	CAR GAC GTA TAC AAA ATC GG	20	733	c	356
rcM53.2	GCA ATG TGR GCI GTG TGG CA	20	1088		
M52.7	GTC AAG GAR YTG CGT CGT GG	20	931		356
rcM4	ACA GCV ACK GTY TGY CTC ATR TC	23	1286		
(iii) M13 Sequencing Primers					
M13-21	TGT AAA ACG ACG GCC AGT	18	-		-
M13-rev	CAG GAA ACA GCT ATG ACC	18	-		-

IUPAC Ambiguity Codes: R=AG, Y=CT, M=AC, K=GT, S=CG, W=AT | H=ACT, B=CGT, V=ACG, D=AGT | N=ACGT | I=inosine



**Table 4. Dopa Decarboxylase (DDC) Primers.** Exhaustive compilation of oligonucleotide primers developed in the Regier Lab and used historically to amplify DDC across Arthropoda. Primers are sorted by position along the reference sequence in Figure 5, and alternate versions of a single primer are grouped together. ‘F’ suffix in the Primer Name denotes forward primer, which anneals to the antisense strand and promotes synthesis of the sense strand. ‘R’ suffix in the Primer Name denotes reverse primer, which anneals to the sense strand and promotes synthesis of the antisense strand. Primers used in this study are marked with an asterisk (\*) and those used in the RT phase are marked with \*\*. Primers preferred in Regier Lab protocols are marked with a cross (†) and those used in the RT phase are marked with ‡. Oligonucleotide primer sequence is written 5’ to 3’, irrespective of orientation in Figure 5 (i.e., reverse primers can be oriented by taking their reverse complement). Underlined nucleotides mark sites of mismatch with the *Manduca sexta* DDC sequence (GenBank accession U03909). Bases at these positions exhibit high variability across Lepidoptera in multiple sequence alignments, so conflict with *Manduca* was not unexpected. Italicized bases indicate cases in which degeneracy has been increased at that position in past primer orders (e.g., I substituted for N; N substituted for B). Stricken 7.5sR primer contains an error (underlined).

Primer Name	Sequence (5' ⇒ 3')	Primer Length	Position in Figure 5	Ref	Note
* 1.0F	TTY AAR GAY TTY GCW AAR RCD ATG	24	1	2	a
1.1nF	ACI GAY TAY ATH RCI GAN T	19	25	5	
M1.1F	<u>G</u> GAC TAY ATC <u>GCG</u> <u>GAA</u> TAT <u>TTG</u> G	23	27	5	b
† 1.1vF	GAY TAY ATY RCR GAR TA	17	28	5	
† 1.2F	GAR AAY ATY AGA GAY AGR CAR GT	23	49	5	
1.4F	TTT <u>CAT</u> <u>GCT</u> TAT TTT <u>CCT</u> <u>ACT</u> GC	23	211	1	c
* 1.7F	GCT ATT GCT TGT ATT GGT TTT ACT TGG AT	29	274	1	
† 1.7sF	GCH TGY ATY GGN TTY WCN TGG AT	23	280	4	d
1.7dF	GCY TGY ATY GGW TTY ACY TGG AT	23	280	1	
† 1.8R	CAT NAC NAC YTC IAR YTC IGT RCA	24	316	5	
† 1.9sF	ATG HTN GAY TGG YTV GGY CAR ATG	24	337	4	
* 1.9dF	ATG YTR GAY TGG YTR GGY CAR ATG	24	337	1	
1.9'dF	GAY TGG CTN GGN CAR ATG	18	343	2	e
‡ 1.9sR	CAT YTG RCC BAR CCA RTC NAD CAT	24	337	[4]	
* 1.9dR	CAT YTG RCC TAR CCA RTC YAR CAT	24	337	2	
† 3.2sF	TGG YTN CAY GTN GAY GCN GCN TAY GC	26	784	4	
* 3.2dF	TGG YTR CAY GTS GAY GCD GCY TAY GC	26	784	1	f
3.2dR	TAR GCH GCR TCS ACR TGY ARC CA	23	806	1	
† 3.3sF	TTY AAY TTY AAY CCN CAY AAR TGG	24	874	[4]	
3.3'F	AAY TTY AAY CCN CAY AAR TGG	21	877	2	g
*† 3.3sR	CCA YTT RTG NGG RTT RAA RTT RAA	24	874	4	
3.3R	CCA YTT RTG NGG RTT RAA RTT	21	877	2	
**† 4sR	GGD <u>ATY</u> TGC CAR TGH CKR TAR TC	23	1012	4	
4ddR	GGK <u>ATY</u> TGC CAR TGM CGR TAR TC	23	1012	1	h
** 4dnR	GGG <u>ATT</u> TGC CAR TGA CGR TAR TC	23	1012	1	
7.0sR	GTR AAN CGN GAR CAD ATN GC	20	1324	3	i
7.5R	TCC CAR GAN ACR TGV ATR TC	20	1354	2	
**† 7.5sR	TCC CAN GAN ACR TGV ATR TC	20	1354	3	j
7.5sR	TCC CAN GAN ACR TGV <u>TAR</u> TC	20	1354	x	
M13-21	TGT AAA ACG ACG GCC AGT	18	-	-	
M13-rev	CAG GAA ACA GCT ATG ACC	18	-	-	

#### Table 4 (continued)

IUPAC Ambiguity Codes: R=AG, Y=CT, M=AC, K=GT, S=CG, W=AT | H=ACT, B=CGT, V=ACG, D=AGT | N=ACGT | I=inosine

'Position in Figure 5' denotes coordinate of the 5' end of the primer relative to the sense strand in the *Manduca sexta* DDC reference sequence shown in Figure 5; coordinate '1' corresponds to the 192nd nucleotide in the original GenBank accession U03909.

References: (1) Fang, *et al.* (1997); (2) Friedlander, *et al.* (1998); (3) Mitchell (1998); (4) Mitchell, *et al.* (2000); (5) Regier Lab Optimized Protocols.

#### Notes:

- (a) 1.0F primer nt15 (W) conflicts with G at position 206 in U03909.
- (b) 1.1vF is the least degenerate and most consistent version of this primer. Version 1.1nF (unknown author) includes an extra 3nt at the 5' end and excludes 1nt at the 3' end. Version M1.1F (unknown author) includes an extra 1nt at the 5' end and 5nt at the 3' end, and has five direct conflicts with U03909: G at primer nt1 with T at position 218; G's at nt11&13 with A's at positions 228&230; A at nt16 with G at position 233; and T at nt20 with C at position 237.
- (c) 1.4F is anchored at position 424 (3' end), according to Table 2 (Fang 1997, p. 272). In this orientation, T's at primer nt3,6,9&15 conflict with C's at positions 404,407,410&416 in U03909; and T's at primer nt18&21 conflict with G's at positions 419&422 in U03909.
- (d) Version 1.7dF is nested entirely within 1.7F (6nt shorter on the 5' end) and incorporates more degeneracy. Version 1.7sF is a more degenerate version of 1.7dF.
- (e) Version 1.9sF retains a purine (V = C+R) at nt15, but R conflicts with C at position 542 in U03909. Is this possibly a carryover error from version 1.9dF (Fang 1997)? Version 1.9'dF (Friedlander 1998) is nested entirely within 1.9dF (6nt shorter on the 5' end) and slightly more degenerate. Version 1.9sRC (Mitchell 2000) slightly increases degeneracy at nt10,19&21, relative to 1.9dRC.
- (f) 3.2dRC is the reverse complement of 3.2dF, excluding 3nt on the 5' end (i.e., it ends at nt997 in U03909).
- (g) Version 3.3sRC includes an additional 3nt on 3' end relative to 3.3RC (Friedlander 1998). Version 3.3sF is simply the reverse complement of 3.3sRC (Mitchell 2000), and includes an additional 3nt on 5' end relative to 3.3'F (Friedlander 1998).
- (h) Version 4ddRC is a slightly more degenerate version of 4dnRC, but G or K at primer nt3 in both 4dnRC and 4ddRC conflicts with the T complement at position 1223 in U03909. Version 4sRC incorporates more degeneracy, and retains the keto (D = A+K) at primer nt3 which does not complement with T at position 1223 in U03909.
- (i) "Two additional DDC primers, allowing the amplification of an extra 312 bp or 342 bp of the 3'-end of DDC, became available during this study. These primers are 7.0sRC (5'-GTR AAN CGN GAR CAD ATN GC-3') and 7.5sRC (5'-TCC CAN GAN ACR TGV ATR TC-3'), respectively." (Mitchell 1998, p. ???)
- (j) Version 7.5sRC replaces R with N at nt6 to slightly increase degeneracy relative to 7.5RC. Note that a typo in some versions of 7.5sRC switches **AT** to **TA** at primer nt16-nt17 (TCC CAN GAN ACR TGV **TAR** TC; unknown author).

**Table 5. Amplification strategies for DDC employed (a) in this study and (b) in the Regier Lab.** Primers are grouped into pairs generating overlapping fragments which have been successfully assembled to obtain continuous sequence for DDC. Primer pairs used in RT-PCR and nested PCR phases of amplification are indicated separately. 'Fragment Size' indicates the amplicon size for each primer pair along with amplicon abbreviation in parentheses, where a naming convention has been established. Table 4 describes all other notations and presents more detailed information about individual DDC primers.

(a) Primer pairs employed in this study

Primer Name	Sequence (5' ⇒ 3')	Primer Length	Position in Figure 5	Ref	Fragment Size
<i>RT-PCR Amplification</i>					
1.0F	TTY AAR GAY TTY GCW AAR RCD ATG	24	1	2	1,373
7.5sR	CAT YTG RCC BAR CCA RTC NAD CAT	24	1354	[4]	
1.0F	TTY AAR GAY TTY GCW AAR RCD ATG	24	1	2	1,034
4dnR	GGG ATT TGC CAR TGA CGR TAR TC	23	1012	1	
3.2dF	TGG YTR CAY GTS GAY GCD GCY TAY GC	26	784	1	590
7.5sR	TCC CAN GAN ACR TGV ATR TC	20	1354	3	
<i>Nested PCR Reamplification</i>					
1.0F	TTY AAR GAY TTY GCW AAR RCD ATG	24	1	2	360 (X)
1.9dR	CAT YTG RCC TAR CCA RTC YAR CAT	24	337	2	
1.7F	GCT ATT GCT TGT ATT GGT TTT ACT TGG AT	29	274	1	624 (Y)
3.3sR	CCA YTT RTG NGG RTT RAA RTT RAA	24	874	4	
3.2dF	TGG YTR CAY GTS GAY GCD GCY TAY GC	26	784	1	590 (Z)
7.5sR	TCC CAN GAN ACR TGV ATR TC	20	1354	3	
1.9dF	ATG YTR GAY TGG YTR GGY CAR ATG	24	337	1	698 (W)
4sR	GGD ATY TGC CAR TGH CKR TAR TC	23	1012	4	

(b) Primer pairs employed in Regier Lab protocols

Primer Name	Sequence (5' ⇒ 3')	Primer Length	Position in Figure 5	Ref	Fragment Size
<i>RT-PCR Amplification</i>					
1.1vF	GAY TAY ATY RCR GAR TA	17	28	5	333 (A)
1.9sR	CAT YTG RCC BAR CCA RTC NAD CAT	24	337	[4]	
1.7sF	GCH TGY ATY GGN TTY WCN TGG AT	23	280	4	755 (B)
4sR	GGD ATY TGC CAR TGH CKR TAR TC	23	1012	4	
3.2sF	TGG YTN CAY GTN GAY GCN GCN TAY GC	26	784	4	590 (C)
7.5sR	TCC CAN GAN ACR TGV ATR TC	20	1354	3	
<i>Nested PCR Reamplification</i>					
1.1vF	GAY TAY ATY RCR GAR TA	17	28	5	312 (z)
1.8R	CAT NAC NAC YTC IAR YTC IGT RCA	24	316	5	
1.7sF	GCH TGY ATY GGN TTY WCN TGG AT	23	280	4	618 (y)
3.3sR	CCA YTT RTG NGG RTT RAA RTT RAA	24	874	4	
1.9sF	ATG HTN GAY TGG YTV GGY CAR ATG	24	337	4	698 (w)
4sR	GGD ATY TGC CAR TGH CKR TAR TC	23	1012	4	
3.3sF	TTY AAY TTY AAY CCN CAY AAR TGG	24	874	[4]	500 (v)
7.5sR	TCC CAN GAN ACR TGV ATR TC	20	1354	3	

IUPAC Ambiguity Codes: R=AG, Y=CT, M=AC, K=GT, S=CG, W=AT | H=ACT, B=CGT, V=ACG, D=AGT | N=ACGT | I=inosine

**Table 6. RT-PCR and Nested PCR reaction conditions.** Composition of individual reverse transcription (RT) reactions and subsequent polymerase chain reactions (PCR) is presented in (a) and (b), respectively. Concentration of stock components, volume of that stock added to a single reaction, and the resulting final component concentration in each reaction is given separately for each gene. RT thermal cycling conditions were identical for both genes and consisted of a 42C incubation for 35 minutes followed by a 99C incubation for 5 minutes. Touchdown thermal cycling parameters used in the PCR portion of these RT-PCR reactions were also identical for both genes, and are presented in (c). Composition of individual Nested PCR reactions and thermal cycling conditions are presented separately for each gene in (d) and (e), respectively.

(a) Composition of RT reactions

Component	[stock]	EF		DDC	
		Volume	[reaction]	Volume	[reaction]
MgCl <sub>2</sub>	25 mM	2.0uL	5mM	2.0uL	5mM
dNTP	10mM ea	2.0uL	2mM ea	2.0uL	2mM ea
PCR Buffer	10X	1.0uL	1X	1.0uL	1X
RT primer	20uM	1.0uL	2uM	1.5uL	3uM
RNase Inhibitor	20U/uL	0.5uL	1U/uL	0.5uL	1U/uL
Reverse Transcriptase	50U/uL	0.5uL	2.5U/uL	0.5uL	2.5U/uL
Purified Water	-	2.9uL	-	2.0uL	-
Nucleic Acid extract	-	0.1uL	-	0.5uL	-
<b><i>total RT reaction</i></b>		<b><i>10.0uL</i></b>		<b><i>10.0uL</i></b>	

(b) Composition of PCR reactions

Component	[stock]	EF		DDC	
		Volume	[reaction]	Volume	[reaction]
MgCl <sub>2</sub>	25 mM	3.0uL	2.5mM	4.0uL	3mM
PCR Buffer	10X	4.0uL	1X	4.0uL	1X
forward primer	20uM	1.25uL	0.5uM	2.5uL	1uM
reverse primer	20uM	0.5uL	0.6uM	1.25uL	0.9uM
AmpliTaq DNA Polymerase with TaqStart Antibody	5U/uL 7uM	0.5uL	0.05U/uL 0.07uM	0.5uL	0.05U/uL 0.07uM
Purified Water	-	30.75uL	-	27.75uL	-
RT reaction contents	-	10uL	-	10uL	-
<b><i>total RT reaction</i></b>		<b><i>50.0uL</i></b>		<b><i>50.0uL</i></b>	

**Table 6. (continued)****(c) Touchdown PCR thermal cycling parameters**

<b>Phase</b>	<b>first 25X cycles</b>		<b>last 13X cycles</b>	
	<b>Temp (°C)</b>	<b>Time (sec)</b>	<b>Temp (°C)</b>	<b>Time (sec)</b>
Denaturation	94	30	94	30
Annealing	55 (-0.4/cycle)	30	45	30
Extension	72	60 (+2/cycle)	72	120 (+3/cycle)

**(d) Composition of nested PCR reactions**

<b>Component</b>	<b>[stock]</b>	<b>EF or DDC</b>	
		<b>Volume</b>	<b>[reaction]</b>
MgCl <sub>2</sub>	25 mM	4.0uL	2.0mM
PCR Buffer	10X	5.0uL	1X
dNTP	10mM (each)	1.0uL	0.2mM (each)
forward primer	20uM	1.25uL	0.5uM
reverse primer	20uM	1.25uL	0.5uM
AmpliTaq DNA Polymerase with TaqStart Antibody	5U/uL 7uM	0.5uL	0.05U/uL 0.07uM
Purified Water	-	36uL	-
gel pure RT-PCR template	-	1.0uL	-
<b><i>total RT reaction</i></b>		<b><i>50.0uL</i></b>	

**(e) Nested PCR thermal cycling parameters**

<b>Phase</b>	<b>EF</b>		<b>DDC</b>	
	<b>22X cycles</b>		<b>22X cycles</b>	
	<b>Temp (°C)</b>	<b>Time (sec)</b>	<b>Temp (°C)</b>	<b>Time (sec)</b>
Denaturation	94	30	94	30
Annealing	60	30	50	30
Extension	72	60 (+2/cycle)	72	60 (+2/cycle)

**Table 7. Survey of GenBank accessions for EF and DDC across Lepidoptera.**

Number of hits recovered from various search strings requesting (a) EF or (b) DDC sequences for all Lepidoptera in the NCBI GenBank Nucleotides Database, entered into the Entrez Search Engine on 06 April 2004. General format of each search string was “<gene> AND <taxon>[organism]”. Distribution of hits across Superfamilies, Families and Genera indicates the range of taxonomic diversity recovered from each search string. Compiling results from several searches results in a more exhaustive exploration of database contents.

(a) GenBank hits to EF in Lepidoptera

<b>Search String</b>	<b>Hits</b>	<b>Superfamilies</b>	<b>Families</b>	<b>Genera</b>
"elongat* AND lepidopt*[organism]"	<b>419</b>	9	20	248
"elong* fact* AND lepidopt*[organism]"	<b>417</b>	9	20	247
"EF AND lepidopt*[organism]"	<b>259</b>	9	17	184

(b) GenBank hits to DDC in Lepidoptera

<b>Search String</b>	<b>Hits</b>	<b>Superfamilies</b>	<b>Families</b>	<b>Genera</b>
"dopa AND lepidopt*[organism]"	<b>238</b>	13	26	150
"decarboxylas* AND lepidopt*[organism]"	<b>237</b>	10	25	148
"dopa decarb* AND lepidopt*[organism]"	<b>234</b>	10	25	148
"DDC AND lepidopt*[organism]"	<b>133</b>	3	8	81



Table 8. (continued)

Taxonomy	Genus	species	UMD Accession	Taxon Label	type	sex	Locality	country	Date	Collector / Determiner	Notes	Wing <sup>V</sup>	Extr. Date	Extr. Tissue	EF	DDC			
SMERINTHINAE	Amblycini	<i>Atheremis</i>	JKA-02-1642	Atheremis1642	A	na	Tumzambale, San Luis Potosi	Mexico	6Aug02	Adams, JK		1642	15Jan03	head	*	*			
		<i>Proamblyx</i>	WJK-03-1945	Proamblyx1945	A	na	Mocosa-Santiago Province (1270m)	Ecuador	1Jan03	Kelly, WJ & Wolfe, KL		1945	25Feb03	head & proborax	*	*			
	Smerinthini	<i>Amerpha</i>	Juglandis	CWB-02-1595	Amerpha1595	A	na	Concan, Uvalde Co., Texas	USA	6Sep02	Bordelon, CW & Knudson, EC	these specimens stored together, partially submerged in EOH	1595	15Jan03	head	*	*		
		<i>Leucost</i>	populi	UK-02-0012	Leucost0012	A	M	London, SE3	England	1999	Goddell, G & Kitching, UJ	emerged March 2000 (obtained from BMNH, 18Nov02)	na	25Feb03	head, portion	*	*		
		<i>Merumba</i>	quercus	UK-02-0118	Merumba0118	A	F	Provence, near Toulon	France	2000	Pitaway, AR & Kitching, UJ	head	na	25Feb03	head & proborax	*	*		
		<i>Mimas</i>	tiliae	UK-02-5836	Mimas5836	A	M	London, Raynes Park	England	2001	Kitching, UJ	UK accession no. 69536 (obtained from BMNH, 18Nov02)	5836	25Feb03	proborax	*	*		
		<i>Pachyphax</i>	mederae	(RSP-96-0626)	PachyphaxGB	A	F	Denver, Colorado	USA	1Jul96	Pegler, RS		na	27Sep00	thorax	AF234573	na		
		<i>Pa.</i>	occidentalis	JPT-02-1528	Pachyphax1528	A	na	Paragonia Mtns, Santa Cruz Co., Arizona	USA	20Jan02	Tuttle, JP		1528	4Feb03	head & proborax	*	*		
		<i>Pentias</i>	excelsa	(CWM-96-0573)	PentiasGB	A	na	Malinas, West Virginia	USA	8Jul96	Mittler, CW	specimens from live	na	27Sep00	thorax	AF234572	na		
		<i>Pa.</i>	myops	JPT-02-1540	Pentias1540	A	na	Atascosa Mtns, Santa Cruz Co., Arizona	USA	26Jul02	Mooney, B & Moore, J & Tuttle, UJ	white residue in vial	1540	27Feb03	proborax	*	*		
		<i>Pseudocentis</i>	paucica	UK-02-5839	Pseudocentis5839	A	M	unknown	South Africa	2000	Kitching, UJ	ex head stock, UK accession no. 695839 (obtained from BMNH, 18Nov02)	5839	27Feb03	head & proborax	*	*		
		<i>Smerinthus</i>	centyl	(JJK-95-0827)	SmerinthusGB	P	na	Hull, Portage Co., Wisconsin	USA	28May95	Kruec, JJ	w/1 female complete at LV light, ex. ovoviparous July-Aug 1995 and from pupae 1995	na	14Mar00	thorax	AF234576	AF234595		
		<i>Sm.</i>	saliceti	JBW-02-1511	Smerinthus1511	A	na	Santa Rita Mtns, Pima Co., Arizona (1067m)	USA	2Aug02	Walsh, B	specimens listed as 100% EOH, shipped cold but delayed in shipping for 10 days	1511	6Feb03	head & proborax	*	*		
		<i>Hoplacroma</i>	brachycera	MIM-96-0233	Hoplacroma0233	A	na	NT, SA or ACT	Australia	1996	Matthews, MJ		na	6Feb03	proborax	*	*		
		SPHINGINAE	Acherontini	<i>Acheronia</i>	UK-02-5989	Acheronia5989	A	M	Palawan, Bataraza, Malibud	Philippines	1Jul01	Zwick, A & Kitching, UJ	head ex. larva, UK accession no. 69989 (obtained from BMNH, 28Nov02)	na	27Feb03	proborax	*	*	
				<i>Agrus</i>	WJK-02-1941	Agrus1941	A	na	Blackberry Mountain, Gilmer Co., Georgia	USA	22Sep02	Kelly, WJ	collected at mercury vapor light	1941	15Jan03	head	*	*	
			Sphingini	<i>Crocidia</i>	fulvipes	UK-02-5816	Crocidia5816	A	F	unknown	Zimbabwe	2002	O'Neill, M & Kitching, UJ	ex head stock, UK accession no. 69516 (obtained from BMNH, 18Nov02)	na	27Feb03	head & proborax	*	*
				<i>Crocidia</i>	calypse	DCR-02-1870	Crocidia1870	A	na	Walton, Scott Co., Arkansas	USA	10Sep02	Rudolph, DC	collected live to alcohol	1870	27Feb03	proborax	*	*
				<i>Cx.</i>	undulosa	(RSP-96-09732)	CrocidiaGB	A	na	Barr Lake, Adams Co., Colorado	USA	23Jan95	DLorenz, S		na	14Mar00	thorax	AF234562	AF234584
				<i>Cyclops</i>	dapsichel	DHU-02-2359	Cocytus2359	A	F	Area de Conservacion, Guanacaste	Costa Rica	27Oct02	Jensen, DH	DIU accession no. 02-SRNP-2018 (http://jensen.us/npms/02s)	2359	15Jan03	head	*	*
<i>Dolbe</i>	hyloea			(RSP-xx-1349)	DolbeGB	A	na	unknown	USA	na	Peifer, RS	"specimen badly rotted" (RS Peifer)	1349	11Jul94	unknown	AF234579	AF234598		
<i>Eryops</i>	dogesii			WJK-03-2891	Eryops032891	A	na	Morona-Santiago Province (1270m)	Ecuador	1Jan03	Kelly, WJ & Wolfe, KL		2891	4Mar03	proborax	*	*		
<i>Lepora</i>	confusum			JKA-02-1670	Lepora1670	A	na	Calhoun, Gordon Co., Georgia	USA	1Aug02	Adams, JK		1670	4Mar03	head & proborax	*	*		
<i>Manduca</i>	floreana			JPT-02-1529	Manduca1529	A	na	Paragonia Mtns, Santa Cruz Co., Arizona	USA	24Jul02	Mooney, B & Byrne, H & Tuttle, UJ		1529	4Mar03	head & proborax	*	*		
<i>Me.</i>	muscosa			JBW-02-1508	Manduca1508	A	na	Santa Rita Mtns, Pima Co., Arizona (1067m)	USA	2Aug02	Walsh, B	collected at MV/UV lights	1508	4Mar03	head & proborax	*	*		
<i>Me.</i>	quinguerulatus			DCR-02-1876	Manduca1876	A	na	Walton, Scott Co., Arkansas	USA	11Sep02	Rudolph, DC	collected live to alcohol	1876	6Feb03	head	*	*		
<i>Me.</i>	scote			(TFP-91-2004)	ManducaGB	A	na	Sugar Loaf Mtn., Montgomery Co., Maryland	USA	3Jul81	Friedlander, TP & Peifer, RS	larva on tomato plant, previously misidentified as <i>M. quinguerulatus</i> , original label "2001"	na	unknown	larva	AF234571	[U03099]		
<i>Neocentrus</i>	chernis			WJK-03-1949	Neocentrus1949	A	na	Tinalandia, Pichincha Province (710m)	Ecuador	3Jan03	Kelly, WJ & Wolfe, KL		1949	4Mar03	proborax	na	*		
<i>Pantora</i>	plachia			WJK-02-1939	Pantora1939	A	na	ElIlyo, Gilmer Co., Georgia	USA	29Aug02	Kelly, WJ	collected at MV light	1939	6Feb03	head & proborax	*	*		
<i>Polygramma</i>	incisa			UK-02-5988	Polygramma5988	A	M	Palawan, Bataraza, Malibud	Philippines	1Jul01	Zwick, A & Kitching, UJ	head ex. larva, UK accession no. 69988 (obtained from BMNH, 18Nov02)	na	4Mar03	head & proborax	*	*		
<i>Sphinx</i>	chernis			(JPT-xx-0839)	SphinxGB	P	na	Pena Blanca Lake, Santa Cruz	USA	na	Mooney, B & Byrne, H & Tuttle, UJ		1532	6Feb03	head & proborax	*	*		
<i>Sp.</i>	delili			JPT-02-1532	Sphinx1532	A	na	Paragonia Mtns, Santa Cruz Co., Arizona	USA	24Jul02	Mooney, B & Byrne, H & Tuttle, UJ		1532	6Feb03	head & proborax	*	*		
<i>Sp.</i>	lister			CWB-02-1591	Sphinx1591	A	na	Concan, Uvalde Co., Texas	USA	6Sep02	Bordelon, CW & Knudson, EC		1591	4Mar03	proborax	*	*		
<i>Sp.</i>	halimae			WJK-02-1938	Sphinx1938	A	na	ElIlyo, Gilmer Co., Georgia	USA	28Aug02	Kelly, WJ	collected at MV light	1938	4Mar03	head & proborax	*	*		



**Table 9. Owing samples (Lepidoptera) for which EF and/or DDC sequences were obtained.** Species are listed alphabetically by higher taxonomic assignment, determined from multiple sources (Arnett 2001, Borror 1989, Kristiansen 1999, Scoble 1992, Wagner 2001; also see Table 1). UMD accession numbers are provided for each specimen derived from the UMD Lepidoptera Collections; "unknown" indicates UMD sequence data which could not be traced to a particular specimen; entries in square brackets provide published ID or other citation information for sequence data obtained from other sources. "Taxon" indicates the taxonomic group to which the specimen belongs. "Type" indicates specimen life stage: "A", adult; "P", pupa; "L", larva. Tissue position and date of nucleic acid extraction are noted in "ExtrDate" and "ExtrTime", respectively. Incomplete data is indicated by "na". Complete specimen information can be obtained from the University of Maryland Lepidoptera Collections (see Figure 3). GenBank accession numbers listed in the "EF" and "DDC" columns. Blank cells indicate sequence obtained for only one gene and these taxa were omitted from combined EF/DDC analysis. Brackets around D13338 (*Bombus morio*) indicate this was the EF reference sequence against which all other samples were aligned (see Figure 4).

Taxon Superfamily	Family	Subfamily	Type	Genus	Species	UMD Accession	Extr. Label	Large Int. Locality	Data	Collector/Distributor	Notes	Wing V. Extr. Date	Extr. Time	EF	DDC																
Zoopliptera	Microgasterinae	Microgasterinae	Microgasterinae	Microgasterinae	Microgasterinae	Microgasterinae	Microgasterinae	Microgasterinae	Microgasterinae	Microgasterinae	Microgasterinae	Microgasterinae	Microgasterinae	Microgasterinae	Microgasterinae																
																Microgasterinae	Microgasterinae	Microgasterinae	Microgasterinae	Microgasterinae	Microgasterinae	Microgasterinae	Microgasterinae	Microgasterinae	Microgasterinae	Microgasterinae	Microgasterinae	Microgasterinae	Microgasterinae	Microgasterinae	
																Microgasterinae	Microgasterinae	Microgasterinae	Microgasterinae	Microgasterinae	Microgasterinae	Microgasterinae	Microgasterinae	Microgasterinae	Microgasterinae	Microgasterinae	Microgasterinae	Microgasterinae	Microgasterinae	Microgasterinae	Microgasterinae
																Microgasterinae	Microgasterinae	Microgasterinae	Microgasterinae	Microgasterinae	Microgasterinae	Microgasterinae	Microgasterinae	Microgasterinae	Microgasterinae	Microgasterinae	Microgasterinae	Microgasterinae	Microgasterinae	Microgasterinae	Microgasterinae
																Microgasterinae	Microgasterinae	Microgasterinae	Microgasterinae	Microgasterinae	Microgasterinae	Microgasterinae	Microgasterinae	Microgasterinae	Microgasterinae	Microgasterinae	Microgasterinae	Microgasterinae	Microgasterinae	Microgasterinae	Microgasterinae
																Microgasterinae	Microgasterinae	Microgasterinae	Microgasterinae	Microgasterinae	Microgasterinae	Microgasterinae	Microgasterinae	Microgasterinae	Microgasterinae	Microgasterinae	Microgasterinae	Microgasterinae	Microgasterinae	Microgasterinae	Microgasterinae
																Microgasterinae	Microgasterinae	Microgasterinae	Microgasterinae	Microgasterinae	Microgasterinae	Microgasterinae	Microgasterinae	Microgasterinae	Microgasterinae	Microgasterinae	Microgasterinae	Microgasterinae	Microgasterinae	Microgasterinae	Microgasterinae
																Microgasterinae	Microgasterinae	Microgasterinae	Microgasterinae	Microgasterinae	Microgasterinae	Microgasterinae	Microgasterinae	Microgasterinae	Microgasterinae	Microgasterinae	Microgasterinae	Microgasterinae	Microgasterinae	Microgasterinae	Microgasterinae
																Microgasterinae	Microgasterinae	Microgasterinae	Microgasterinae	Microgasterinae	Microgasterinae	Microgasterinae	Microgasterinae	Microgasterinae	Microgasterinae	Microgasterinae	Microgasterinae	Microgasterinae	Microgasterinae	Microgasterinae	Microgasterinae
																Microgasterinae	Microgasterinae	Microgasterinae	Microgasterinae	Microgasterinae	Microgasterinae	Microgasterinae	Microgasterinae	Microgasterinae	Microgasterinae	Microgasterinae	Microgasterinae	Microgasterinae	Microgasterinae	Microgasterinae	Microgasterinae

**Table 10. New Sphingidae specimens.** Novel material (350 specimens) collected expressly for this study was accessioned into the University of Maryland Lepidoptera Collections and is available for molecular sequence data collection (see Figures 2 and 3). Number of specimens and their distribution across taxonomic levels was tabulated for each collector.

<b>Collector</b>	<b>Series</b>	<b>Subfamilies</b>	<b>Genera</b>	<b>Species</b>	<b>Specimens</b>
<b>James K. Adams</b>	JKA-02	3	11	19	21
<b>Charles W. Bordelon</b>	CWB-02	3	8	12	28
<b>David Boucher</b>	DB-03	2	4	4	4
<b>John DeBenedictis</b>	JAD-02	2	2	2	4
<b>Ian J. Kitching</b>	IJK-02&03	3	32	58	99
<b>Daniel H. Janzen</b>	DHJ-02	3	9	18	30
<b>William J. Kelly</b>	WJK-02&03	3	16	37	42
<b>Peter J. Landolt</b>	PJL-02	1	2	2	6
<b>Andre A. Mignault</b>	AAM-02	1	3	3	21
<b>Charles W. Mitter</b>	CWM-02	1	1	1	1
<b>Marcela More</b>	MM-03	2	7	13	17
<b>Mogens C. Nielsen</b>	MCN-03	3	4	5	5
<b>James Oberfoell</b>	JO-03	2	3	3	5
<b>Richard S. Peigler</b>	RSP-02	1	1	1	1
<b>D. Craig Rudolph</b>	DCR-02	2	7	9	14
<b>Glen Smart</b>	GS-02	3	10	14	19
<b>James P. Tuttle</b>	JPT-02	3	10	18	20
<b>J. Bruce Walsh</b>	JBW-02	3	8	10	13

**Table 11 Distribution of EF and DDC sequence accessions in GenBank across Lepidoptera.** Search strings querying EF and DDC sequences across Lepidoptera were submitted to the Entrez Browser in the NCBI GenBank Nucleotides Database on 06 April 2004 (see Table 7). Hits to these queries are plotted separately for each gene across all families in a classification of Lepidoptera [Hexapoda: Ectognatha(Insecta): Dicondylia: Pterygota: Neoptera: Holometabola(Endopterygota): Panoroidea: Amphimesenoptera] compiled from Borror 1989, Wagner 2001, Arnett 2000, Kristensen 1999, Scoble 1992. Raw and cumulative numbers of described species per superfamily and family are also included to provide diversity measures.

#	SUPERFAMILY	spp	%	cum	cum%	Family	spp	Common Name	EF	DDC
<b>Zeugloptera</b>										
1	MICROPTERIGOIDEA	121	0.07	121	0.07	Micropterigidae	121	mandibulate archaic moths	2	2
<b>Aglossata</b>										
2	AGATHIPHAGOIDEA	2	0.00	123	0.07	Agathiphagidae	2	kauri moths		
<b>Heterobathmiina</b>										
3	HETEROBATHMIOIDEA	9	0.01	132	0.07	Heterobathmiidae	9	valdivian archaic moths		
<b>Glossata</b>										
4	ERIOCRANIOIDEA	24	0.01	156	0.09	Eriocraniidae	24	sparkling archaic sun moths		2
<b>Glossata&gt;Coelolepida</b>										
5	ACANTHOPTEROCETOIDEA	5	0.00	161	0.09	Acanthopteroctetidae	5	archaic sun moths		
6	LOPHOCORONOIDEA	6	0.00	167	0.09	Lophocoronidae	6	australian archaic sun moths		
<b>Glossata&gt;Coelolepida&gt;Myoglossata</b>										
7	NEOPSEUSTOIDEA	11	0.01	178	0.10	Neopseustidae	11	archaic bell moths		
<b>Glossata&gt;Coelolepida&gt;Myoglossata&gt;Neolepidoptera&gt;Exoporia</b>										
8	HEPIALOIDEA	569	0.32	747	0.42	Anomosetidae	1	australian primitive ghost moths		
						Hepialidae	550	ghost moths & swifts		2
						Neotheoridae	1	amazonian primitive ghost moths		
						Palaeosetidae	8	miniature ghost moths		
						Prototheoridae	9	african primitive ghost moths		
						Mnesarchaeidae	14	new zealand primitive moths		
9	MNESARCHAEOIDEA	14	0.01	761	0.43					
<b>Glossata&gt;Coelolepida&gt;Myoglossata&gt;Neolepidoptera&gt;Heteroneura</b>										
10	NEPTICULOIDEA	902	0.51	1,663	0.93	Nepticulidae	800	leaf miners & pygmy moths		1
						Opostegidae	102	eye-cap moths		1
11	INCURVARIOIDEA	594	0.33	2,257	1.27	Adelidae	300	long-horned fairy moths		3
						Cecidosidae	7	gall moths		2
						Crinopterygidae	1	shield bearers & leaf miners		2
						Heliozelidae	106	leaf-cutter moths		1
						Incurvarilidae	100	yucca moths		7
						Prodoxidae	80	gondwanaland moths		1
						Tischeriidae	80	apple-leaf trumpet miners		2
12	PALAEPHATOIDEA	60	0.03	2,317	1.30					
13	TISCHERIOIDEA	80	0.04	2,397	1.35					
<b>Glossata&gt;Coelolepida&gt;Myoglossata&gt;Neolepidoptera&gt;Heteroneura&gt;Ditrysia</b>										
14	SIMAETHISTOIDEA	4	0.00	2,401	1.35	Simaethistidae	4			
15	TINEOIDEA	4,350	2.45	6,751	3.79	Acrolophidae	270	tube moths		
						Arrhenophanidae	8	tropical lattice moths		
						Eriocottidae	71	old world spiny-winged moths		
						Lypusidae	1			
						Psychidae	1,000	bag worm moths		1
						Tineidae	3,000	fungus & clothes moths		2
16	GELECHIOIDEA	16,631	9.35	23,382	13.14	Amphisbatidae	65			
						Autostichidae	308			
						Batrachedridae	100			
						Chimabachidae	6			
						Coleophoridae	1,418	casebearer moths		
						Cosmopterigidae	1,628	cosmet moths		
						Deoclonidae	4			
						Elachistidae	3,270	grass miner moths		
						Gelechiidae	4,530	twirler moths		
						Glyphidoceridae	50			
						Lecithoceridae	875	tropical longhorned moths		
						Oecophoridae	3,150	concealer moths		
						Peleopodidae	25			
						Schistonoeidae	2			
						Xyloryctidae	1,200			
17	GRACILLARIOIDEA	2,316	1.30	25,698	14.44	Bucculatricidae	250	ribbed cocoon-maker moths		
						Douglasidae	26	douglas moths		
						Gracillariidae	2,000	leaf miner moths		1
						Roeslerstammlidae	40			
18	YPONOMEUTOIDEA	1,869	1.05	27,567	15.49	Acrolepiidae	95	false diamond-back moths		
						Bedelliidae	18			
						Glyphipterygidae	390	sedge moths		
						Heliolindidae	55	sun moths		
						Lyonetiidae	210	lyonet moths		
						Plutellidae	380	diamond-back moths		
						Yponomeutidae	591	ermine moths		
						Ypsolophidae	130			

Table 11. (continued)

Glossata>Coelolepida>Myoglossata>Neolepidoptera>Heteroneura>Ditrysia>Apoditrysia											
19	ALUCITOIDEA	164	0.09	27,731	15.59	Alucitidae	146	many-plumed moths			
						Tineodidae	18	false plume moths			
20	PTEROPHOROIDEA	986	0.55	28,717	16.14	Pterophoridae	986	plume moths			
21	CHOREUTOIDEA	415	0.23	29,132	16.37	Choreutidae	415	metalmark moths			
22	COSSOIDEA	676	0.38	29,808	16.75	Cossidae	670	carpenter & goat moths			
						Dudgeoneidae	6	dudgeon carpenter worm moths			
23	SESIOIDEA	1,372	0.77	31,180	17.53	Brachodidae	100	little bear moths			
						Castniidae	137	giant butterfly moths			
						Sesidae	1,135	clearwing moths			
24	ZYGAENOIDEA	2,783	1.56	33,963	19.09	Aididae	6				
						Anomoerotidae	40				
						Cyclotornidae	12	australian parasite moths			
						Dalceridae	50	tropical slug caterpillar moths			
						Epipyropidae	55	planthopper parasite moths			
						Heterogynidae	10	mediterranean burnet moths			
						Himantopteridae	40	long-tailed burnet moths			
						Lacturidae	125	tropical burnet moths			
						Limacodidae	1,080	slug & saddleback caterpillar moths			
						Megalopygidae	265	flannel moths			
						Somabrachyidae	?	mediterranean flannel moths			
						Zygaenidae	1,100	smoky moths & burnets			
25	EPERMENIOIDEA	83	0.05	34,046	19.14	Epermeniidae	83	fringe-tufted moths			
26	GALACTICOIDEA	17	0.01	34,063	19.15	Galactiidae	17				
27	SCHRECKENSTEINOIDEA	5	0.00	34,068	19.15	Schreckensteiniidae	5	bristle-legged moths			
28	TORTRICOIDEA	8,000	4.50	42,068	23.65	Tortricidae	8,000	leafroller moths			
29	URODOIDEA	80	0.04	42,148	23.69	Urodidae	80	false burnet moths			
Glossata>Coelolepida>Myoglossata>Neolepidoptera>Heteroneura>Ditrysia>Apoditrysia>Obtectomera											
30	COPROMORPHOIDEA	330	0.19	42,478	23.88	Carposinidae	275	fruitworm moths			
						Copromorphidae	55	tropical fruitworm moths			
31	HYBLAEOIDEA	18	0.01	42,496	23.89	Hyblaeidae	18	teak moths			
32	IMMOIDEA	246	0.14	42,742	24.02	Immidae	246	imma moths			
33	PYRALOIDEA	17,763	9.98	60,505	34.01	Crambidae	11,630	close-wings & grassmoths			
						Pyralidae	6,133	snout & grass moths	27	1	
34	THYRIDOIDEA	760	0.43	61,265	34.44	Thyrididae	760	picture-winged leaf moths			
35	WHALLEYANOIDEA	2	0.00	61,267	34.44	Whalleyanidae	2				
Glossata>Coelolepida>Myoglossata>Neolepidoptera>Heteroneura>Ditrysia>Apoditrysia>Obtectomera>Macrolepidoptera											
36	BOMBYCOIDEA	3,553	2.00	64,820	36.43	Bombycidae	350	silkworm moths	4	3	
						Brahmaeidae	20	brahmin moths	2	2	
						Carthaeidae	1	australian silkworm moths			
						Endromidae	1	glory moths	1		
						Eupterotidae	300	giant lappet moths			
						Lemonidae	20	autumn silkworm moths	1		
						Mirinae	2				
						Saturniidae	1,590	emperor & giant silkworm moths	76	53	
						Sphingidae	1,269	hawk, hornworm & sphinx moths	29	18	
37	LASIOCAMPOIDEA	2,125	1.19	66,945	37.63	Anthelidae	75	australian lappet moths			
						Lasiocampidae	2,050	tent caterpillars & lappet moths	13		
38	MIMALONOIDEA	255	0.14	67,200	37.77	Mimallonidae	255	sack-bearer moths			
39	NOCTUOIDEA	70,000	39.35	137,200	77.12	Arctiidae	11,000	tiger, footman & wasp moths	4	4	
						Ctenuchidae	?	wasp moths			
						Doidae	?				
						Lymantriidae	2,500	tussock & gypsy moths	3	3	
						Noctuidae	35,000	dagger, owlet & forester moths	81	91	
						Noilidae	?				
						Notodontidae	2,800	prominent moths	6	5	
						Oenosandridae	?				
						Pantheidae	?				
40	DREPANOIDEA	815	0.46	138,015	77.58	Drepanidae	790	hook-tip moths			
						Epicopeiidae	25	oriental swallowtail moths			
41	GEOMETROIDEA	21,740	12.22	159,755	89.79	Geometridae	21,000	measuringworms, cankerworms	1		
						Sematuridae	40	american swallowtail moths			
						Uraniidae	700	swallowtail moths			
42	AXIOIDEA	6	0.00	159,761	89.80	Axiidae	6	gold moths			
43	CALLIDULOIDEA	60	0.03	159,821	89.83	Callidulidae	60	old world butterfly moths			
44	HEDYLOIDEA	40	0.02	159,861	89.85	Hedyllidae	40	american butterfly moths	1		
45	HESPEROIDEA	3,675	2.07	163,536	91.92	Hesperidae	3,675	skippers	3		
46	PAPILIONOIDEA	14,375	8.08	177,911	100.00	Lycanidae	6,575	blues, coppers, hairstreaks	2		
						Nymphalidae	6,000	brushfooted, fritillaries, checkerspots, satyrs	106	27	
						Papilionidae	575	swallowtails & parnassians	41	1	
						Peridae	1,225	yellow-white & orange-tips, sulfurs	16		
		<i>total no. species</i>				<i>total no. species</i>				<i>EF DDC</i>	
		(superfamily estimates) : 177,911				(family estimates) : 151,411				total GenBank hits : 419 238	

**Table 12. Summary of character information content and nucleotide composition in data matrices by gene, taxon set and partition.** For the (a) EF, (b) DDC and (c) EF&DDC combined data matrices, the number ('chars') and percentage (%) of invariant, autapomorphic and parsimony informative amino acid and nucleotide characters is tabulated for each partition across four taxon sets: (i) all Lepidoptera, (ii) all Bombycoidea, (iii) all Sphingidae and (iv) shared Sphingidae (n=64) along with Bombycidae and Saturniini outgroups. Mean nucleotide base frequencies for each partition were calculated in PAUP\* and are adjusted for missing data. Complete empirical nucleotide base composition for every ingroup and outgroup sequence is available in Tables 15 and 16, respectively.

**(a) EF: Elongation Factor 1-alpha (1,228nt; 409aa)**

TAXON SET	PART	TOTAL	INVARIANT		AUTAP		PARS INF		BASE FREQUENCIES (%)			
			chars	%	chars	%	chars	%	A	C	G	T
(i) Lepidoptera ntax=118	aa	409	359	87.8%	29	7.1%	21	5.1%	.	.	.	.
	ntall	1,228	776	63.2%	59	4.8%	393	32.0%	25.26	28.52	25.10	21.12
	nt1	409	361	88.3%	18	4.4%	30	7.3%	29.03	18.37	37.73	14.86
	nt2	409	379	92.7%	19	4.6%	11	2.7%	32.47	25.00	15.80	26.73
	nt3	410	36	8.8%	22	5.4%	352	85.9%	14.28	42.18	21.79	21.76
(ii) Bombycoidea ntax=82	aa	409	384	93.9%	11	2.7%	14	3.4%	.	.	.	.
	ntall	1,228	830	67.6%	49	4.0%	349	28.4%	25.14	28.80	25.26	20.80
	nt1	409	376	91.9%	10	2.4%	23	5.6%	29.03	18.40	37.60	14.96
	nt2	409	396	96.8%	7	1.7%	6	1.5%	32.51	25.00	15.84	26.65
	nt3	410	58	14.1%	32	7.8%	320	78.0%	13.87	42.99	22.36	20.78
(iii) Sphingidae ntax=67	aa	409	393	96.1%	5	1.2%	11	2.7%	.	.	.	.
	ntall	1,228	890	72.5%	69	5.6%	269	21.9%	24.78	29.35	25.48	20.39
	nt1	409	388	94.9%	4	1.0%	17	4.2%	29.03	18.43	37.61	14.94
	nt2	409	401	98.0%	3	0.7%	5	1.2%	32.52	25.01	15.84	26.63
	nt3	410	101	24.6%	62	15.1%	247	60.2%	12.79	44.61	23.01	19.59
(iv) Sphingidae &2OG ntax=66	aa	409	391	95.6%	7	1.7%	11	2.7%	.	.	.	.
	ntall	1,228	871	70.9%	70	5.7%	287	23.4%	24.85	29.28	25.41	20.46
	nt1	409	386	94.4%	6	1.5%	17	4.2%	29.03	18.43	37.58	14.96
	nt2	409	399	97.6%	5	1.2%	5	1.2%	32.53	25.03	15.83	26.61
	nt3	410	86	21.0%	59	14.4%	265	64.6%	13.00	44.37	22.84	19.80

**(b) DDC: Dopa Decarboxylase (1,329nt; 443aa)**

TAXON SET	PART	TOTAL	INVARIANT		AUTAP		PARS INF		BASE FREQUENCIES (%)			
			chars	%	chars	%	chars	%	A	C	G	T
(i) Lepidoptera ntax=105	aa	443	256	57.8%	57	12.9%	130	29.3%	.	.	.	.
	ntall	1,329	599	45.1%	81	6.1%	649	48.8%	24.99	23.09	25.79	26.13
	nt1	443	251	56.7%	42	9.5%	150	33.9%	22.33	22.03	35.38	20.26
	nt2	443	330	74.5%	37	8.4%	76	17.2%	29.15	21.7	19.72	29.43
	nt3	443	18	4.1%	2	0.5%	423	95.5%	23.5	25.55	22.27	28.68

Table 12. (continued)

Table 12. (continued)

(ii) Bombycoidea	aa	443	305	68.8%	40	9.0%	98	22.1%	.	.	.	.
ntax=73	ntall	1,329	693	52.1%	60	4.5%	576	43.3%	25.55	22.45	25.24	26.76
	nt1	443	302	68.2%	36	8.1%	105	23.7%	22.85	21.96	34.67	20.53
	nt2	443	372	84.0%	22	5.0%	49	11.1%	29.21	21.39	19.76	29.65
	nt3	443	19	4.3%	2	0.5%	422	95.3%	24.6	24	21.28	30.12
(iii) Sphingidae	aa	443	329	74.3%	29	6.5%	85	19.2%	.	.	.	.
ntax=65	ntall	1,329	736	55.4%	49	3.7%	544	40.9%	25.48	22.51	25.21	26.80
	nt1	443	326	73.6%	26	5.9%	91	20.5%	22.88	21.99	34.56	20.58
	nt2	443	391	88.3%	17	3.8%	35	7.9%	29.15	21.47	19.73	29.66
	nt3	443	19	4.3%	6	1.4%	418	94.4%	24.42	24.06	21.34	30.18
(iv) Sphingidae &2OG	aa	443	315	71.1%	37	8.4%	91	20.5%	.	.	.	.
ntax=66	ntall	1,329	711	53.5%	61	4.6%	557	41.9%	25.46	22.50	25.23	26.81
	nt1	443	313	70.7%	35	7.9%	95	21.4%	22.84	22.01	34.57	20.57
	nt2	443	379	85.6%	23	5.2%	41	9.3%	29.16	21.44	19.73	29.67
	nt3	443	19	4.3%	3	0.7%	421	95.0%	24.38	24.04	21.38	30.20

(c) EF&DDC: Combined Data (2,557nt; 852aa)

TAXON SET	PART TOTAL	INVARIANT		AUTAP		PARS INF		BASE FREQUENCIES (%)				
		chars	%	chars	%	chars	%	A	C	G	T	
(i) Lepidoptera	aa	852	651	76.4%	76	8.9%	125	14.7%	.	.	.	.
ntax=91	ntall	2,557	1449	56.7%	148	5.8%	960	37.5%	25.19	26.01	25.30	23.51
	nt1	852	646	75.8%	58	6.8%	148	17.4%	25.97	20.06	36.41	17.56
	nt2	852	736	86.4%	53	6.2%	63	7.4%	30.99	23.40	17.63	27.99
	nt3	853	67	7.9%	37	4.3%	749	87.8%	18.61	34.57	21.85	24.97
(ii) Bombycoidea	aa	852	695	81.6%	47	5.5%	110	12.9%	.	.	.	.
ntax=72	ntall	2,557	1546	60.5%	108	4.2%	903	35.3%	25.28	25.79	25.27	23.66
	nt1	852	687	80.6%	42	4.9%	123	14.4%	25.97	20.17	36.16	17.71
	nt2	852	770	90.4%	28	3.3%	54	6.3%	30.89	23.22	17.77	28.13
	nt3	853	89	10.4%	38	4.5%	726	85.1%	18.99	33.97	21.91	25.13
(iii) Sphingidae	aa	852	723	84.9%	33	3.9%	96	11.3%	.	.	.	.
ntax=64	ntall	2,557	1630	63.7%	116	4.5%	811	31.7%	25.12	25.95	25.35	23.59
	nt1	852	716	84.0%	29	3.4%	107	12.6%	25.93	20.23	36.07	17.77
	nt2	852	792	93.0%	20	2.3%	40	4.7%	30.84	23.24	17.79	28.14
	nt3	853	122	14.3%	67	7.9%	664	77.8%	18.57	34.39	22.20	24.84
(iv) Sphingidae &2OG	aa	852	706	82.9%	44	5.2%	102	12.0%	.	.	.	.
ntax=66	ntall	2,557	1582	61.9%	131	5.1%	844	33.0%	25.16	25.88	25.32	23.65
	nt1	852	699	82.0%	41	4.8%	112	13.1%	25.92	20.23	36.07	17.78
	nt2	852	778	91.3%	28	3.3%	46	5.4%	30.83	23.23	17.79	28.15
	nt3	853	105	12.3%	62	7.3%	686	80.4%	18.71	34.18	22.11	25.00











**Table 15. Empirical base compositions for EF and DDC among legrupp taxa (Bombacoideae, Spingioideae).** Empirical frequencies of six character state categories were calculated separately for each gene across every legrupp sequence obtained de novo or in silico in this study. Percentage adenine (A), cytosine (C), guanine (G), thymine (T), missing data (X), binary (IUPAC ambiguity codes) was calculated by dividing the count of each category in the final aligned sequence by the matrix sequence length (1,274bp for EF, 1,373bp for DDC). In contrast to the final matrix length, 'real' bp reports the number of nucleotide characters (N) were appended at either end to standardize length across taxa. For sequences whose 'real' bp < 'final matrix length', the 'start' column indicates the position of the first real nucleotide relative to the reference sequences depicted in Figure 4 (EF) and Figure 5 (DDC). Values in the 'start' and 'real' bp columns are especially important descriptions of sequences collected in silico in this study (indicated by a 'GB' suffix on the Taxon Label), as GenBank accessions were extremely variable in length.

Taxonomy	Genus	species	Taxon Label	Elongation Factor 1-alpha (EF)						Decarbonylase (DDC)									
				Accession	%A	%C	%G	%T	%X	%I	Accession	%A	%C	%G	%T	%X	%I		
MACROGLOSSINAE	Diplophonotini		Aethlios399	DHI-02-2399	24.10	30.37	25.65	19.63	0.00	0.24	1274	DHI-02-2399	25.06	22.95	25.81	25.96	0.00	0.23	1373
			Adipos369	AF234559	23.94	30.21	25.65	20.03	0.00	0.16	1240	AF234559	25.06	22.95	25.81	25.96	0.00	0.23	1373
			Callionotus966	RFD-06-0966	23.94	30.70	25.90	19.46	0.00	0.00	1274	RFD-06-0966	25.06	22.95	25.81	25.96	0.00	0.23	1373
			Catantia273	AF234562	23.94	30.70	25.90	19.46	0.00	0.00	1274	AF234562	25.06	22.95	25.81	25.96	0.00	0.23	1373
			Catantia273	AF234562	23.94	30.70	25.90	19.46	0.00	0.00	1274	AF234562	25.06	22.95	25.81	25.96	0.00	0.23	1373
			Ca. Erythra	JK-A-02-1646	24.59	30.71	25.21	19.74	0.00	0.08	1274	JK-A-02-1646	25.51	23.52	25.28	27.69	0.00	0.20	1373
			Ca. Erythra	JK-A-02-1646	24.59	30.71	25.21	19.74	0.00	0.08	1274	JK-A-02-1646	25.51	23.52	25.28	27.69	0.00	0.20	1373
			Ca. Erythra	JK-A-02-1646	24.59	30.71	25.21	19.74	0.00	0.08	1274	JK-A-02-1646	25.51	23.52	25.28	27.69	0.00	0.20	1373
			Ca. Erythra	JK-A-02-1646	24.59	30.71	25.21	19.74	0.00	0.08	1274	JK-A-02-1646	25.51	23.52	25.28	27.69	0.00	0.20	1373
			Ca. Erythra	JK-A-02-1646	24.59	30.71	25.21	19.74	0.00	0.08	1274	JK-A-02-1646	25.51	23.52	25.28	27.69	0.00	0.20	1373
			Ca. Erythra	JK-A-02-1646	24.59	30.71	25.21	19.74	0.00	0.08	1274	JK-A-02-1646	25.51	23.52	25.28	27.69	0.00	0.20	1373
			Ca. Erythra	JK-A-02-1646	24.59	30.71	25.21	19.74	0.00	0.08	1274	JK-A-02-1646	25.51	23.52	25.28	27.69	0.00	0.20	1373
			Ca. Erythra	JK-A-02-1646	24.59	30.71	25.21	19.74	0.00	0.08	1274	JK-A-02-1646	25.51	23.52	25.28	27.69	0.00	0.20	1373
			Ca. Erythra	JK-A-02-1646	24.59	30.71	25.21	19.74	0.00	0.08	1274	JK-A-02-1646	25.51	23.52	25.28	27.69	0.00	0.20	1373
			Ca. Erythra	JK-A-02-1646	24.59	30.71	25.21	19.74	0.00	0.08	1274	JK-A-02-1646	25.51	23.52	25.28	27.69	0.00	0.20	1373
			Ca. Erythra	JK-A-02-1646	24.59	30.71	25.21	19.74	0.00	0.08	1274	JK-A-02-1646	25.51	23.52	25.28	27.69	0.00	0.20	1373
			Ca. Erythra	JK-A-02-1646	24.59	30.71	25.21	19.74	0.00	0.08	1274	JK-A-02-1646	25.51	23.52	25.28	27.69	0.00	0.20	1373
			Ca. Erythra	JK-A-02-1646	24.59	30.71	25.21	19.74	0.00	0.08	1274	JK-A-02-1646	25.51	23.52	25.28	27.69	0.00	0.20	1373
			Ca. Erythra	JK-A-02-1646	24.59	30.71	25.21	19.74	0.00	0.08	1274	JK-A-02-1646	25.51	23.52	25.28	27.69	0.00	0.20	1373
			Ca. Erythra	JK-A-02-1646	24.59	30.71	25.21	19.74	0.00	0.08	1274	JK-A-02-1646	25.51	23.52	25.28	27.69	0.00	0.20	1373
			Ca. Erythra	JK-A-02-1646	24.59	30.71	25.21	19.74	0.00	0.08	1274	JK-A-02-1646	25.51	23.52	25.28	27.69	0.00	0.20	1373
			Ca. Erythra	JK-A-02-1646	24.59	30.71	25.21	19.74	0.00	0.08	1274	JK-A-02-1646	25.51	23.52	25.28	27.69	0.00	0.20	1373
			Ca. Erythra	JK-A-02-1646	24.59	30.71	25.21	19.74	0.00	0.08	1274	JK-A-02-1646	25.51	23.52	25.28	27.69	0.00	0.20	1373
Ca. Erythra	JK-A-02-1646	24.59	30.71	25.21	19.74	0.00	0.08	1274	JK-A-02-1646	25.51	23.52	25.28	27.69	0.00	0.20	1373			
Ca. Erythra	JK-A-02-1646	24.59	30.71	25.21	19.74	0.00	0.08	1274	JK-A-02-1646	25.51	23.52	25.28	27.69	0.00	0.20	1373			
Ca. Erythra	JK-A-02-1646	24.59	30.71	25.21	19.74	0.00	0.08	1274	JK-A-02-1646	25.51	23.52	25.28	27.69	0.00	0.20	1373			
Ca. Erythra	JK-A-02-1646	24.59	30.71	25.21	19.74	0.00	0.08	1274	JK-A-02-1646	25.51	23.52	25.28	27.69	0.00	0.20	1373			
Ca. Erythra	JK-A-02-1646	24.59	30.71	25.21	19.74	0.00	0.08	1274	JK-A-02-1646	25.51	23.52	25.28	27.69	0.00	0.20	1373			
Ca. Erythra	JK-A-02-1646	24.59	30.71	25.21	19.74	0.00	0.08	1274	JK-A-02-1646	25.51	23.52	25.28	27.69	0.00	0.20	1373			
Ca. Erythra	JK-A-02-1646	24.59	30.71	25.21	19.74	0.00	0.08	1274	JK-A-02-1646	25.51	23.52	25.28	27.69	0.00	0.20	1373			
Ca. Erythra	JK-A-02-1646	24.59	30.71	25.21	19.74	0.00	0.08	1274	JK-A-02-1646	25.51	23.52	25.28	27.69	0.00	0.20	1373			
Ca. Erythra	JK-A-02-1646	24.59	30.71	25.21	19.74	0.00	0.08	1274	JK-A-02-1646	25.51	23.52	25.28	27.69	0.00	0.20	1373			
Ca. Erythra	JK-A-02-1646	24.59	30.71	25.21	19.74	0.00	0.08	1274	JK-A-02-1646	25.51	23.52	25.28	27.69	0.00	0.20	1373			
Ca. Erythra	JK-A-02-1646	24.59	30.71	25.21	19.74	0.00	0.08	1274	JK-A-02-1646	25.51	23.52	25.28	27.69	0.00	0.20	1373			
Ca. Erythra	JK-A-02-1646	24.59	30.71	25.21	19.74	0.00	0.08	1274	JK-A-02-1646	25.51	23.52	25.28	27.69	0.00	0.20	1373			
Ca. Erythra	JK-A-02-1646	24.59	30.71	25.21	19.74	0.00	0.08	1274	JK-A-02-1646	25.51	23.52	25.28	27.69	0.00	0.20	1373			
Ca. Erythra	JK-A-02-1646	24.59	30.71	25.21	19.74	0.00	0.08	1274	JK-A-02-1646	25.51	23.52	25.28	27.69	0.00	0.20	1373			
Ca. Erythra	JK-A-02-1646	24.59	30.71	25.21	19.74	0.00	0.08	1274	JK-A-02-1646	25.51	23.52	25.28	27.69	0.00	0.20	1373			
Ca. Erythra	JK-A-02-1646	24.59	30.71	25.21	19.74	0.00	0.08	1274	JK-A-02-1646	25.51	23.52	25.28	27.69	0.00	0.20	1373			
Ca. Erythra	JK-A-02-1646	24.59	30.71	25.21	19.74	0.00	0.08	1274	JK-A-02-1646	25.51	23.52	25.28	27.69	0.00	0.20	1373			
Ca. Erythra	JK-A-02-1646	24.59	30.71	25.21	19.74	0.00	0.08	1274	JK-A-02-1646	25.51	23.52	25.28	27.69	0.00	0.20	1373			
Ca. Erythra	JK-A-02-1646	24.59	30.71	25.21	19.74	0.00	0.08	1274	JK-A-02-1646	25.51	23.52	25.28	27.69	0.00	0.20	1373			
Ca. Erythra	JK-A-02-1646	24.59	30.71	25.21	19.74	0.00	0.08	1274	JK-A-02-1646	25.51	23.52	25.28	27.69	0.00	0.20	1373			
Ca. Erythra	JK-A-02-1646	24.59	30.71	25.21	19.74	0.00	0.08	1274	JK-A-02-1646	25.51	23.52	25.28	27.69	0.00	0.20	1373			
Ca. Erythra	JK-A-02-1646	24.59	30.71	25.21	19.74	0.00	0.08	1274	JK-A-02-1646	25.51	23.52	25.28	27.69	0.00	0.20	1373			
Ca. Erythra	JK-A-02-1646	24.59	30.71	25.21	19.74	0.00	0.08	1274	JK-A-02-1646	25.51	23.52	25.28	27.69	0.00	0.20	1373			
Ca. Erythra	JK-A-02-1646	24.59	30.71	25.21	19.74	0.00	0.08	1274	JK-A-02-1646	25.51	23.52	25.28	27.69	0.00	0.20	1373			
Ca. Erythra	JK-A-02-1646	24.59	30.71	25.21	19.74	0.00	0.08	1274	JK-A-02-1646	25.51	23.52	25.28	27.69	0.00	0.20	1373			
Ca. Erythra	JK-A-02-1646	24.59	30.71	25.21	19.74	0.00	0.08	1274	JK-A-02-1646	25.51	23.52	25.28	27.69	0.00	0.20	1373			
Ca. Erythra	JK-A-02-1646	24.59	30.71	25.21	19.74	0.00	0.08	1274	JK-A-02-1646	25.51	23.52	25.28	27.69	0.00	0.20	1373			
Ca. Erythra	JK-A-02-1646	24.59	30.71	25.21	19.74	0.00	0.08	1274	JK-A-02-1646	25.51	23.52	25.28	27.69	0.00	0.20	1373			
Ca. Erythra	JK-A-02-1646	24.59	30.71	25.21	19.74	0.00	0.08	1274	JK-A-02-1646	25.51	23.52	25.28	27.69	0.00	0.20	1373			
Ca. Erythra	JK-A-02-1646	24.59	30.71	25.21	19.74	0.00	0.08	1274	JK-A-02-1646	25.51	23.52	25.28	27.69	0.00	0.20	1373			
Ca. Erythra	JK-A-02-1646	24.59	30.71	25.21	19.74	0.00	0.08	1274	JK-A-02-1646	25.51	23.52	25.28	27.69	0.00	0.20	1373			
Ca. Erythra	JK-A-02-1646	24.59	30.71	25.21	19.74	0.00	0.08	1274	JK-A-02-1646	25.51	23.52	25.28	27.69	0.00	0.20	1373			
Ca. Erythra	JK-A-02-1646	24.59	30.71	25.21	19.74	0.00	0.08	1274	JK-A-02-1646	25.51	23.52	25.28	27.69	0.00	0.20	1373			
Ca. Erythra	JK-A-02-1646	24.59	30.71	25.21	19.74	0.00	0.08	1274	JK-A-02-1646	25.51	23.52	25.28	27.69	0.00	0.20	1373			
Ca. Erythra	JK-A-02-1646	24.59	30.71	25.21	19.74	0.00	0.08	1274	JK-A-02-1646	25.51	23.52	25.28	27.69	0.00	0.20	1373			
Ca. Erythra	JK-A-02-1646	24.59	30.71	25.21	19.74	0.00	0.08	1274	JK-A-02-1646	25.51	23.52	25.28	27.69	0.00	0.20	1373			
Ca. Erythra	JK-A-02-1646	24.59	30.71	25.21	19.74														















Table 18. (continued)

69	174	71	72	73	74	75	76	77	78	79	80	81	82	83	84	85	86	87	88	89	90	91	92	93	94	95	96	97	98	99	100																																																																														
100	101	102	103	104	105	106	107	108	109	110	111	112	113	114	115	116	117	118	119	120	121	122	123	124	125	126	127	128	129	130	131	132	133	134	135	136	137	138	139	140	141	142	143	144	145	146	147	148	149	150	151	152	153	154	155	156	157	158	159	160	161	162	163	164	165	166	167	168	169	170	171	172	173	174	175	176	177	178	179	180	181	182	183	184	185	186	187	188	189	190	191	192	193	194	195	196	197	198	199	200									
191	192	193	194	195	196	197	198	199	200	201	202	203	204	205	206	207	208	209	210	211	212	213	214	215	216	217	218	219	220	221	222	223	224	225	226	227	228	229	230	231	232	233	234	235	236	237	238	239	240	241	242	243	244	245	246	247	248	249	250	251	252	253	254	255	256	257	258	259	260	261	262	263	264	265	266	267	268	269	270	271	272	273	274	275	276	277	278	279	280	281	282	283	284	285	286	287	288	289	290	291	292	293	294	295	296	297	298	299	300
301	302	303	304	305	306	307	308	309	310	311	312	313	314	315	316	317	318	319	320	321	322	323	324	325	326	327	328	329	330	331	332	333	334	335	336	337	338	339	340	341	342	343	344	345	346	347	348	349	350	351	352	353	354	355	356	357	358	359	360	361	362	363	364	365	366	367	368	369	370	371	372	373	374	375	376	377	378	379	380	381	382	383	384	385	386	387	388	389	390	391	392	393	394	395	396	397	398	399	400										
401	402	403	404	405	406	407	408	409	410	411	412	413	414	415	416	417	418	419	420	421	422	423	424	425	426	427	428	429	430	431	432	433	434	435	436	437	438	439	440	441	442	443	444	445	446	447	448	449	450	451	452	453	454	455	456	457	458	459	460	461	462	463	464	465	466	467	468	469	470	471	472	473	474	475	476	477	478	479	480	481	482	483	484	485	486	487	488	489	490	491	492	493	494	495	496	497	498	499	500										
501	502	503	504	505	506	507	508	509	510	511	512	513	514	515	516	517	518	519	520	521	522	523	524	525	526	527	528	529	530	531	532	533	534	535	536	537	538	539	540	541	542	543	544	545	546	547	548	549	550	551	552	553	554	555	556	557	558	559	560	561	562	563	564	565	566	567	568	569	570	571	572	573	574	575	576	577	578	579	580	581	582	583	584	585	586	587	588	589	590	591	592	593	594	595	596	597	598	599	600										
601	602	603	604	605	606	607	608	609	610	611	612	613	614	615	616	617	618	619	620	621	622	623	624	625	626	627	628	629	630	631	632	633	634	635	636	637	638	639	640	641	642	643	644	645	646	647	648	649	650	651	652	653	654	655	656	657	658	659	660	661	662	663	664	665	666	667	668	669	670	671	672	673	674	675	676	677	678	679	680	681	682	683	684	685	686	687	688	689	690	691	692	693	694	695	696	697	698	699	700										
701	702	703	704	705	706	707	708	709	710	711	712	713	714	715	716	717	718	719	720	721	722	723	724	725	726	727	728	729	730	731	732	733	734	735	736	737	738	739	740	741	742	743	744	745	746	747	748	749	750	751	752	753	754	755	756	757	758	759	760	761	762	763	764	765	766	767	768	769	770	771	772	773	774	775	776	777	778	779	780	781	782	783	784	785	786	787	788	789	790	791	792	793	794	795	796	797	798	799	800										
801	802	803	804	805	806	807	808	809	810	811	812	813	814	815	816	817	818	819	820	821	822	823	824	825	826	827	828	829	830	831	832	833	834	835	836	837	838	839	840	841	842	843	844	845	846	847	848	849	850	851	852	853	854	855	856	857	858	859	860	861	862	863	864	865	866	867	868	869	870	871	872	873	874	875	876	877	878	879	880	881	882	883	884	885	886	887	888	889	890	891	892	893	894	895	896	897	898	899	900										
901	902	903	904	905	906	907	908	909	910	911	912	913	914	915	916	917	918	919	920	921	922	923	924	925	926	927	928	929	930	931	932	933	934	935	936	937	938	939	940	941	942	943	944	945	946	947	948	949	950	951	952	953	954	955	956	957	958	959	960	961	962	963	964	965	966	967	968	969	970	971	972	973	974	975	976	977	978	979	980	981	982	983	984	985	986	987	988	989	990	991	992	993	994	995	996	997	998	999	1000										

**Table 19. Preliminary maximum parsimony (MP) heuristic searches.** A range of MP heuristic search strategies across various taxon sets was conducted for (a) EF, (b) DDC and (c) combined EF&DDC data matrices. Identical heuristic searches for smaller taxon sets were repeated four times under 10, 100, 1,000 or 10,000 random sequence addition replicates to illustrate the efficiency of treespace exploration by a TBR-based search algorithm. Parsimony-based tree statistics (length, CI, RI) are reported for each set of found trees, along with the number of islands across which those trees are distributed. Filtering saved trees for optimal parsimony score significantly reduced the size of MP tree sets required for further evaluation. Three analyses conducted for the Sphingidae&ZOG taxon set and reported in Figures 6, 7 & 8 are shaded. Third codon position was excluded from analyses only in the combined EF&DDC data matrix, as the low number of parsimony informative characters precluded analysis for each gene separately. '-dups' indicates taxon set was trimmed of samples containing identical EF amino acid haplotypes, in an effort to reduce computation time by eliminating minimally informative taxa.

(a) EF Data Matrix														
Log Taxon Set	ntax	Data Partition	nchar	Reps	Random Seed	Rearrangements	Time	Length	CI	RI	Trees	Islands	Filtered Islands	Bootstrap Replicates
5 Lepidoptera	118	EF ntall	452	200	1607577416	237,160,000,000	45h5m38s	4,932	0.156	0.470	680	1	680	116
6 Bombycoidea	82	EF ntall	398	1,000	1139344340	36,127,000,000	4h49m35s	2,695	0.241	0.520	7,316	406	280	2
12A Sphingidae	64	EF ntall	336	10	2063643223	125,356,440	0h1m0s	1,494	0.315	0.574	630	8	243	3
12B Sphingidae	64	EF ntall	336	100	2063643223	1,232,234,304	0h9m55s	1,494	0.315	0.574	2,605	74	243	3
12C Sphingidae	64	EF ntall	336	1,000	2063643223	9,682,800,000	1h32m0s	1,494	0.315	0.574	5,862	383	243	3
11D Sphingidae	64	EF ntall	336	10,000	2063643223	86,192,000,000	13h18m6s	1,494	0.315	0.574	9,871	1,188	243	3
25A Sphingidae	67	EF ntall	338	10	1074512411	134,174,600	0h1m14s	1,525	0.311	0.590	357	8	184	2
25B Sphingidae	67	EF ntall	338	100	1074512411	1,099,848,504	0h10m15s	1,525	0.311	0.590	2,407	74	244	3
25C Sphingidae	67	EF ntall	338	1,000	1074512411	9,353,000,000	1h28m6s	1,525	0.311	0.590	6,216	470	244	3
25D Sphingidae	67	EF ntall	338	10,000	1074512411	89,681,000,000	14h22m28s	1,525	0.311	0.590	11,584	1,293	244	3
18A Sphingidae&ZOG	66	EF ntall	357	10	52841009	255,317,280	0h1m0s	1,705	0.300	0.549	652	10	161	3
18B Sphingidae&ZOG	66	EF ntall	357	100	52841009	1,390,727,616	0h9m55s	1,705	0.300	0.549	2,544	65	161	3
18C Sphingidae&ZOG	66	EF ntall	357	1,000	52841009	12,085,000,000	1h32m0s	1,705	0.300	0.549	7,363	349	161	3
18D Sphingidae&ZOG	66	EF ntall	357	10,000	52841009	110,270,000,000	13h18m6s	1,705	0.300	0.549	12,709	937	161	3
26A Sphingidae&ZOG	69	EF ntall	358	10	654765370	252,768,884	0h1m53s	1,736	0.297	0.565	1,632	9	560	3
26B Sphingidae&ZOG	69	EF ntall	358	100	654765370	2,294,900,000	0h17m3s	1,736	0.297	0.565	6,151	81	580	4
26C Sphingidae&ZOG	69	EF ntall	358	1,000	654765370	17,051,000,000	2h9m15s	1,736	0.297	0.565	15,184	525	580	4
26D Sphingidae&ZOG	69	EF ntall	358	10,000	654765370	156,710,000,000	20h40m27s	1,736	0.297	0.565	28,971	1,945	580	4

(b) DDC Data Matrix														
Log Taxon Set	ntax	Data Partition	nchar	Reps	Random Seed	Rearrangements	Time	Length	CI	RI	Trees	Islands	Filtered Islands	Bootstrap Replicates
2 Bombycoidea	73	DDC ntall	636	10,000	1636539794	52,303,000,000	17h18m23s	5059(5062)	0.232	0.604	2,210	376	20	1
4 Lepidoptera	105	DDC ntall	730	1,000	1636539794	61,444,000,000	22h44m49s	8318(8320)	0.170	0.543	707	32	240	2
13A Sphingidae	64	DDC ntall	591	10	65489846	19,519,816	0h0m21s	4,035	0.262	0.634	66	9	20	1
13B Sphingidae	64	DDC ntall	591	100	65489846	236,273,898	0h4m37s	4,035	0.262	0.634	204	34	20	1
13C Sphingidae	64	DDC ntall	591	1,000	65489846	19,519,816	0h39m12s	4,035	0.262	0.634	608	116	20	1
13D Sphingidae	64	DDC ntall	591	10,000	65489846	19,519,816	6h53m21s	4,035	0.262	0.634	1,372	297	20	1
27A Sphingidae	65	DDC ntall	593	10	1641822553	36,696,460	0h0m36s	4,117	0.259	0.633	117	7	20	1
27B Sphingidae	65	DDC ntall	593	100	1641822553	235,332,752	0h4m2s	4,117	0.259	0.633	282	38	20	1
27C Sphingidae	65	DDC ntall	593	1,000	1641822553	2,283,800,000	0h40m54s	4,117	0.259	0.633	591	99	20	1
27D Sphingidae	65	DDC ntall	593	10,000	1641822553	23,298,000,000	7h36m36s	4,117	0.259	0.633	1,259	237	20	1
15A Sphingidae&ZOG	66	DDC ntall	618	10	315856485	56,764,988	0h1m14s	4,484	0.249	0.611	54	7	10	1
15B Sphingidae&ZOG	66	DDC ntall	618	100	315856485	361,051,904	0h7m55s	4,484	0.249	0.611	167	30	10	1
15C Sphingidae&ZOG	66	DDC ntall	618	1,000	315856485	3,245,700,000	1h1m0s	4,484	0.249	0.611	353	70	10	1
15D Sphingidae&ZOG	66	DDC ntall	618	10,000	315856485	33,006,000,000	12h5m14s	4,484	0.249	0.611	800	173	10	1

Table 19. (continued)

Log Taxon Set	ntax	Data Partition	nchar	Reps	Random Seed	Rearrangements	Time	Length	CI	RI	Filtered			Bootstrap Replicates	
											Trees	Islands	Trees		
28A Sphingidae&2OG	67	DDC ntall	620	10	1953784988	40,715,536	0h0m43s	4,566	0.246	0.610	47	5	20	1	5000
28B Sphingidae&2OG	67	DDC ntall	620	100	1953784988	337,945,312	0h5m56s	4,566	0.246	0.610	228	41	20	1	
28C Sphingidae&2OG	67	DDC ntall	620	1,000	1953784988	2,885,300,000	0h53m7s	4,566	0.246	0.610	511	136	20	1	
28D Sphingidae&2OG	67	DDC ntall	620	10,000	1953784988	29,322,000,000	9h25m29s	4,566	0.246	0.610	1,047	278	20	1	
(c) EF&DDC Data Matrix															
7 Lepidoptera	91	EF&DDC ntall	1,108	1,000	370101926	6,466,100,000	2h27m21s	10,119	0.196	0.538	35	19	2	1	1000
8 Bombycoidea	72	EF&DDC ntall	1,011	1,000	1636539794	1,750,946,322	0h52m20s	7,243	0.242	0.577	43	32	1	1	1000
10A Sphingidae	64	EF&DDC ntall	927	10	984651357	14,471,140	0h0m22s	5,612	0.272	0.613	19	7	3	1	2520
10B Sphingidae	64	EF&DDC ntall	927	100	984651357	114,652,264	0h2m59s	5,612	0.272	0.613	57	26	3	1	
10C Sphingidae	64	EF&DDC ntall	927	1,000	984651357	1,089,478,592	0h28m34s	5,612	0.272	0.613	111	57	3	1	
10D Sphingidae	64	EF&DDC ntall	927	10,000	984651357	10,649,000,000	4h37m6s	5,612	0.272	0.613	237	1335	3	1	
16A Sphingidae&2OG	66	EF&DDC ntall	975	10	644781007	12,183,998	0h0m15s	6,280	0.259	0.588	18	8	3	1	2160
16B Sphingidae&2OG	66	EF&DDC ntall	975	100	644781007	136,286,734	0h2m43s	6,280	0.259	0.588	39	20	3	1	
16C Sphingidae&2OG	66	EF&DDC ntall	975	1,000	644781007	1,296,544,020	0h26m3s	6,280	0.259	0.588	82	44	3	1	
16D Sphingidae&2OG	66	EF&DDC ntall	975	10,000	644781007	12,742,000,000	4h17m3s	6,280	0.259	0.588	216	125	3	1	
22 Lepidoptera-dups	77	EF&DDC nt1&2	322	421	281468754	116,140,000,000	42h47m5s	1,209	0.343	0.629	6369	112	243	43	2435
9 Bombycoidea	72	EF&DDC nt1&2	247	337	436992825	81,847,000,000	26h21m53s	814	0.365	0.715	36177	200	1296	2	2000
20A Sph+Bomby-dups	58	EF&DDC nt1&2	247	10	137523599	95,099,680	0h0m32s	779	0.379	0.671	295	5	234	3	821
20B Sph+Bomby-dups	58	EF&DDC nt1&2	247	100	137523599	1,346,074,986	0h7m34s	779	0.379	0.671	1494	55	234	3	
20C Sph+Bomby-dups	58	EF&DDC nt1&2	247	1,000	137523599	10,309,000,000	0h58m12s	779	0.379	0.671	5942	431	234	3	
20D Sph+Bomby-dups	58	EF&DDC nt1&2	247	10,000	137523599	100,430,000,000	9h44m56s	779	0.379	0.671	13777	1697	234	3	
21A Sph&2OG-dups	52	EF&DDC nt1&2	226	10	870775331	61,188,966	0h0m29s	667	0.385	0.660	583	9	223	4	885
21B Sph&2OG-dups	52	EF&DDC nt1&2	226	100	870775331	495,436,250	0h3m30s	667	0.385	0.660	1684	79	235	6	
21C Sph&2OG-dups	52	EF&DDC nt1&2	226	1,000	870775331	3,781,100,000	0h31m0s	667	0.385	0.660	6131	545	235	6	
21D Sph&2OG-dups	52	EF&DDC nt1&2	226	10,000	870775331	35,156,000,000	4h44m29s	667	0.385	0.660	16593	2127	235	6	
19A Sphingidae-dups	50	EF&DDC nt1&2	195	10	80275767	79,361,196	0h0m32s	559	0.392	0.693	1731	8	994	1	35
19B Sphingidae-dups	50	EF&DDC nt1&2	195	100	80275767	446,032,648	0h3m1s	559	0.392	0.693	3867	72	994	1	
19C Sphingidae-dups	50	EF&DDC nt1&2	195	1,000	80275767	3,546,100,000	0h28m38s	559	0.392	0.693	12034	490	994	1	
19D Sphingidae-dups	50	EF&DDC nt1&2	195	10,000	80275767	25,879,000,000	3h10m15s	559	0.392	0.693	29375	2468	994	1	

**Table 20. Performance of data on alternative topologies, evaluated under the criterion of maximum parsimony (MP).** Variable (i.e., autapomorphic and parsimony-informative) characters from EF, DDC and combined EF&DDC data matrices were mapped onto the sets of MP topologies derived from independent analyses on the Sphingidae&2OG taxon set from each data matrix. Each row in the data table indicates a unique topology: for EF, 2 of 161MP trees filtered for compatibility with the 50% majority rule consensus tree; for DDC, all 10MP trees; for combined EF&DDC, all 3MP trees. Data from the three matrices was optimized onto each topology, and four parsimony-based performance measures were recorded: 'length' indicates total of all inferred character state changes across a topology, and is minimized when the original data set is mapped onto its own tree (see shaded cells); '%diff' indicates the percentage increase in tree length incurred for a given data set relative to the minimal observed length (shaded cells); 'ci' and 'ri' are the consensus and retention indices, respectively. Mean values for all four measures were calculated across the three data matrices for each tree, as a measure of overall parsimony penalty imposed by mapping one data set on another's topology. That topology with lowest mean 'length' and '%diff' and highest 'ci' and 'ri' was selected as the optimal MP tree for a given data set. These trees are indicated by an asterisk and were used as seed topologies for maximum likelihood parameter estimation and heuristic searches. The procedure was repeated for (a) all nt and (b) nt1 & nt2 only within each data set.

(a) all nt positions

		Data Partition															
		EF				DDC				ED				Mean Values			
Trees		length	%diff	ci	ri	length	%diff	ci	ri	length	%diff	ci	ri	length	%diff	ci	ri
EF	i	1705	0.00	0.300	0.549	4785	6.71	0.233	0.576	6490	3.34	0.251	0.570	4327	3.35	0.261	0.565
	*ii	1705	0.00	0.300	0.549	4782	6.65	0.233	0.577	6487	3.30	0.251	0.570	4325	3.31	0.261	0.565
DDC	i	1802	5.69	0.284	0.512	4484	0.00	0.249	0.611	6286	0.10	0.259	0.588	4191	1.93	0.264	0.570
	ii	1808	6.04	0.283	0.510	4484	0.00	0.249	0.611	6292	0.19	0.259	0.587	4195	2.08	0.264	0.569
	iii	1800	5.57	0.284	0.513	4484	0.00	0.249	0.611	6284	0.06	0.259	0.588	4189	1.88	0.264	0.571
	iv	1807	5.98	0.283	0.510	4484	0.00	0.249	0.611	6291	0.18	0.259	0.588	4194	2.05	0.264	0.570
	*v	1798	5.45	0.284	0.514	4484	0.00	0.249	0.611	6282	0.03	0.259	0.588	4188	1.83	0.264	0.571
	vi	1800	5.57	0.284	0.513	4484	0.00	0.249	0.611	6284	0.06	0.259	0.588	4189	1.88	0.264	0.571
	vii	1805	5.87	0.283	0.511	4484	0.00	0.249	0.611	6289	0.14	0.259	0.588	4193	2.00	0.264	0.570
	viii	1806	5.92	0.283	0.511	4484	0.00	0.249	0.611	6290	0.16	0.259	0.588	4193	2.03	0.264	0.570
	ix	1800	5.57	0.284	0.513	4484	0.00	0.249	0.611	6284	0.06	0.259	0.588	4189	1.88	0.264	0.571
	x	1806	5.92	0.283	0.511	4484	0.00	0.249	0.611	6290	0.16	0.259	0.588	4193	2.03	0.264	0.570
E+Dntall	*i	1787	4.81	0.286	0.518	4493	0.20	0.248	0.610	6280	0.00	0.259	0.588	4187	1.67	0.264	0.572
	ii	1786	4.75	0.286	0.518	4494	0.22	0.248	0.610	6280	0.00	0.259	0.588	4187	1.66	0.264	0.572
	iii	1787	4.81	0.286	0.518	4493	0.20	0.248	0.610	6280	0.00	0.259	0.588	4187	1.67	0.264	0.572

(b) nt1 & nt2 positions only (nt3 excluded)

		Data Partition, excluding nt3															
		EFnt12				DDCnt12				EDnt12				Mean Values			
Trees		length	%diff	ci	ri	length	%diff	ci	ri	length	%diff	ci	ri	length	%diff	ci	ri
EF	i	135	0.00	0.267	0.610	643	9.17	0.350	0.678	778	6.87	0.335	0.667	519	5.35	0.317	0.652
	ii	135	0.00	0.267	0.610	643	9.17	0.350	0.678	778	6.87	0.335	0.667	519	5.35	0.317	0.652
DDC	i	139	2.96	0.259	0.594	590	0.17	0.381	0.719	729	0.14	0.358	0.699	486	1.09	0.333	0.671
	ii	139	2.96	0.259	0.594	591	0.34	0.381	0.718	730	0.27	0.358	0.698	487	1.19	0.333	0.670
	iii	139	2.96	0.259	0.594	590	0.17	0.381	0.719	729	0.14	0.358	0.699	486	1.09	0.333	0.671
	iv	139	2.96	0.259	0.594	591	0.34	0.381	0.718	730	0.27	0.358	0.698	487	1.19	0.333	0.670
	*v	138	2.22	0.261	0.598	589	0.00	0.382	0.720	727	-0.14	0.359	0.700	485	0.69	0.334	0.673
	vi	138	2.22	0.261	0.598	589	0.00	0.382	0.720	727	-0.14	0.359	0.700	485	0.69	0.334	0.673
	vii	138	2.22	0.261	0.598	590	0.17	0.381	0.719	728	0.00	0.359	0.699	485	0.80	0.334	0.672
	viii	138	2.22	0.261	0.598	590	0.17	0.381	0.719	728	0.00	0.359	0.699	485	0.80	0.334	0.672
	ix	138	2.22	0.261	0.598	589	0.00	0.382	0.720	727	-0.14	0.359	0.700	485	0.69	0.334	0.673
	x	138	2.22	0.261	0.598	590	0.17	0.381	0.719	728	0.00	0.359	0.699	485	0.80	0.334	0.672
E+Dntall	*i	140	3.70	0.257	0.591	588	-0.17	0.383	0.721	728	0.00	0.359	0.699	485	1.18	0.333	0.670
	ii	140	3.70	0.257	0.591	588	-0.17	0.383	0.721	728	0.00	0.359	0.699	485	1.18	0.333	0.670
	iii	140	3.70	0.257	0.591	588	-0.17	0.383	0.721	728	0.00	0.359	0.699	485	1.18	0.333	0.670

**Table 21. Iterative maximum likelihood (ML) model parameter estimation and heuristic searches.** For each data matrix, ten parameters in the GTR+I+G nucleotide substitution model were estimated from the data based on all three starting topologies derived from MP analyses of EF, DDC and combined EF&DDC data (see Figures 6, 7 & 8, and Table 20). Parameter values from this first stage (estimate i) were then fixed in the GTR+I+G model, and TBR branch swapping was conducted on the original MP starting topology until a maximum likelihood heuristic search located a globally optimal topology (tree A). That tree was in turn used as input for parameter re-estimation (estimate ii), and those parameters fixed for a random addition sequence heuristic search using SPR branch swapping to locate the ML topology (tree B). This cycle was repeated two more times for each data set, and the estimate at which parameter values first converged is indicated in boldface. Topologies generated after each iteration were compared across starting trees, and identical topologies are indicated by shared symbols: 'e' for EF data, 'd' for DDC data and 'c' for combined data. Notes about the heuristic search itself are presented in italics, including ranges of likelihood scores for suboptimal trees encountered on different islands. All characters, including invariant and autapomorphic sites, were included in these analyses. This procedure was repeated for each of three MP starting topologies within a given data set, and all three convergent parameter estimates from each data set (boldface) are presented in the summary table. The two topologies generated by ML analysis of combined EF&DDC data differ only in relative placement of Pachyphix and Pionis. Note, cases in which -lnL scores differ between the tree and the previous estimate (iv) are attributable to use of different numbers of discrete rate categories (4 vs. 8) to approximate the gamma distribution.

Start Tree	Iteration	-lnL	Tree	Equilibrium Base Frequencies					Relative Rate Parameters					Gamma Shape		
				A	C	G	T	I	AC	AG	AT	CG	CT		GT	
EF	estimate i	9866.40890	e	0.270037	0.264224	0.224773	0.240966	2.083831	13.309599	5.201402	2.215088	22.999231	1.0	0.624215	0.724428	
	tree A	9848.71090	e	<i>95,173 rearrangements</i>												
	estimate ii	<b>9836.20528</b>	e	<b>0.271855</b>	<b>0.260711</b>	<b>0.224495</b>	<b>0.242939</b>	<b>2.261761</b>	<b>13.998292</b>	<b>5.385792</b>	<b>2.310256</b>	<b>25.061543</b>	<b>1.0</b>	<b>0.616341</b>	<b>0.679515</b>	
	tree B	9849.20925	e	<i>84,390 rearrangements; 6 other islands [9849.30124...9874.18398]</i>												
	estimate iii	9836.20528	e	0.271855	0.260711	0.224495	0.242939	2.261761	13.998292	5.385792	2.310256	25.061543	1.0	0.616341	0.679515	
	tree C	9849.20925	e	<i>100,170 rearrangements; 2 identical ML trees (including two trichotomies) from two separate islands; 3 other islands [9849.30124...9875.47942]</i>												
	estimate iv	9836.20528	e	0.271855	0.260711	0.224495	0.242939	2.261761	13.998292	5.385792	2.310256	25.061543	1.0	0.616341	0.679515	
	tree D	9849.20925	e	<i>309,393 rearrangements; 13 other islands [9849.30124...9889.82807]</i>												
	DDC	estimate i	10013.46872	e	0.268910	0.259672	0.224306	0.247112	2.208843	13.597483	4.878705	2.189306	23.425677	1.0	0.623982	0.693267
	tree A	9836.54721	e	<i>72,110 rearrangements</i>												
estimate ii	9836.26202	e	0.272504	0.260927	0.223731	0.242837	2.290440	14.341559	5.432694	2.354036	25.382307	1.0	0.615662	0.675366		
tree B	9849.33662	e	<i>68,598 rearrangements; 2 different ML trees from same island; 4 other islands [9853.83292...9871.80406]</i>													
estimate iii	9836.26202	e	0.272504	0.260927	0.223731	0.242837	2.290440	14.341559	5.432694	2.354036	25.382307	1.0	0.615662	0.675366		
tree C	9849.28293	e	<i>131,160 rearrangements; 7 other islands [9849.33662...9893.33645]</i>													
estimate iv	<b>9836.20528</b>	e	<b>0.271855</b>	<b>0.260711</b>	<b>0.224495</b>	<b>0.242939</b>	<b>2.261761</b>	<b>13.998292</b>	<b>5.385792</b>	<b>2.310256</b>	<b>25.061543</b>	<b>1.0</b>	<b>0.616341</b>	<b>0.679515</b>		
tree D	9836.20528	e	<i>79,726 rearrangements; 7 other islands [9836.28013...9866.91601]</i>													
EF&DDC	estimate i	10009.72970	e	0.267098	0.262628	0.224041	0.246232	2.211722	13.461395	4.920453	2.166527	22.954691	1.0	0.624388	0.702701	
tree A	9836.56188	e	<i>76,198 rearrangements</i>													
estimate ii	9836.26202	e	0.272504	0.260927	0.223731	0.242837	2.290440	14.341559	5.432694	2.354036	25.382307	1.0	0.615662	0.675366		
tree B	9836.22323	e	<i>30,139 rearrangements; 8 other islands [9840.1406...9833.41953]</i>													
estimate iii	<b>9836.20528</b>	e	<b>0.271855</b>	<b>0.260711</b>	<b>0.224495</b>	<b>0.242939</b>	<b>2.261761</b>	<b>13.998292</b>	<b>5.385792</b>	<b>2.310256</b>	<b>25.061543</b>	<b>1.0</b>	<b>0.616341</b>	<b>0.679515</b>		
tree C	9836.20528	e	<i>84,440 rearrangements; 4 other islands [9836.28013...9868.09629]</i>													
estimate iv	9836.20528	e	0.271855	0.260711	0.224495	0.242939	2.261761	13.998292	5.385792	2.310256	25.061543	1.0	0.616341	0.679515		
tree D	9836.20528	e	<i>110,395 rearrangements; 7 other islands [9836.28013...9875.26308]</i>													

(b) DDC data

Start Tree	Iteration	-lnL	Tree	Equilibrium Base Frequencies					Relative Rate Parameters					Gamma Shape		
				A	C	G	T	I	AC	AG	AT	CG	CT		GT	
EF	estimate i	21315.34521	d	0.265803	0.218021	0.216613	0.298963	1.548052	5.708376	1.352207	1.136922	6.707771	1.0	0.513455	1.415038	
	tree A	20776.05376	d	<i>84,873 rearrangements</i>												
	estimate ii	<b>20771.82306</b>	d	<b>0.274066</b>	<b>0.219258</b>	<b>0.215995</b>	<b>0.290681</b>	<b>1.502608</b>	<b>5.571131</b>	<b>1.333153</b>	<b>1.150866</b>	<b>6.838060</b>	<b>1.0</b>	<b>0.510070</b>	<b>1.399595</b>	
	tree B	20775.55706	d	<i>51,995 rearrangements; 1 other island [20781.32586]</i>												
	estimate iii	20771.82306	d	0.274066	0.219258	0.215995	0.290681	1.502608	5.571131	1.333153	1.150866	6.838060	1.0	0.510070	1.399595	
	tree C	20775.55706	d	<i>69,039 rearrangements; 1 other island [20781.32586]</i>												
	estimate iv	20771.82306	d	0.274066	0.219258	0.215995	0.290681	1.502608	5.571131	1.333153	1.150866	6.838060	1.0	0.510070	1.399595	
	tree D	20775.55706	?	<i>output lost, tree not saved</i>												
	DDC	estimate i	20809.12010	d	0.275327	0.220694	0.217132	0.286847	1.446916	5.408308	1.341116	1.129692	6.707951	1.0	0.511308	1.440494
	tree A	20776.21237	d	<i>77,580 rearrangements</i>												
estimate ii	<b>20771.82036</b>	d	<b>0.274066</b>	<b>0.219258</b>	<b>0.215995</b>	<b>0.290681</b>	<b>1.502608</b>	<b>5.571131</b>	<b>1.333153</b>	<b>1.150866</b>	<b>6.838060</b>	<b>1.0</b>	<b>0.510070</b>	<b>1.399595</b>		
tree B	20775.55706	d	<i>55,811 rearrangements; 1 other island [20781.32586]</i>													

Table 21. (continued)

Start	Iteration	-lnL	Tree	A	C	G	T	AC	AG	AT	CG	CT	GT	plnv	Gamma Shape
estimate iii	20771.82036			0.274066	0.219258	0.215995	0.290681	1.502608	5.571131	1.333513	1.150866	6.838060	1.0	0.510070	1.399595
tree C	20775.55706	d		<i>70,081 rearrangements; 1 other island [20781.32586]</i>											
estimate iv	20771.82036			0.274066	0.219258	0.215995	0.290681	1.502608	5.571131	1.333513	1.150866	6.838060	1.0	0.510070	1.399595
tree D	20775.55706	d		<i>173,018 rearrangements; 1 other island [20781.32586]</i>											
EF&DDC	estimate i	20807.90239	d	0.274008	0.220909	0.216143	0.288940	1.450891	5.456497	1.338920	1.112771	6.649230	1.0	0.511846	1.458255
	tree A	20772.05824	d	<i>81,920 rearrangements</i>											
estimate ii	20771.82036			0.274066	0.219258	0.215995	0.290681	1.502608	5.571131	1.333513	1.150866	6.838060	1.0	0.510070	1.399595
tree B	20771.82036	d		<i>105,992 rearrangements; 1 other island [20777.34186]</i>											
estimate iii	20771.82036			0.274066	0.219258	0.215995	0.290681	1.502608	5.571131	1.333513	1.150866	6.838060	1.0	0.510070	1.399595
tree C	20771.82036	d		<i>103,945 rearrangements; 1 other island [20777.34186]</i>											
estimate iv	20771.82036			0.274066	0.219258	0.215995	0.290681	1.502608	5.571131	1.333513	1.150866	6.838060	1.0	0.510070	1.399595
tree D	20771.82036	d		<i>72,654 rearrangements; 1 other island [20777.34186]</i>											

(c) combined EF&DDC EF&DDC data

Start	Iteration	-lnL	Tree	Equilibrium Base Frequencies				Relative Rate Parameters				Gamma Shape			
				A	C	G	T	AC	AG	AT	CG	CT	GT	plnv	Gamma Shape
EF	estimate i	31641.43966		0.261769	0.241367	0.222335	0.274529	1.428825	6.378758	1.823303	1.097377	7.833578	1.0	0.574423	1.020463
	tree A	31249.93690		<i>79,321 rearrangements</i>											
	estimate ii	31241.97825		0.266192	0.241775	0.218030	0.274002	1.423766	6.397491	1.809089	1.115201	8.133311	1.0	0.573487	1.043336
	tree B	31230.35368	cl	<i>24,589 rearrangements; 2 other islands [31240.66054...31290.45183]</i>											
	estimate iii	31221.47311		0.268178	0.240423	0.220771	0.270628	1.413892	6.385676	1.835360	1.105062	8.201244	1.0	0.573686	1.039287
	tree C	31230.19768	cl	<i>45,127 rearrangements; 3 other islands [31231.03992...31277.35428]</i>											
	estimate iv	31221.47311		0.268178	0.240423	0.220771	0.270628	1.413892	6.385676	1.835360	1.105062	8.201244	1.0	0.573686	1.039287
	tree D	31230.19768	cl	<i>48,987 rearrangements; 8 other islands [31231.67144...31289.87335]</i>											
DDC	estimate i	31265.28480		0.267618	0.241289	0.221067	0.270025	1.386938	6.299045	1.819246	1.096481	8.030910	1.0	0.575522	1.062515
	tree A	31230.09800	cl	<i>74,134 rearrangements</i>											
	estimate ii	31221.47311		0.268178	0.240423	0.220771	0.270628	1.413892	6.385676	1.835360	1.105062	8.201244	1.0	0.573686	1.039287
	tree B	31230.19768	cl	<i>64,591 rearrangements; 3 other islands [31238.09353...31260.53561]</i>											
	estimate iii	31221.47311		0.268178	0.240423	0.220771	0.270628	1.413892	6.385676	1.835360	1.105062	8.201244	1.0	0.573686	1.039287
	tree C	31230.19768	cl	<i>50,298 rearrangements; 4 other islands [31233.92263...31281.97766]</i>											
	estimate iv	31221.47311		0.268178	0.240423	0.220771	0.270628	1.413892	6.385676	1.835360	1.105062	8.201244	1.0	0.573686	1.039287
	tree D	31230.19768	cl	<i>69,814 rearrangements; 5 other islands [31230.22379...31285.65724]</i>											
EF&DDC	estimate i	31263.23365		0.265896	0.242508	0.220701	0.270894	1.399164	6.336312	1.831596	1.087868	7.967988	1.0	0.575700	1.070484
	tree A	31221.48129	e2	<i>81,979 rearrangements</i>											
	estimate ii	31221.29642		0.268032	0.240620	0.220863	0.270486	1.411799	6.379233	1.834034	1.101840	8.187761	1.0	0.574004	1.043732
	tree B	31221.29642	e2	<i>32,506 rearrangements; 2 other islands [31271.57985...31274.37460]</i>											
	estimate iii	31221.29642		0.268032	0.240620	0.220863	0.270486	1.411799	6.379233	1.834034	1.101840	8.187761	1.0	0.574004	1.043732
	tree C	31221.29642	e2	<i>23,593 rearrangements; 3 other islands [31254.30769...31271.14336]</i>											
	estimate iv	31221.29642		0.268032	0.240620	0.220863	0.270486	1.411799	6.379233	1.834034	1.101840	8.187761	1.0	0.574004	1.043732
	tree D	31221.29642	?	<i>17,046 rearrangements; output test; tree not saved</i>											

(d) Summary

Data	Starting MP Tree	Iteration	-lnL	Tree	Equilibrium Base Frequencies				Relative Rate Parameters				Gamma Shape			
					A	C	G	T	AC	AG	AT	CG	CT	GT	plnv	Gamma Shape
EF	EF	estimate ii	9836.20528	e	0.271855	0.260711	0.224495	0.242939	2.261761	13.998292	5.385792	2.310256	25.061543	1.0	0.616341	0.679515
EF	DDC	estimate iv	9836.20528	e	0.271855	0.260711	0.224495	0.242939	2.261761	13.998292	5.385792	2.310256	25.061543	1.0	0.616341	0.679515
	EF&DDC	estimate iii	9836.20528	d	0.271855	0.260711	0.224495	0.242939	2.261761	13.998292	5.385792	2.310256	25.061543	1.0	0.616341	0.679515
	EF	estimate ii	20771.82036	d	0.274066	0.219258	0.215995	0.290681	1.502608	5.571131	1.333513	1.150866	6.838060	1.0	0.510070	1.399595
	DDC	estimate ii	20771.82036	d	0.274066	0.219258	0.215995	0.290681	1.502608	5.571131	1.333513	1.150866	6.838060	1.0	0.510070	1.399595
	EF&DDC	estimate iii	20771.82036	d	0.274066	0.219258	0.215995	0.290681	1.502608	5.571131	1.333513	1.150866	6.838060	1.0	0.510070	1.399595
	EF	estimate iii	31221.47311	cl	0.268178	0.240423	0.220771	0.270628	1.413892	6.385676	1.835360	1.105062	8.201244	1.0	0.573686	1.039287
	DDC	estimate ii	31221.47311	cl	0.268178	0.240423	0.220771	0.270628	1.413892	6.385676	1.835360	1.105062	8.201244	1.0	0.573686	1.039287
	EF&DDC	estimate ii	31221.29642	e2	0.268032	0.240620	0.220863	0.270486	1.411799	6.379233	1.834034	1.101840	8.187761	1.0	0.574004	1.043732

**Table 22. Performance of data on alternative topologies, evaluated under the criterion of maximum likelihood (ML).** Parameters of the GTR+I+G model specific to each data matrix were fixed (see Table 21d) and used to calculate likelihood scores by fitting the EF, DDC and combined EF&DDC data to the sets of (a) four ML topologies (Table 21) and (b) fifteen MP topologies (Table 20) derived from separate analyses on the Sphingidae&2OG taxon set. Each row in the data table indicates a unique topology, and the columns correspond to the single models optimized for EF and DDC, and the two models optimized for the combined EF&DDC data. Values in bold indicate topologies with maximum likelihood, which best explain the observed distribution of character states given the specified model of nucleotide substitution.

(a) Maximum Likelihood topologies

Topology	Model			
	EF	DDC	EF&DDCi	EF&DDCii
EF	<b>9831.17404</b>	21287.25301	31582.35831	31582.35202
DDC	10028.65251	<b>20772.01394</b>	31238.01742	31238.00865
EF&DDC i	9986.24572	20784.15003	31221.28558	31221.27737
EF&DDC ii	9989.40732	20782.12303	<b>31221.11648</b>	<b>31221.11370</b>

(b) Maximum Parsimony topologies

Topology	Model			
	EF	DDC	EF&DDCi	EF&DDCii
EF i	<b>9855.42474</b>	21315.95287	31639.78980	31639.79569
EF ii	9857.96464	21310.96800	31637.28333	31637.28812
DDC i	10010.20405	20811.23203	31267.72705	31267.71504
DDC ii	10016.50019	20811.86241	31275.90706	31275.89242
DDC iii	10008.63221	20811.54285	31265.84700	31265.83585
DDC iv	10014.91693	20812.17336	31274.03314	31274.01942
DDC v	10008.63221	20809.34130	31264.49019	31264.47856
DDC vi	10010.20405	20809.34130	31265.77540	31265.76321
DDC vii	10014.91693	20809.97158	31272.67753	31272.66333
DDC viii	10016.50020	20809.97158	31273.95927	31273.94445
DDC ix	10010.20405	20809.34130	31265.77540	31265.76321
DDC x	10016.50020	20809.97158	31273.95927	31273.94445
EF&DDC i	10004.78418	20808.06890	31262.74412	31262.72189
EF&DDC ii	10001.32864	<b>20805.01000</b>	<b>31257.69963</b>	<b>31257.68088</b>
EF&DDC iii	10003.75880	20809.61940	31264.33443	31264.31172





**Figure 2. Instructions distributed to sphingid collectors.** The following one-page instruction sheet was distributed to participating collectors in Fall 2002 and Spring 2003 as part of a Sphingidae collection kit containing labeled vials filled with 100% ethanol, glassine envelopes, blank data sheets and return postage. Special emphasis was placed on conveying the importance of complete immersion in 100% ethanol immediately after death to ensure viable tissue for nucleic acid extraction (see guideline #2).

## Collecting Adult Sphingidae for DNA Analysis

UNIVERSITY OF MARYLAND  
Department of Entomology (MCSE)  
Plant Sciences Building, room 4138  
College Park, MD 20742 USA



ANDRÉ MIGNAULT  
tel: 301-405-2089  
fax: 301-314-9290  
email: [mignault@wam.umd.edu](mailto:mignault@wam.umd.edu)

### Project Description:

In conjunction with my advisors, Drs. Charlie Mitter and Jerry Regier, I am pursuing a **molecular phylogeny of the Sphingidae** (Lepidoptera: Bombycoidea) to provide a foundation for understanding life history evolution in this spectacular group. I am collecting adult moths from every sphingid genus worldwide, as delineated in Kitching & Cadiou's (2000) comprehensive taxonomic revision, with special emphasis on obtaining all North American species because of their notably diverse life history strategies.

### Collection Guidelines:

1. Only **one to three specimens of each taxon** freshly collected into 100% ethanol are required for this project. I would gladly accept surplus specimens collected in glassine envelopes in the traditional manner for pinning and incorporation into the collection as voucher specimens.
  2. As soon as a moth dies, its nucleic acids (DNA and RNA) begin to break down. This process is rapid and irreversible, and jeopardizes our ability to obtain useful molecular data from a specimen. It is critical that **as soon as possible after death the moth be processed into 100% ethanol**, a non-toxic preservative which desiccates the specimen and retards processes of cellular degradation. Obtaining viable molecular data from a freshly processed specimen is nearly foolproof. Specimens long-dead or preserved in a medium containing any water may still be useful, but chances for success are diminished.
  3. After capturing a moth, store it in a cool place to keep it alive until processing. Immediately after killing the moth, carefully **remove the wings from the body\*** (e.g., via forceps or surgical scissors) and place them into a glassine envelope labeled in pencil or waterproof pen. **Insert the wingless body into a numbered vial of 100% ethanol** provided for you. The body of an extremely large specimen may be cut into smaller fragments and placed into several vials. Also, multiple smaller specimens (e.g., of the same genus or species) may be safely fit into a single vial to save space.
- \* I realize this unconventional collecting method requires more time and effort than you may be able to invest. If the entire moth can be inserted into the ethanol vial without destroying its wings then I can process the wings after receiving it. Again, it is most critical that the **body (with or without wings) be submerged into the ethanol as soon as possible after death.***
4. Record specimen collection information as specifically as possible. **Location, date and time** of collection are crucial. Moth identification, sex, method of collection, time since death or other notes of interest (e.g., weather, elevation) are also most welcome if you have the occasion to record them.
  5. These vials hold liquid quite well if the caps are screwed on snugly (paraffin is included to wrap the caps if any doubt). Once the specimen has been sealed in the vial and its wings stored in a labeled envelope, it requires no further processing. Preservation is enhanced by keeping specimens **cold and dark**, but storage at room temperature is fine if refrigeration/freezing is not possible.
  6. Return the **vials** containing moth bodies preserved in 100% ethanol, the corresponding **envelopes** containing wings and/or voucher specimens and **field collection data** for each specimen.

Please contact me if you have any questions or comments regarding the procedures described above, or details of the project as a whole. Your participation and input is greatly appreciated, and I look forward to continued correspondence with you. Many thanks for your invaluable aid in this project!

**Figure 3. Data entry page of the University of Maryland Lepidoptera Collections Database.** One of several screens available for viewing records in the UMD Lepidoptera Collections, the main data entry page displays fields in seven modules for all critical information about every specimen available for collection of molecular sequence data. Codes in the 'Identification' module provide unique serial identifiers for every specimen in the collections. Higher taxonomic information in the 'Taxonomy' module is autopopulated upon entry of a valid genus name, via relational lookup to a companion database of all valid genus names in Lepidoptera compiled from varied sources. Detailed collections information is compiled in the 'Specimen Profile' module, including a notes text field to accommodate special information. All specimens are stored at -80C, indexed by coordinates in the 'Specimen Location' module. Individual buttons for each gene in the 'Sequences' module lead to a separate screen detailing information about collected nucleotide sequence, including amplicon primers and GenBank numbers. Function buttons at the top of the screen perform customized scripts, including generation of reports sorted by taxonomy or accession number, and printing of preformatted labels for vials and wing vouchers. The database was created in FileMaker Pro version 3.1, customized for management of the UMD Lepidoptera Collections, and is presently available in FileMaker Pro version 6.0.

**UNIVERSITY OF MARYLAND LEPIDOPTERA COLLECTIONS**

Functions: [Sort by Taxon](#) [Sort by Accession](#) [2mL Vials](#) [1.5mL Vials](#) [Wing Vouchers](#) [Sequences](#)

**Identification**

**Accession** WJK-02-1941

**Lot**  

**Old Accession**  

**CodeName**  

**Taxonomy** Kitching 2000

Order: LEPIDOPTERA

Superfamily: Bombycoidea

Family: Sphingidae  ?

Subfamily: Sphinginae  ?

Tribe: Acherontiini  ?

Section:    ?

Genus: Agrius  ?

species: cingulata  ?

**Extraction**

Nucleic Acids Extracted  yes  no

	1st	2nd	3rd
Preparer	AAM		
Date	15 Jan 2003		
Tissue	head		
Location	S3		
Notes	RNA&DNA prep (Promega kit #Z3100, lot #146082)		

**Sequences**

<b>DDC</b>	<b>EF-1α</b>	<b>Period</b>	<b>PEPCK</b>	<b>18S</b>
<input checked="" type="radio"/> yes	<input checked="" type="radio"/> yes	<input type="radio"/> yes	<input type="radio"/> yes	<input type="radio"/> yes
<input type="radio"/> no	<input type="radio"/> no	<input checked="" type="radio"/> no	<input checked="" type="radio"/> no	<input type="radio"/> no

**Specimen Profile**

Quantity: exactly 1 specimen(s)

Life Stage: Adult

Sex: unknown

Specimen Type: pickled in 100% Ethanol stored at -80YC

Collector(s): Kelly, William J.

Determiner(s): Kelly, William J.

Date Collected: exactly 22 Sep 2002

COUNTRY: U.S.A.

Locality Data: Blackberry Mountain, Gilmer County, Georgia

Elevation:   meters

Specimen Notes: collected at mercury vapor light

Wing Voucher: 1941 prepared by AAM

**Specimen Location**

<b>Freezer</b>	<b>Rack</b>	<b>Box</b>
<span style="background-color: blue; color: white;">regier</span>	<span style="background-color: blue; color: white;">G</span>	<span style="background-color: blue; color: white;">7</span>
Old:		

**Loan Information**

Specimen Loan  yes  no

Data Input by AAM on 30 Oct 2002  
Data Modified by AAM on 27 Sep 2003

**Figure 4. Reference sequence for Elongation Factor 1-alpha.** Top row: *Bombyx mori* (Bombycoidea: Bombycidae) mRNA reference sequence used to standardize alignments in this study. Sequence provided by Kamie, *et al.* (1993), Genbank accession number D13338. Base composition of 1,687 bp fragment: 500nt (29.6%) A; 396nt (23.5%) C; 375nt (22.2%) G; 41nt (2.4%) T. Bottom row: *Acherontia styx medusa* (Sphingidae) exemplar mRNA sphingid sequence. Sequenced *de novo* in this study, UMD Lepidoptera Collections accession number IJK-02-5989. Base composition of 1,274 bp fragment: 317nt (24.9%) A; 366nt (28.7%) C; 322nt (25.3%) G; 262nt (20.6%) T. ‘.’ marks bases identical to the *Bombyx* reference sequence. Terminal primer sequences (30f and m41.21rc) were eliminated from all phylogenetic analyses. Gray boxes denote untranscribed regions, 47bp upstream of the start ATG and 1bp downstream of the stop TAG codon [note: an additional 247 bp of downstream sequence from the original Genbank accession is omitted here]. Sequences of primers used in this study contained within arrows, indicating the direction of amplification. Primer names are inserted at the primer 5' end: forward primer names above the sequence, reverse primer names below (note overlap between some primer versions). Primer sequences from Regier & Shultz (1997) are **boldface**; primers from Cho, *et al.* (1995) are *italicized*. Numbers at the ends of each line denote position relative to the fragment sequenced for this study; for example, position ‘1’ is the 5'-most base of the terminal primer 30f and position ‘1,274’ is the 3'-most base of the terminal primer m41.21rc.

-64	AGTCTATCTC	GCAPATTACC	GCAGTTTGTA	ATCCGTGACT	AACGAAA	GGCAAGGAAA	AGACT	<b>30f</b> <b>CACAT</b>	<b>TAACATTGTC</b>	<b>GTCAATCGGC</b>	AC	25
26	ACGTCGACTC	CGGCAAGTCC	ACCACCAGTC	GTCACCTGAT	CTACAAATGT	GGTGGTATTG	ACAAACGTAC	Y.m41.21rc	ATCGAGAAG	TTCGAGAAGG	TT	115
116	<b>AGGC</b> CCAGGA	AATGGGTAAA	GGATCCTTCA	<b>AAATGCTTTG</b>	GGTATTGGAC	AAACTAAAGG	CTGAGCGTGA	GCCTGGTATC	ACAATCGATA	..C..T..C..		205
206	TTGCTCTCTG	GAAGTTCGAA	ACTAGCAAGT	ACTATGTTAC	CATCATTTGAT	GCTCCTGGAC	ACAGAGATTT	CATCAAGAAC	ATGATCACAG	.....C..		295
296	GAACTCTCA	GGTGAATTGC	GCTGTGCTCA	TGCTAGTGC	CGGTACCCTG	GAATTCCGAA	CTGGTATCTC	TAAGAACCCTG	CAAAACCCCTG	.....G..		385
386	AGCATGCCTT	GCTCGCTTTC	ACCCTCGGTC	TCAAACAGCT	<b>CATCTAGGA</b>	<b>GTAACAAA</b>	<b>TGGTCTCCAC</b>	TGAACCCACA	TACAGTGAGC	.....C..		475
476	CCAGATTTGA	GGAAATCAAG	AAGGAAGTAT	CCTCATACAT	CAAGAAGAT	GCCTTGGTTC	CAGCTGCTGT	CGCTTTCGTG	CCCAATTCCTG	.....A..		565
566	GATGGCAGG	AGACAACATG	TTGGAGCCTT	CAACCAAAT	GCCTTGGTTC	AAGGATGGC	AGGTGGAGCG	TAAGGAAGGC	AAAGCTGAGC	.....G..		655
656	GAAATCCCT	CATTGAAGCT	CTCGATGCCA	TCCTGCCACC	TGCGCGCCCC	ACTGACAAGC	CCCTGCCTCT	TCCCTC	<b>CAA</b>	<b>GACGFATACA</b>	TT	745
746	<b>AAATCGG</b> GG	TATTGGTACC	GTGCCCGTCG	GCAGAGTTGA	AACTGGTGTG	TTGAAACCAG	GTACCAATGT	TGTCCTTTGCC	CCCGCAACA	.....T..		835
836	TCACTACTGA	AGTCAAGTCT	<b>GTGGAGATGC</b>	<b>ACCAGGAAGC</b>	TCTCCAAGAA	CTCTCAAGAA	..C..G..C..	AGTTTTCAC	GTAAGAAGC	.....G..		925
926	TGTCCTGCAA	GGAAATTCCT	CGTGGTTAAG	TTGCTGTGTA	CTCCAATAAC	AACCCACCTA	AGGTGCTGTC	AGATTTTACA	GCTCAAGTCA	.....G..		1015
1016	TTGTGCTTAA	CCATCCTGGT	CAAAATCTCA	ACGGTTACAC	ACCAGTCTTG	<b>GATGGCACA</b>	<b>CTGCCACAT</b>	TGCTGTCAAA	TTTGGCAGAA	.....C..		1105
1106	TCAAAGAAA	AGTTGACCCG	CGTACTGGTA	AAATCTACTGA	AGTCAACCCA	AAATCCATCA	AGTCTGGAGA	TGCAGCCATT	GTCAACTTGG	.....C..		1195
1196	TACCTTCCAA	GCCTCTAATG	GTAGAGTCTT	TCCAGGAATT	CCCACCCCTC	GGTGGT	<b>CTGCTCCCTGA</b>	<b>CATGAGGCAT</b>	ACAGTTGCTG	.....C..		1285
1286	TGGAGTGCAT	CAAGGCTGTC	AACTTCAAGG	AGGTGGTGG	TGGCAAGGTC	ACTAAAGCTG	CCGAAAAGGC	CACCAAGGGC	AAGAAG	.....C..		1375

**Figure 5. Reference sequence for Dopa Decarboxylase.** Top row: *Manduca sexta* (Bombycoidea: Sphingidae) mRNA reference sequence used to standardize alignments in this study. Sequence provided by Hiruma, et al. (1995), Genbank accession number U03909. Base composition of 3,063bp fragment: 922 (30.1%) A; 542 (17.7%) C; 618 (20.2%) G; 981 (32.0%) T. Bottom row: *Acherontia styx medusa* (Sphingidae) exemplar mRNA sphingid sequence. Sequenced *de novo* in this study, UMD Lepidoptera Collections accession number IJK-02-5989. Base composition of 1,373 bp fragment: 354nt (25.8%) A; 306nt (22.3%) C; 343nt (25.0%) G; 358nt (26.1%) T. ' ' marks bases identical to the *Manduca* reference sequence. Terminal primer sequences (1.0F and 7.5sR) were eliminated from all phylogenetic analyses. Gray boxes denote untranscribed regions, 86bp upstream of the start ATG and 7bp downstream of the stop TAG codon [note: an additional 90bp upstream and 1,353 bp downstream sequence from the original Genbank accession is omitted here]. Sequences of primers used in this study are contained within arrows, indicating the direction of amplification. Primer names are inserted at the primer 5' end: forward primer names above the sequence, reverse primer names below (note overlap between some primer versions). Primers developed and used in the Regier Lab are **boldface** (see Tables 4 & 5). Numbers at the ends of each line denote position relative to the fragment sequenced for this study; for example, position '1' is the 5'-most base of the terminal primer 1.0F and position '1,373' is the 3'-most base of the terminal primer 7.5sR.

-100	ATACCTGGG	CIPRAATACCG	AAAGGCTGTG	ATPRAATTGG	AACAGAAAGG	TCTTGCAATTA	GCTGATTGGA	CAAAAACITTT	GAAGTC	-11
-10	ATCCCCGAGA	<b>TTTAAAGAC</b>	<b>TTGCGGAAG</b>	<b>CGATACCTGA</b>	<b>CTACATCACA</b>	<b>GAGTATCTGG</b>	<b>AAACATTTAG</b>	<b>AGATAGACAA</b>	<b>GTAGTGCCGT</b>	79
80	CAGTGAAGCC	AGGCTACCTA	CGTCCCCTAG	TCCAGAGCA	GGCGCCCCAG	CAAGCTGAGC	CCTGGACAGC	AGTGATGGCG	GATATCGAAA	169
170	GGGTGTTCAT	GTCTGGGGTC	ACCCACTGGC	AATCACCTCG	<b>TTTCCACGCC</b>	<b>TATTTCCCGA</b>	<b>CGGCCAACTC</b>	<b>TTACCCTTCT</b>	<b>ATTGTGGCGG</b>	259
260	ATATGTTGAG	CGGCCTATT	<b>GCTTGTATCG</b>	<b>GTATACACCTG</b>	<b>GATTCGAAGC</b>	<b>CCAGCATGTA</b>	<b>CGGAACCTTGA</b>	<b>AGTTCTATG</b>	<b>TTAGACTGGC</b>	349
350	<b>TCGGTCAAT</b>	<b>GTGGGTCCT</b>	CGGACCCAGT	TCTTAGCAGC	TTCTGGCGCA	GAAGTGGCG	GTGTCATCCA	AGGCACATGA	AGTGAAGCCA	439
440	CGTTTGTAGC	TCTCCTTGGT	GCCAAATCTC	GTATGATGCA	CAGAGTCAAA	GAACAAACCC	CCGAGTGGAC	TGAGACAGAC	ATTCTCGGCA	529
530	AGCTTGTAGG	CYACTGCAAT	CAACAGGCC	ATTGCTCAGT	AGAGCGGGCT	GGACTTCTTG	GTGGGGTAAA	ACTTAGATCA	TTGAAACCCG	619
620	ATTCTAAGAG	ACGCCTTTCG	GGGACACTT	TGCGTGAAGC	AATCGACGAG	GACATTCGCA	ATGGACTTAT	TCCCCTCTAT	GTGGTCGCCA	709
710	CAPTAGGTAC	CACTTCTTCG	TGTGCCCTTG	ACGCATTAGA	TGAAATTTGA	GATGTTTGGC	ATGCAAGCGA	TATA <b>TTGGTTG</b>	<b>CATGTGGACG</b>	799
800	<b>CGGCCATAGC</b>	TGGCTCTGCG	TTTATTGTG	CCGAATACCG	TCACCTTTATG	AAAGGGGTTG	AAAAGGCTGA	<b>TTCTTTCAAT</b>	<b>TTCAACCCAC</b>	889
890	<b>ATAATGGAT</b>	GCTTGTCAAT	TTCGACTGCT	CAGTATATGT	GTTCGAAACA	CCGGCATGGA	TTGTTGACGC	GTTCATATGT	GACCCCTCTGT	979
980	ACTTGAAGCA	CGAACAGCAG	GGATFCGGAC	<b>CAGACTACCG</b>	<b>TCACTGGCAA</b>	<b>ATTCGTTTAG</b>	GACGACGATTT	CAGGTCACCTT	AAACTGTGTT	1069
1070	TCGTTTTGAG	GCTGTATGGC	GTGAAAAATC	TTCAAAAATA	CAATTGGAT	CAAATGGAT	TTGCTCACCT	GTTCGAAAAG	CTTTTAACTT	1159
1160	CGGATGAAG	ATTGAGCTA	TTTGAAGAGG	TGACTATGGG	GCTTGTATGT	TTTAGGCTCA	AAGGATCTAA	TGAAATCAAT	GAAGRATTTAT	1249
1250	TGAGACGCAT	AAATGGCCGC	GGAAAAATCC	ATTTAGTCC	CTCTAAAGTC	GATGACGTAT	ACTTCCCTTAG	ATTAGCAATC	<b>TGTTCAACGGT</b>	1339
1340	<b>TCACCTGAAGA</b>	<b>AAGTACATG</b>	<b>CATGTATCTT</b>	<b>GGGAGGAAT</b>	<b>AAAAGATCCG</b>	CTGTATGATGT	TCTTAAAAAG	TAAGGGAGCG	GTGTTTGAUCA	1429
1430	AAATAATCTG	TTCAACAACG	CGTAGGACCA	AAAATATACT	AACCTATATT	AAACAAAAATA	TATTCGGTGA	TGTTAGCCCTT	<b>TACATCTTAT</b>	1519

**Figure 6. Exemplar most parsimonious phylogram reconstructed from phylogenetic inference on EF ntall data for the Sphingidae&2OG taxon set.** Single topology was one of two selected from 161 equally MP trees by filtering for consistency with the 50% majority rule consensus tree. Gray branches denote regions of conflict between the 161 alternative EF MP trees, and these collapse in the strict consensus. Number of inferred synapomorphies is plotted above each branch. Bootstrap proportions (1,145 pseudoreplicates) are italicized and plotted below each branch. Monophyletic recognized higher taxonomic groups are boxed and shaded; outlier taxa deviating from their traditional taxonomic placement are left unshaded. Paraphyletic Smerinthinae is indicated by a dashed bar.

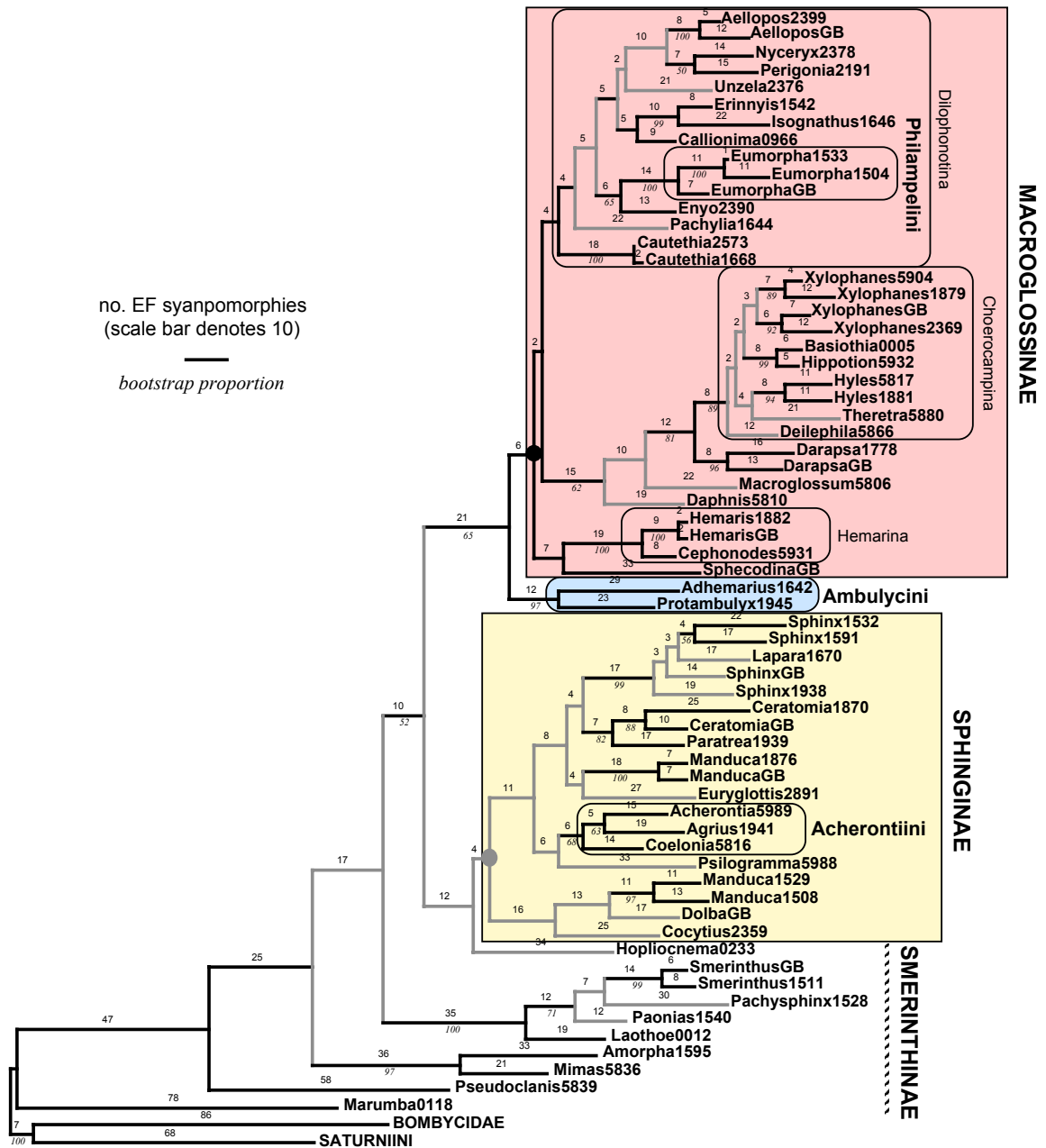


**Figure 7. Exemplar most parsimonious phylogram reconstructed from phylogenetic inference on DDC ntall data for the Sphingidae&2OG taxon set.** Single topology was selected from among 10 equally MP trees on the basis of parsimony mapping criteria (see asterisk in Table 20) . Gray branches denote regions of conflict between the 10 alternative DDC MP trees, and these collapse in the strict consensus. Number of inferred synapomorphies is plotted above each branch. Bootstrap proportions (1,248 pseudoreplicates) are italicized and plotted below each branch. Monophyletic recognized higher taxonomic groups are boxed and shaded; outlier taxa deviating from their traditional taxonomic placement are left unshaded. Paraphyletic MacroGLOSSINAE is indicated by a dashed bar.

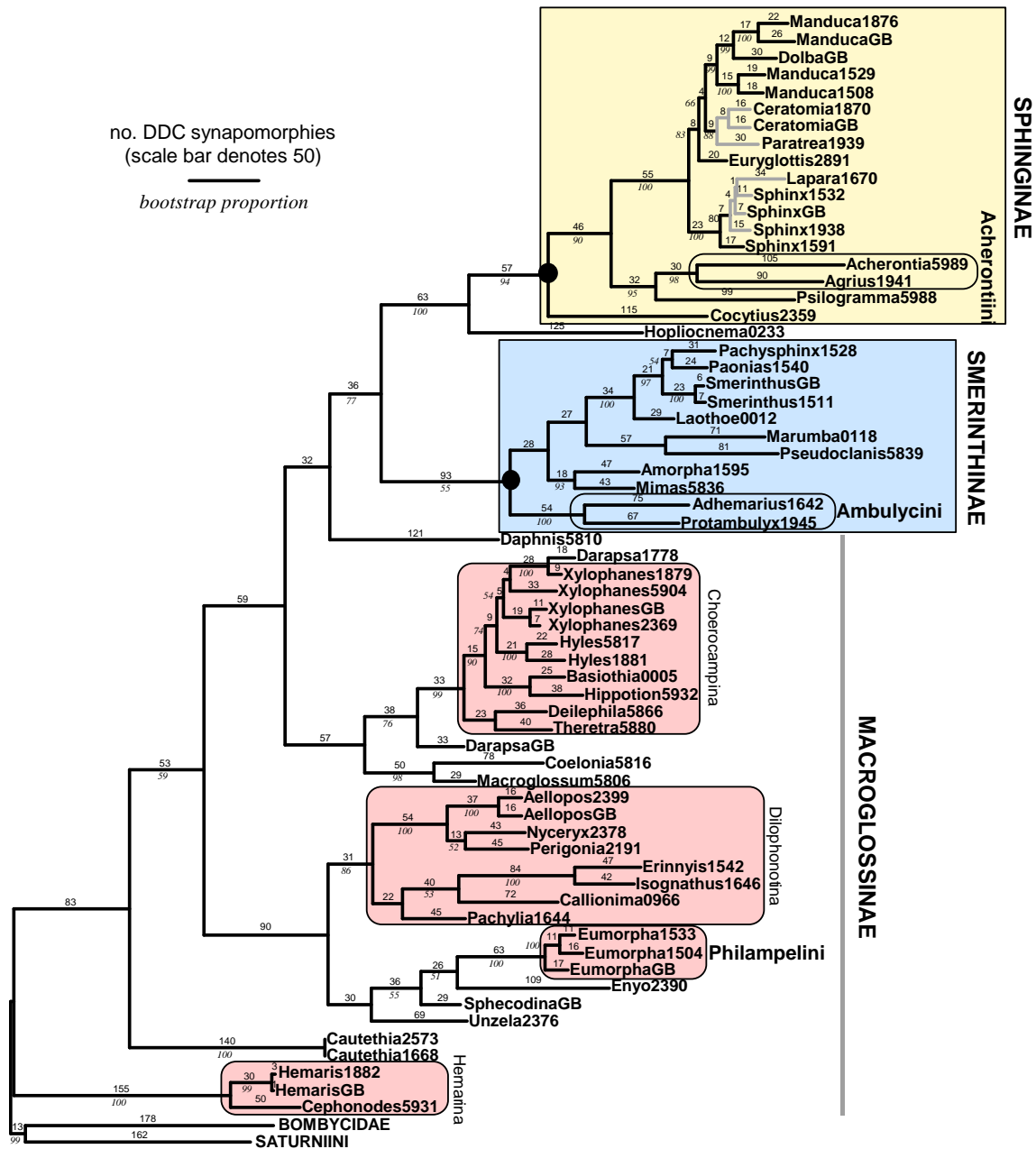


**Figure 8. Exemplar most parsimonious phylogram reconstructed from phylogenetic inference on combined EF&DDC ntall data for the Sphingidae&2OG taxon set.** Single topology was selected randomly from among 3 equally MP trees, as parsimony mapping criteria were equivocal (see Table 20). Gray branches denote regions of conflict between the 3 alternative EF&DDC MP trees, and these collapse in the strict consensus. Number of inferred synapomorphies is plotted above each branch. Bootstrap proportions (2,160 pseudoreplicates) are italicized and plotted below each branch. Monophyletic recognized higher taxonomic groups are boxed and shaded; outlier taxa deviating from their traditional taxonomic placement are left unshaded. Paraphyletic Smerinthinae is indicated by a dashed bar.

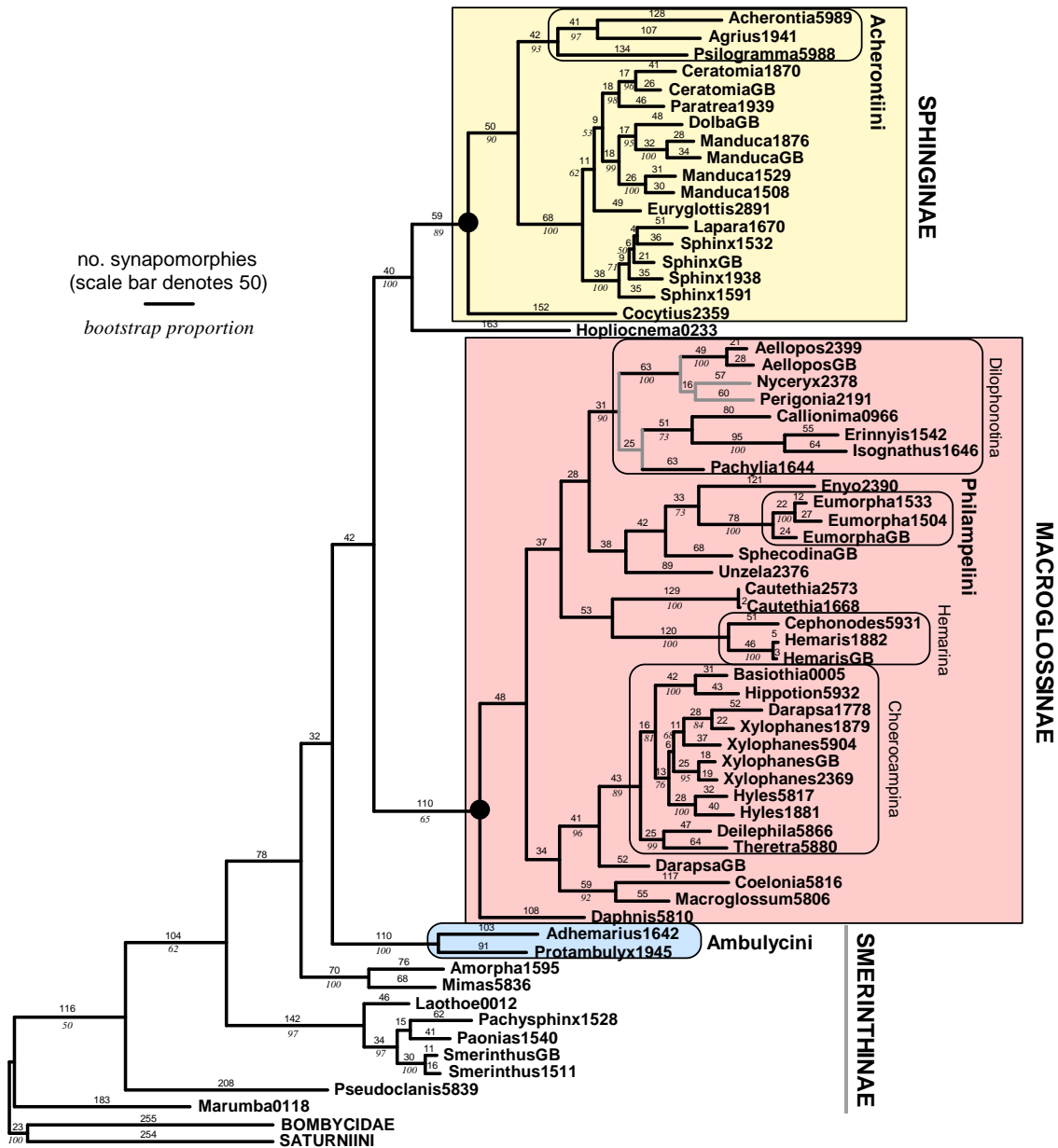




**Figure 9. Maximum likelihood phylogram from phylogenetic inference on EF ntall data for the Sphingidae&2OG taxon set.** Single globally convergent topology (Tree 'e' in Table 21) derived from four cycles of iterative parameter estimation / heuristic searches, using each of the MP trees in Figures 6, 7 and 8 as starting topologies. Branch length values, expressed as 1,000X number of substitutions per site along EF, are indicated above branches. Monophyletic recognized higher taxonomic groups are boxed and shaded; outlier taxa deviating from their traditional taxonomic placement are left unshaded. Paraphyletic Sphinginae and Smerinthinae are indicated by dashed bars. Inset contains maximum likelihood score of this topology and optimized parameters of the underlying GTR+I+G substitution model.

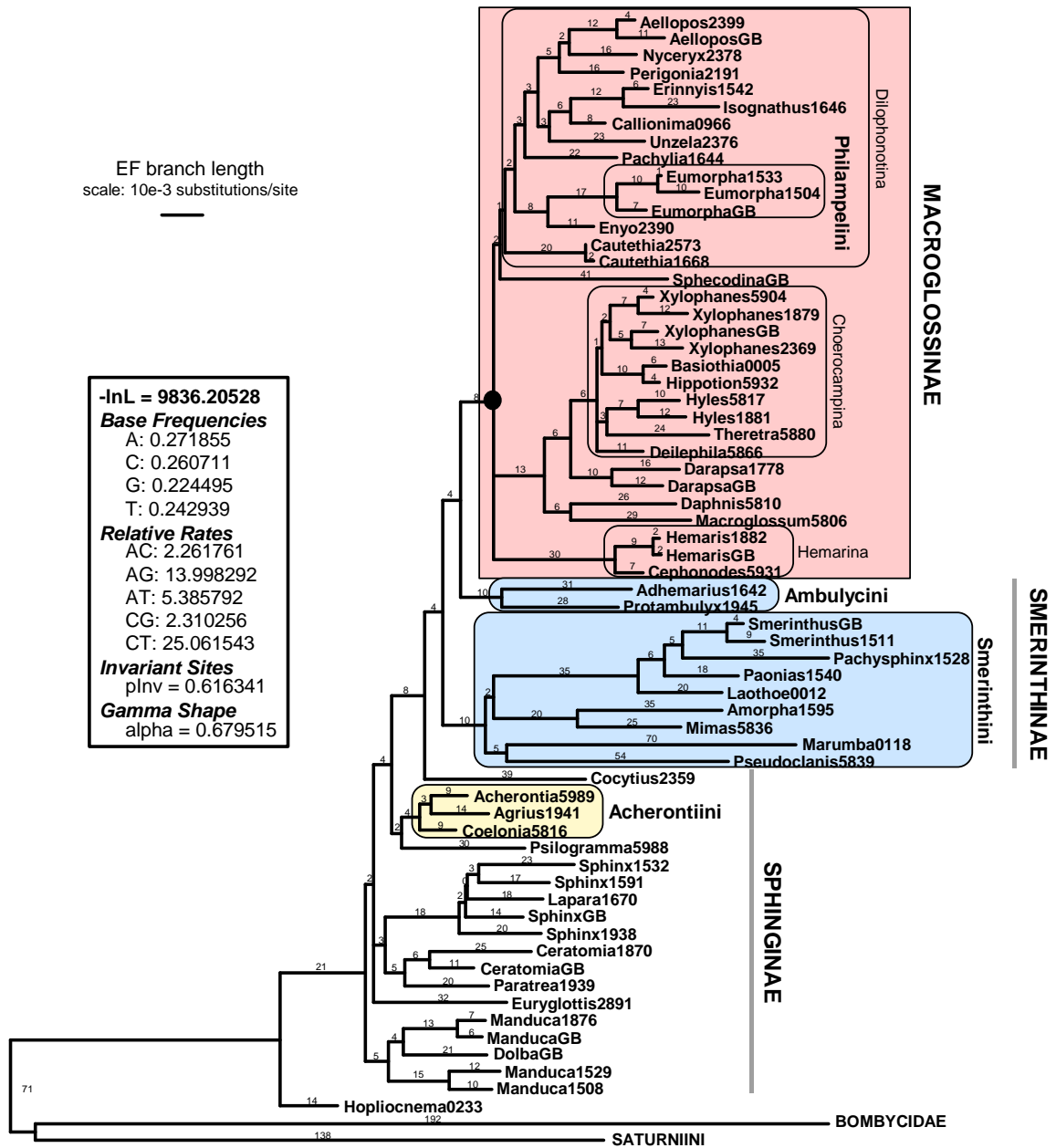


**Figure 10. Maximum likelihood phylogram from phylogenetic inference on DDC ntall data for the Sphingidae&2OG taxon set.** Single globally convergent topology (Tree 'd' in Table 21) derived from four cycles of iterative parameter estimation / heuristic searches, using each of the MP trees in Figures 6, 7 and 8 as starting topologies. Branch length values, expressed as 1,000X number of substitutions per site along EF, are indicated above branches. Monophyletic recognized higher taxonomic groups are boxed and shaded. Inset contains maximum likelihood score of this topology and optimized parameters of the underlying GTR+I+G substitution model.

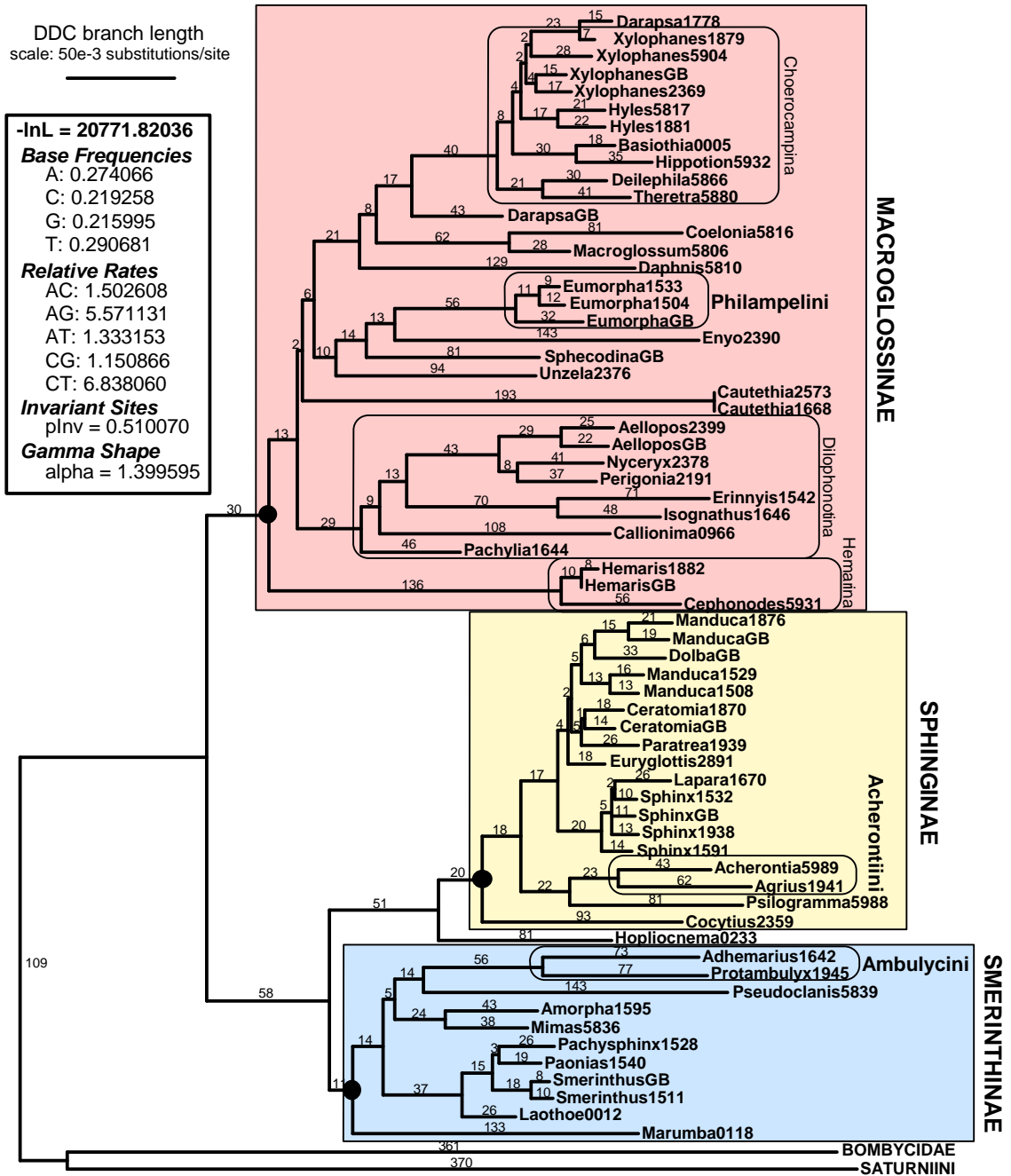


**Figure 11. Exemplar maximum likelihood phylogram from phylogenetic inference on combined EF&DDC ntall data for the Sphingidae&2OG taxon set.** One of two globally convergent topologies (Tree 'c2' in Table 21) derived from four cycles of iterative parameter estimation / heuristic searches, using the combined EF&DDC MP tree in Figure 8 as a starting topology. This ML topology differs from Tree 'c1' only in the relative placement of *Pachysphinx* and *Paonias*. Branch length values, expressed as 1,000X number of substitutions per site along EF, are indicated above branches. Monophyletic recognized higher taxonomic groups are boxed and shaded. Inset contains maximum likelihood score of this topology and optimized parameters of the underlying GTR+I+G substitution model.

